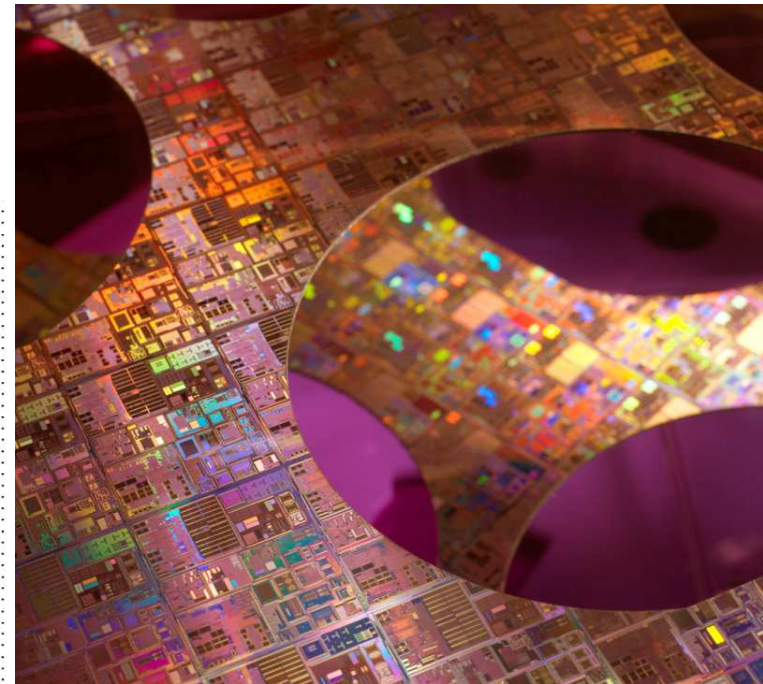
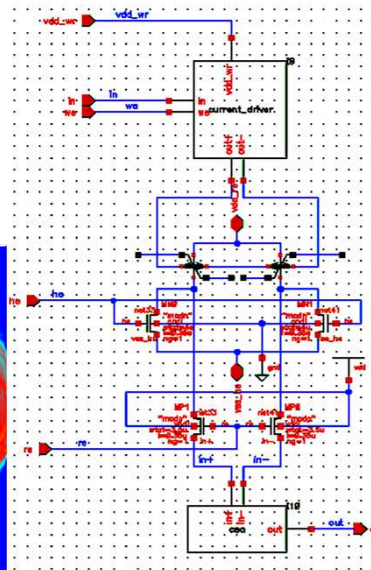
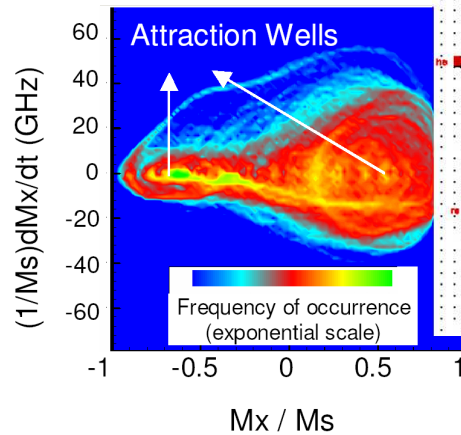
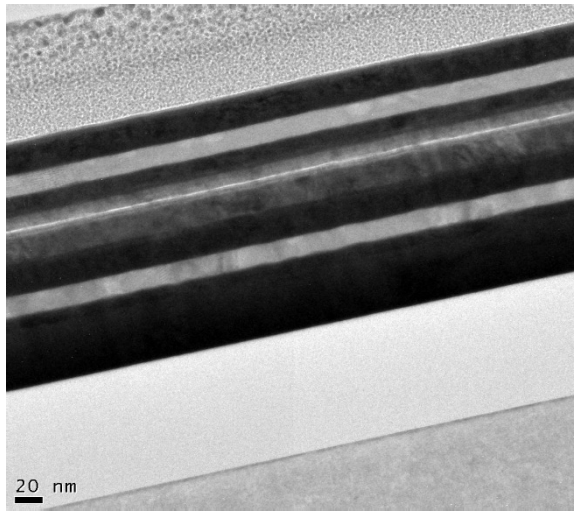
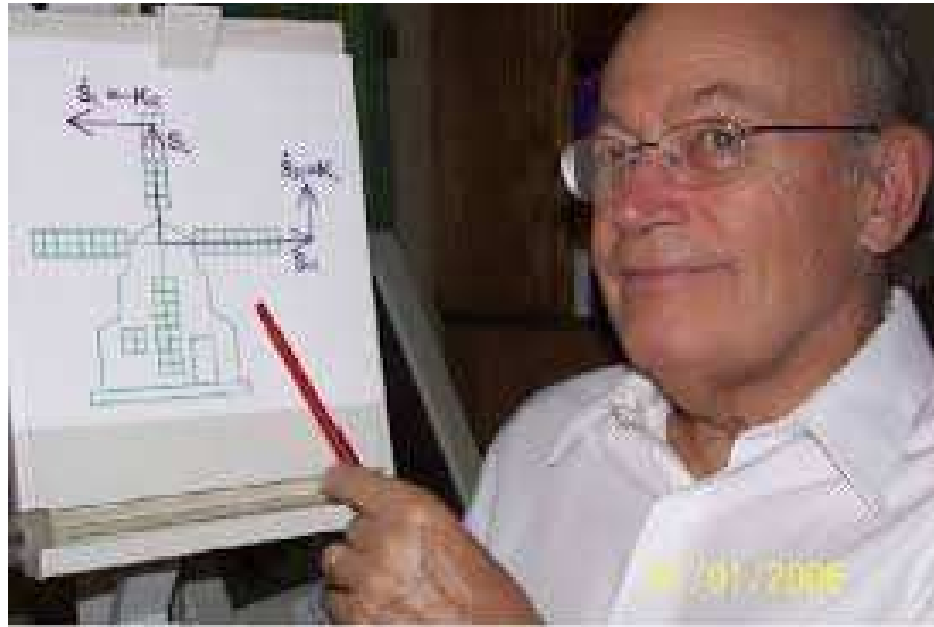


Spinelectronics: From Basic Phenomena to Applications





John Slonczewski

We will miss you, John

Spin-electronics

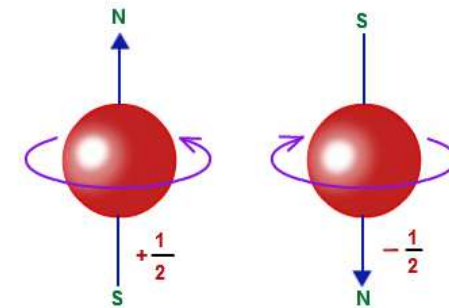
Electronics

Electron charge



Magnetism

Electron Spin

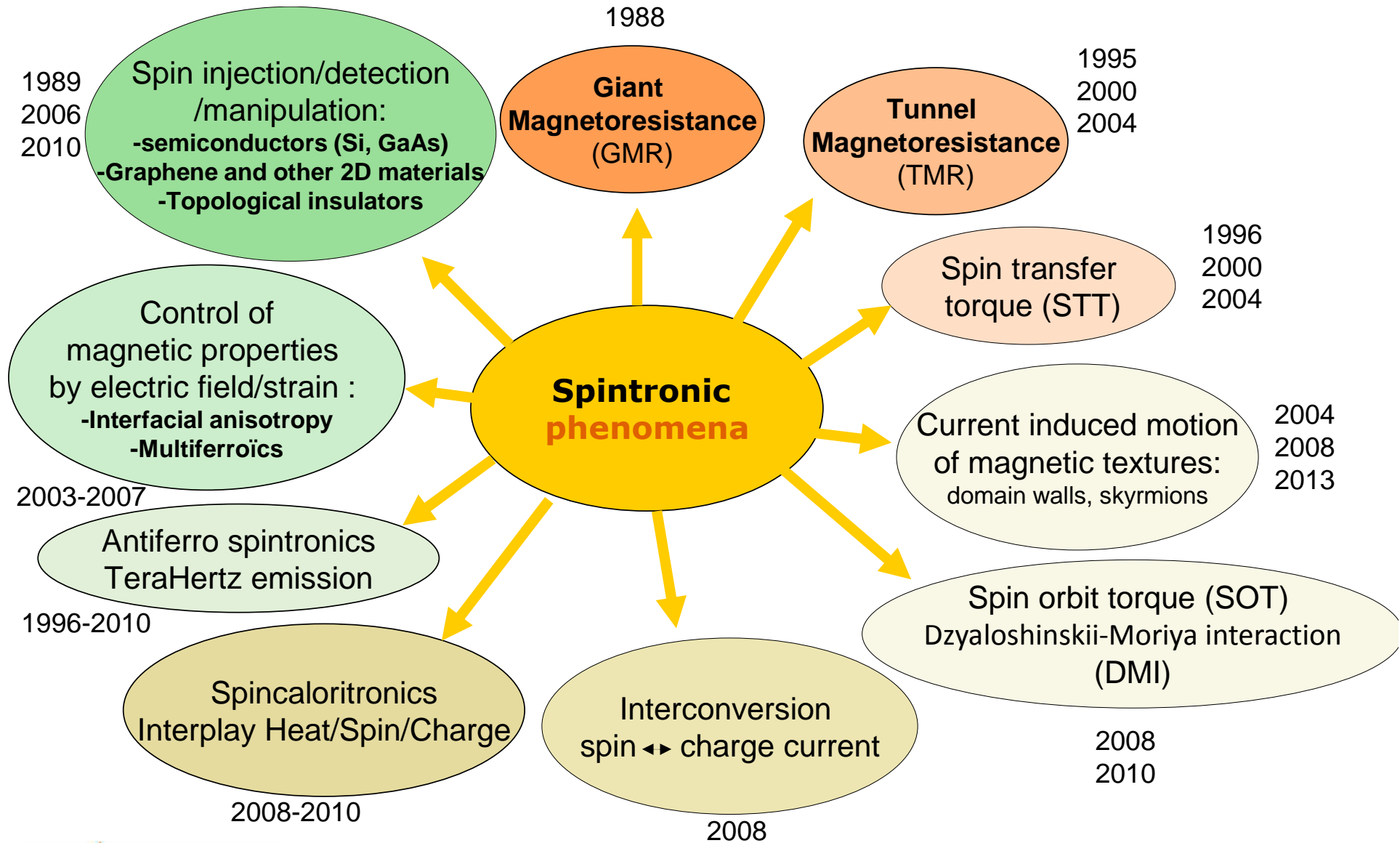


Main goal :

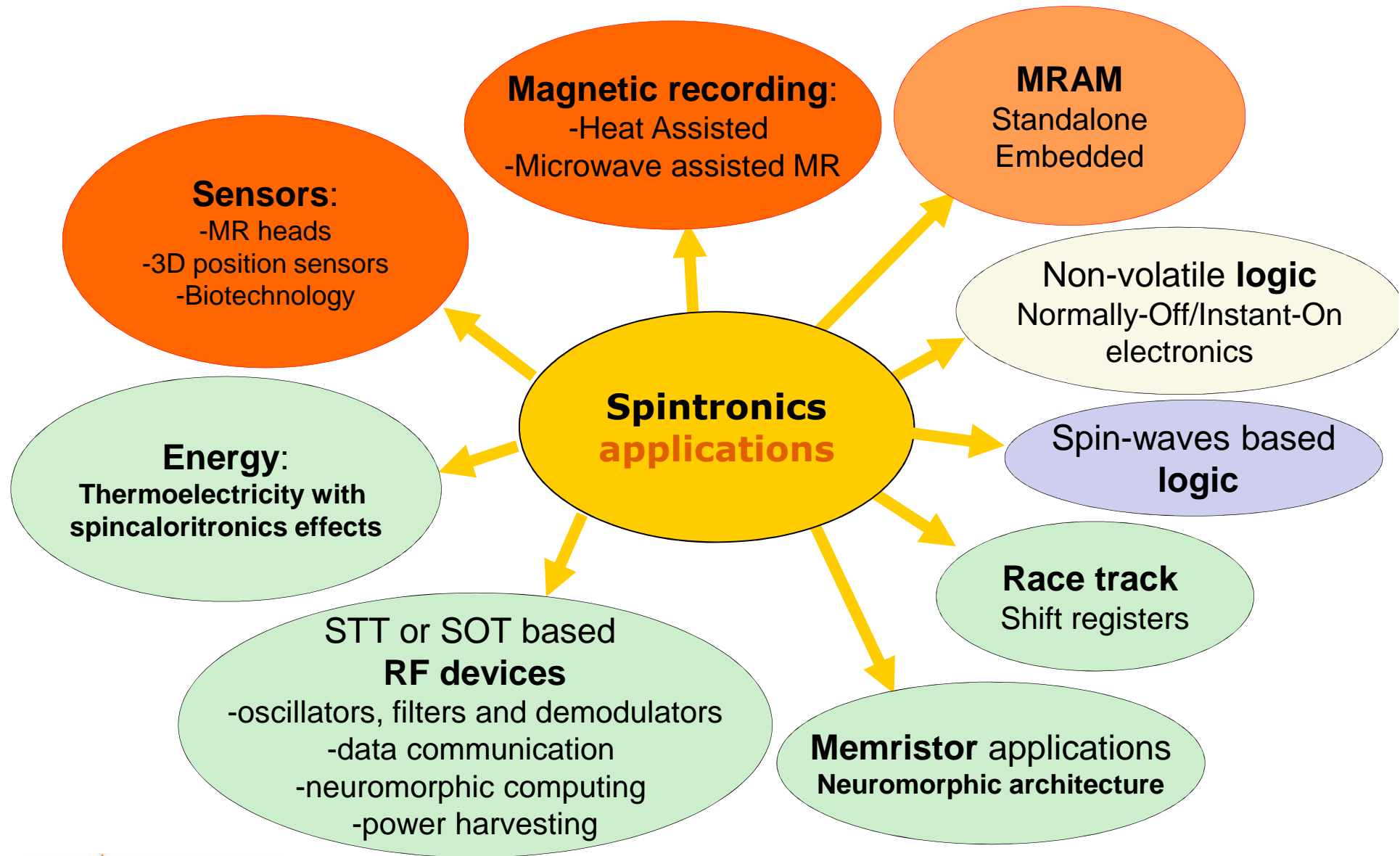
Discover new phenomena taking advantage of the electrons' spin and try to use them in devices having new functionalities or improved performances (higher sensitivity, lower power consumption...etc).

Started in 1988 with the discovery of Giant Magnetoresistance

Spintronics/nanomagnetism broadening spectrum of interest



Spintronics/nanomagnetism broadening spectrum of interest



Spinelectronics: From Basic Phenomena to Applications

OUTLINE

- Part 1 : Basic phenomena in spintronics:
 - Giant Magnetoresistance
 - Tunnel magnetoresistance (TMR)
 - Spin-Transfer Torque (STT)
 - Spin-orbit Torques (SOT)
- Part 2 : Spintronics main applications
 - Magnetic Recording (Hard disk drives Read-heads)
 - MRAMs
 - Magnetic field sensors
 - RF applications

Spinelectronics: From Basic Phenomena to Applications

OUTLINE

- **Part 1 : Basic phenomena in spintronics:**

- **Giant Magnetoresistance**
- Tunnel magnetoresistance (TMR)
- Spin-Transfer Torque (STT)
- Spin-orbit Torques (SOT)

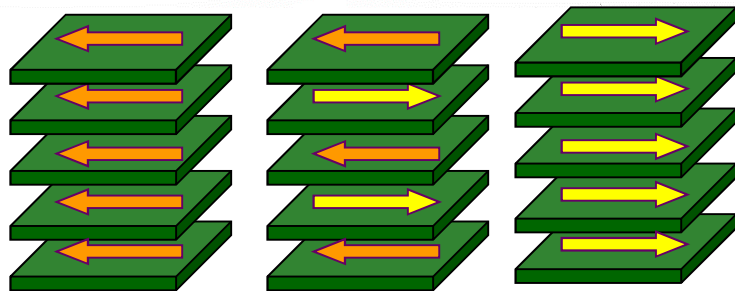
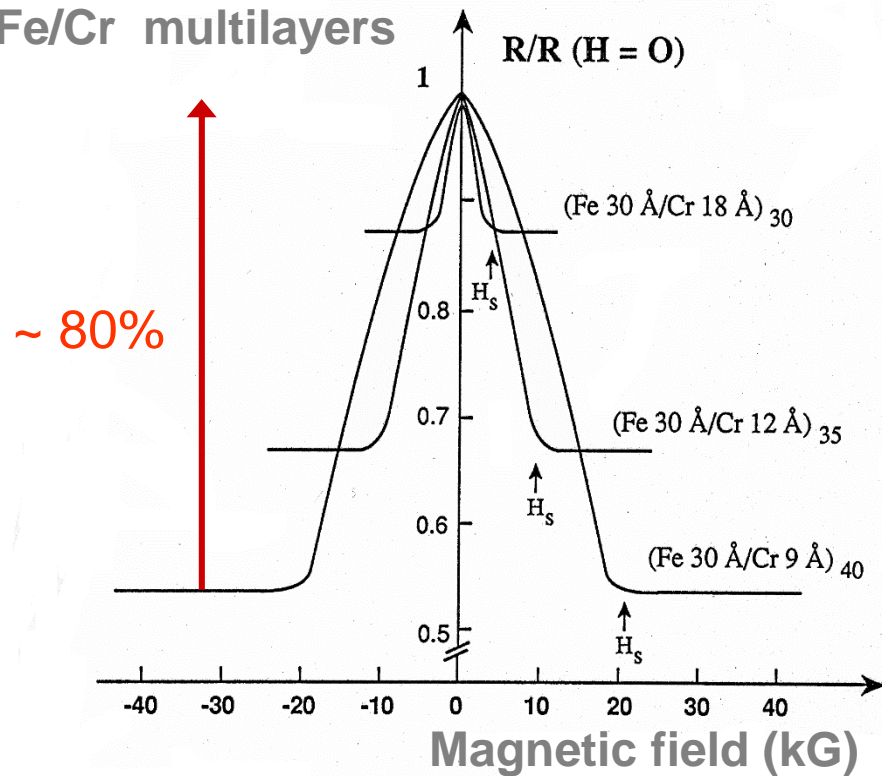
- Part 2 : Spintronics main applications

- Magnetic Recording (Hard disk drives Read-heads)
- MRAMs
- Magnetic field sensors
- RF applications

Giant magnetoresistance (1988)

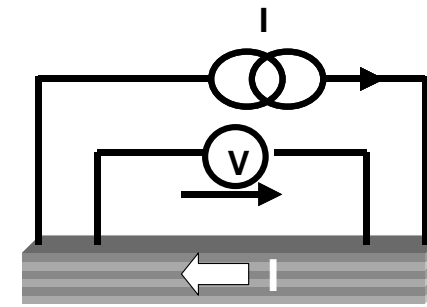
Baibich, M. et al, *Phys.Rev.Lett.*, 61 (1988) 2472.

Fe/Cr multilayers

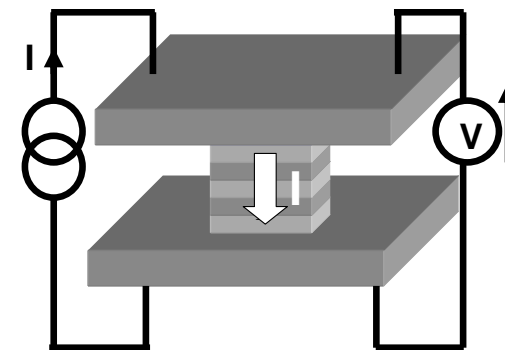


Antiferromagnetically coupled multilayers

Two geometries of measurement:



Current-in-plane



Current-perpendicular-to-plane

$$GMR = \frac{R_{AP} - R_P}{R_P}$$

NOBEL PRIZE IN PHYSICS IN 2007



Photo: U. Montan

Albert Fert



Photo: U. Montan

Peter Grünberg



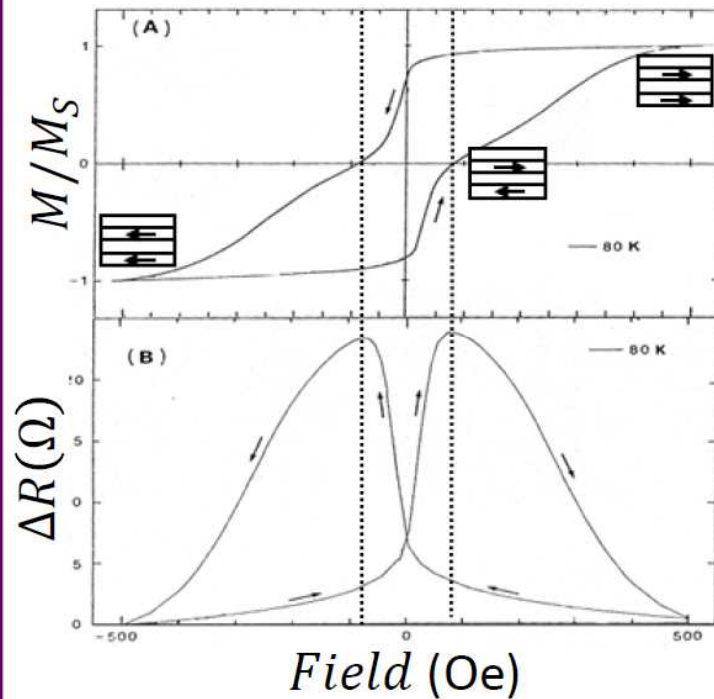
Albert Fert & Peter Grünberg
received the Nobel Prize
from His Majesty King Carl XVI
Gustaf of Sweden
at the Stockholm Concert Hall,
10 December 2007.



Other GMR systems

Multilayers with two different switching fields

(Co 30 Å/Cu 55 Å/NiFe 30 Å)₅

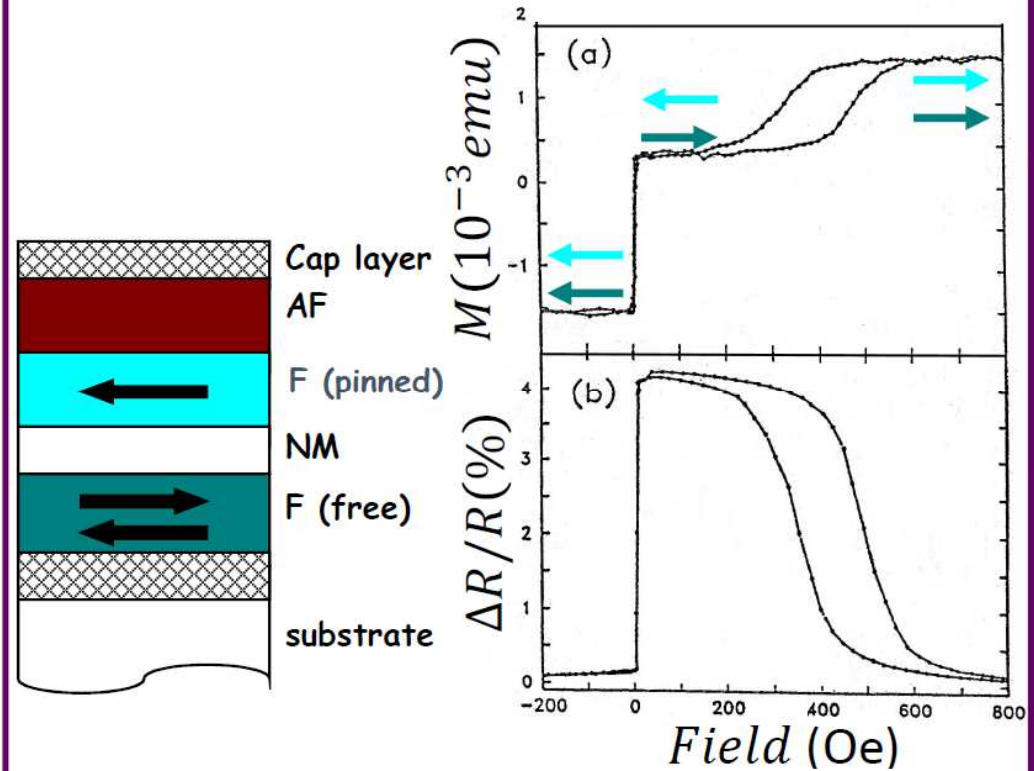


Yamamoto et al., JMMM 1991

Dupas et al, JAP 1990

Spin-valve structures

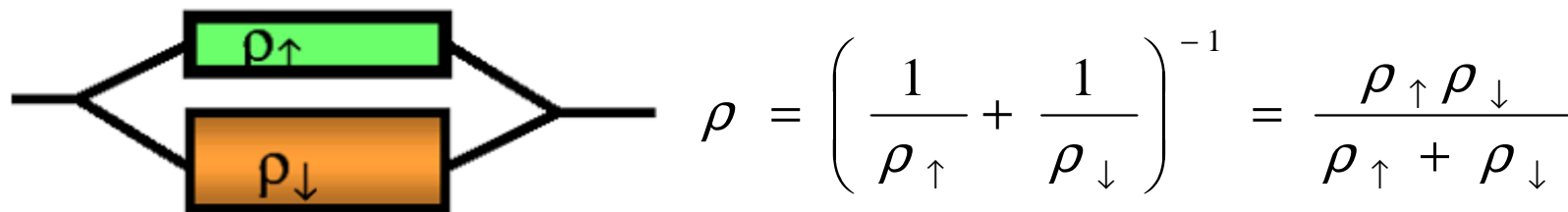
NiFe60Å/Cu22Å/NiFe40Å/FeMn70Å



B.Dieny et al , Phys. Rev.B.(Condensed-Matter) 43 (1991)1297

Two current model (Mott 1930) for transport in magnetic metals

As long as spin-flip is negligible, current can be considered as carried in parallel by two categories of electrons: spin \uparrow and spin \downarrow (parallel and antiparallel to quantization axis)



Sources of spin flip: magnons and spin-orbit scattering

Negligible spin-flip often crude approximation (spin diffusion length in NiFe~4.5nm, 30% spin memory loss at Co/Cu interfaces)

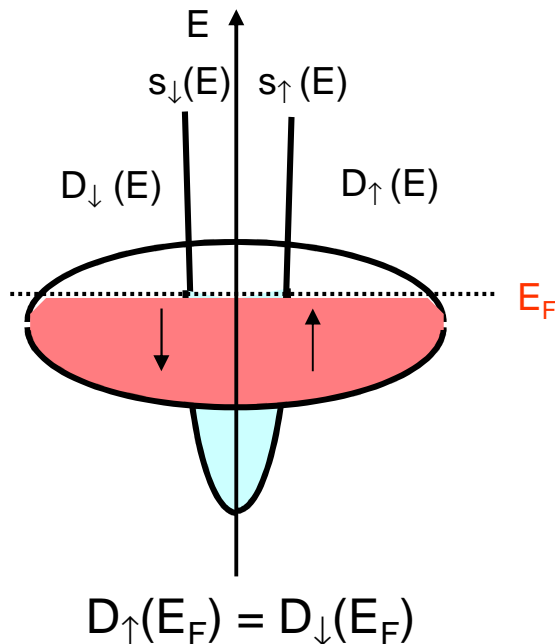
Mott N.F. and H.H.Wills, Proc.Roy.Soc.A156, 368 (1936).

Spin dependent transport in magnetic transition metals (1)

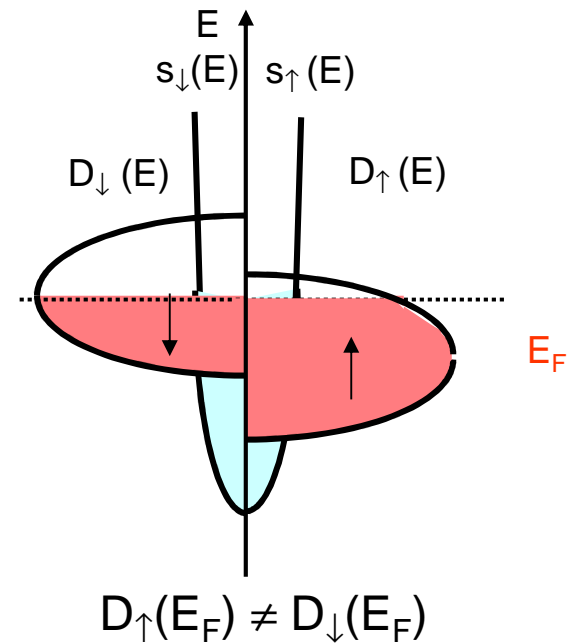
Band structure of 3d transition metals

In transition metals, partially filled bands which participate to conduction are s and d bands

Non-magnetic Cu :



Magnetic Ni :



Most of transport properties are determined by DOS at Fermi energy



Spin-dependent density of state at Fermi energy

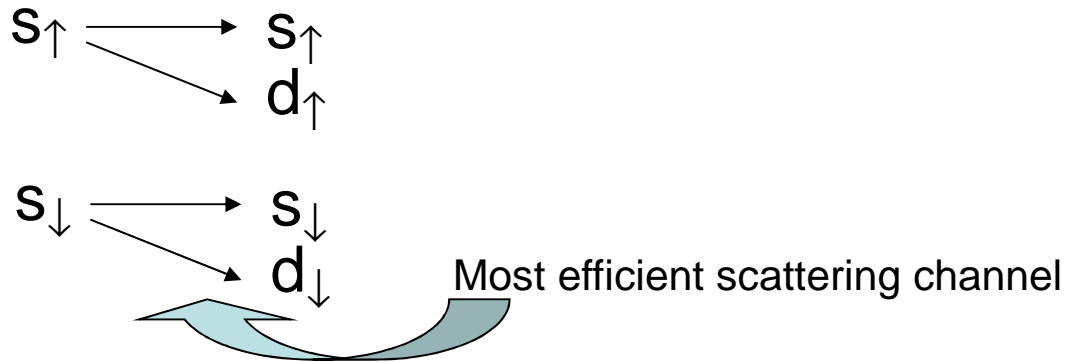
Fert, A., Campbell, I.A., J.Phys.F6, 849 (1976).

Spin dependent transport in magnetic metals (2)

$m^*(d) \gg m^*(s)$  J mostly carried by s electrons in transition metals

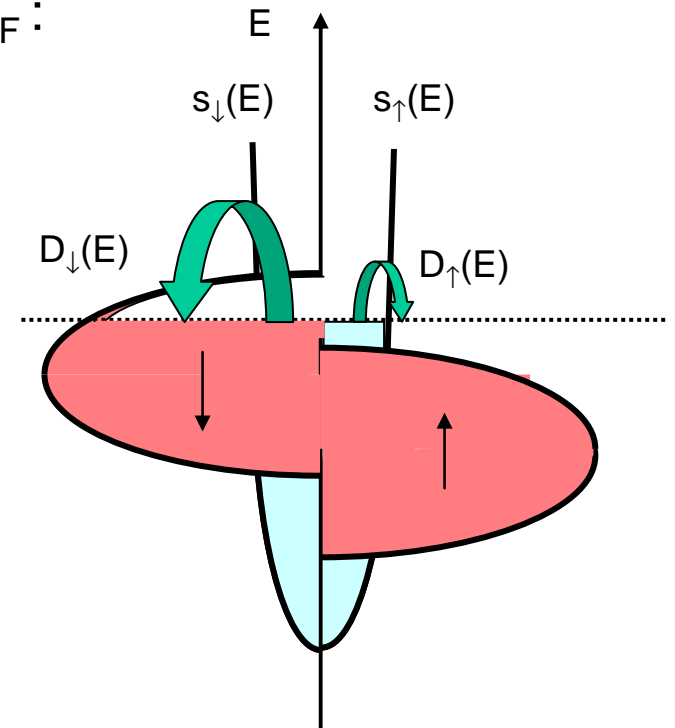
Scattering of electrons determined by DOS at E_F :

Fermi Golden rule : $P^\sigma \propto \langle i|W|f \rangle^2 D_f(E_F)$



Spin-dependent scattering rates in magnetic transition metals

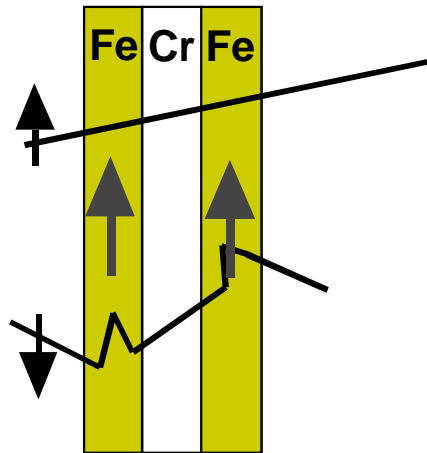
Example: $\lambda_{\uparrow Co} = 10nm$; $\lambda_{\downarrow Co} = 1nm$



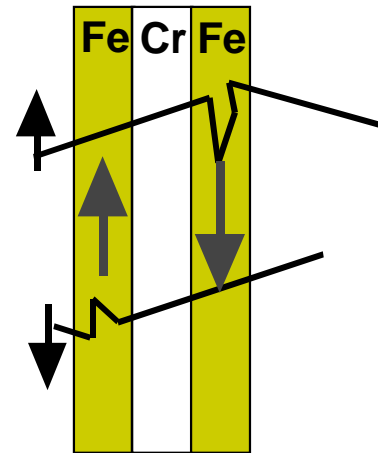
Fert, A., Campbell, I.A., J.Phys.F6, 849 (1976).

Simple model of Giant Magnetoresistance

Parallel config



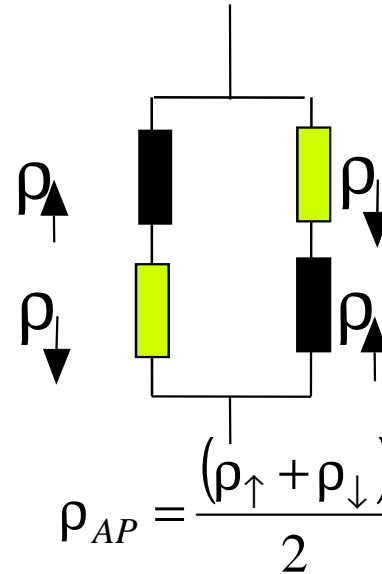
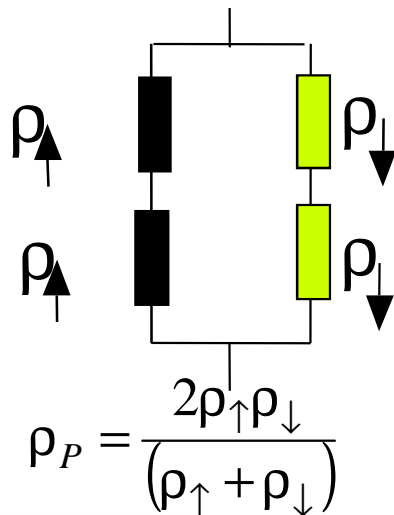
Antiparallel config



Baibich, M. et al,
Phys.Rev.Lett., 61 (1988) 2472.

$$\frac{\Delta\rho}{\rho_{ap}} = \left(\frac{\rho_{\uparrow} - \rho_{\downarrow}}{\rho_{\uparrow} + \rho_{\downarrow}} \right)^2 = \left(\frac{\alpha - 1}{\alpha + 1} \right)^2$$

Equivalent resistances :

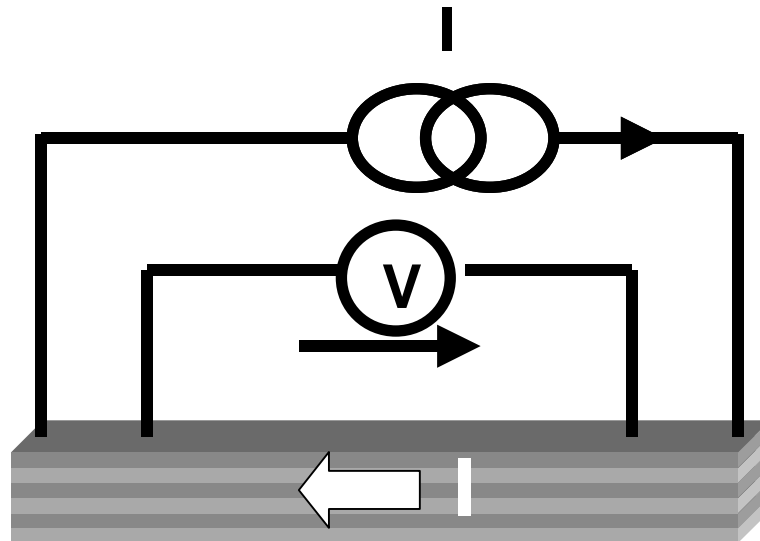


$$\alpha = \frac{\rho_{\uparrow}}{\rho_{\downarrow}}$$

Key role of
scattering contrast α

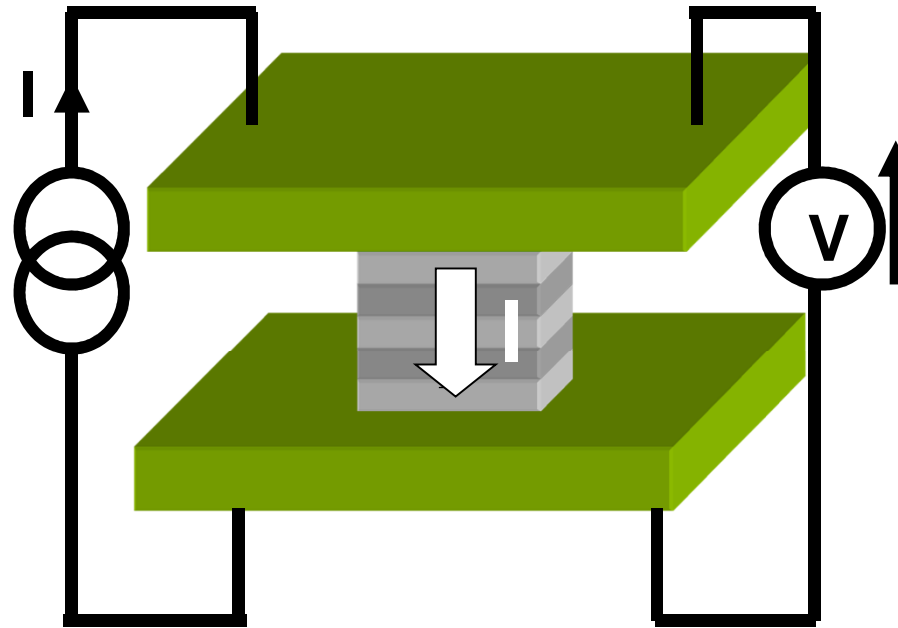
Two configurations of GMR measurement

1) Current in-plane (CIP)



- Straightforward to measure at wafer level, no need for patterning
 - Measured in 4 point probe geometry
- CIP-GMR described by Boltzman formalism
(R. E. Camley and J. Barnaś, *Phys. Rev. Lett.* **63**, 664 (1989))
- Important characteristic lengths : elastic spin-dependent mean free paths
e.g. $\lambda_{NiFe}^{\uparrow} = 7nm$; $\lambda_{NiFe}^{\downarrow} = 1nm$

2) Current Perpendicular to Plane GMR (CPP-GMR)



Much more difficult to measure but richer physics,
Either on macroscopic samples (0.1mm diameter) with superconducting leads
($R \sim \rho \cdot \text{thickness} / \text{area} \sim 10^{-5} \Omega$)
or on patterned microscopic pillars of area $< \mu\text{m}^2$ ($R \sim$ a few Ohms)

Pratt, W.P.Jr, et al, Phys.Rev.Lett. 66 (1991) 3060

Eid, K., Pratt Jr., W.P., and Bass, J. Journ.Appl.Phys.93, 3445 (2003).

Michigan State Univ

Current Perpendicular to Plane GMR

VOLUME 66, NUMBER 23

PHYSICAL REVIEW LETTERS

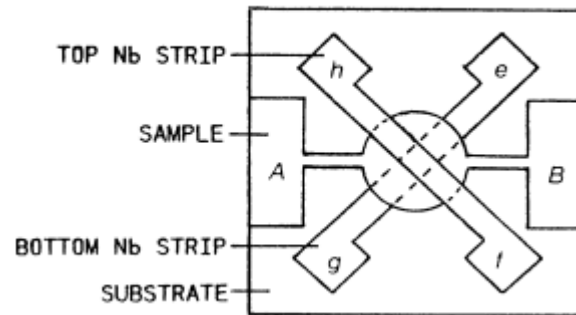
10 JUNE 1991

Perpendicular Giant Magnetoresistances of Ag/Co Multilayers

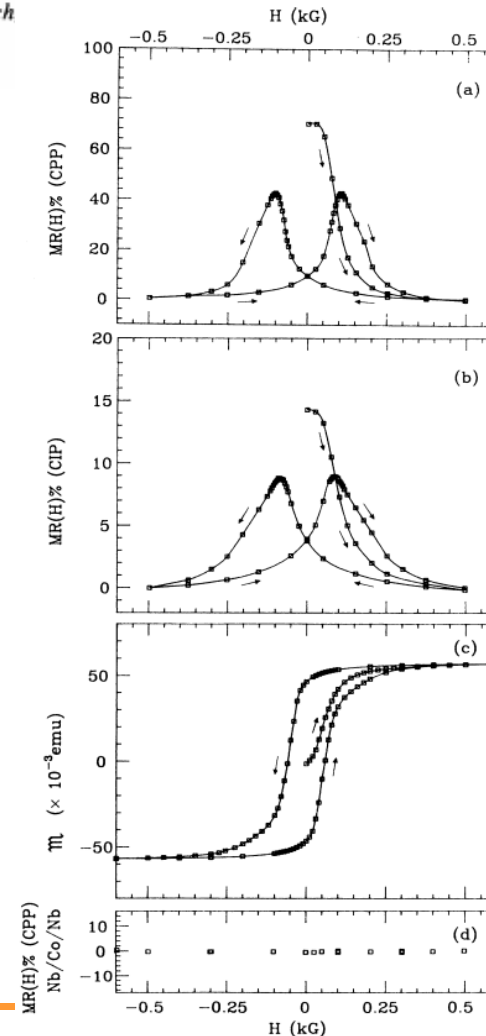
W. P. Pratt, Jr., S.-F. Lee, J. M. Slaughter,^(a) R. Loloee, P. A. Schroeder, and J. Bass

*Department of Physics and Astronomy and Center for Fundamental Materials Research
Michigan State University, East Lansing, Michigan 48824*

(Received 22 January 1991; revised manuscript received 11 April 1991)



Measurement limited at 4K

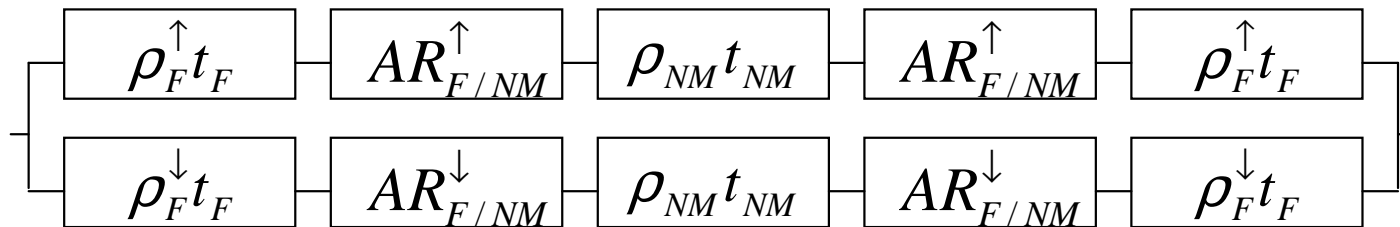


Serial resistance model for CPP-GMR

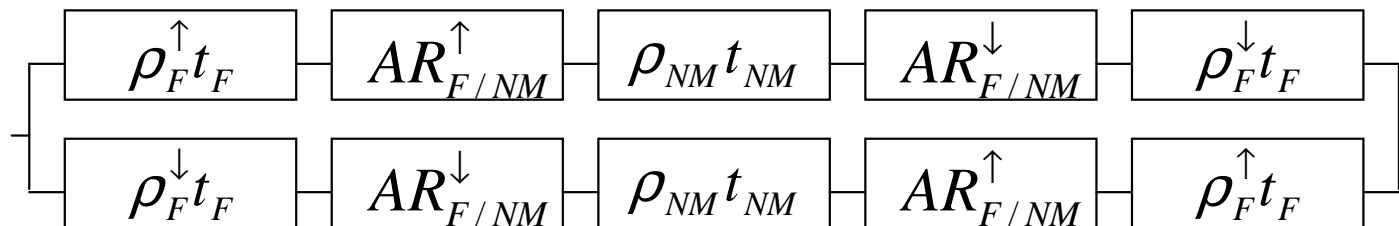
Without spin-film, serial resistance network can be used for CPP transport

CPP transport through F/NM/F sandwich described by:

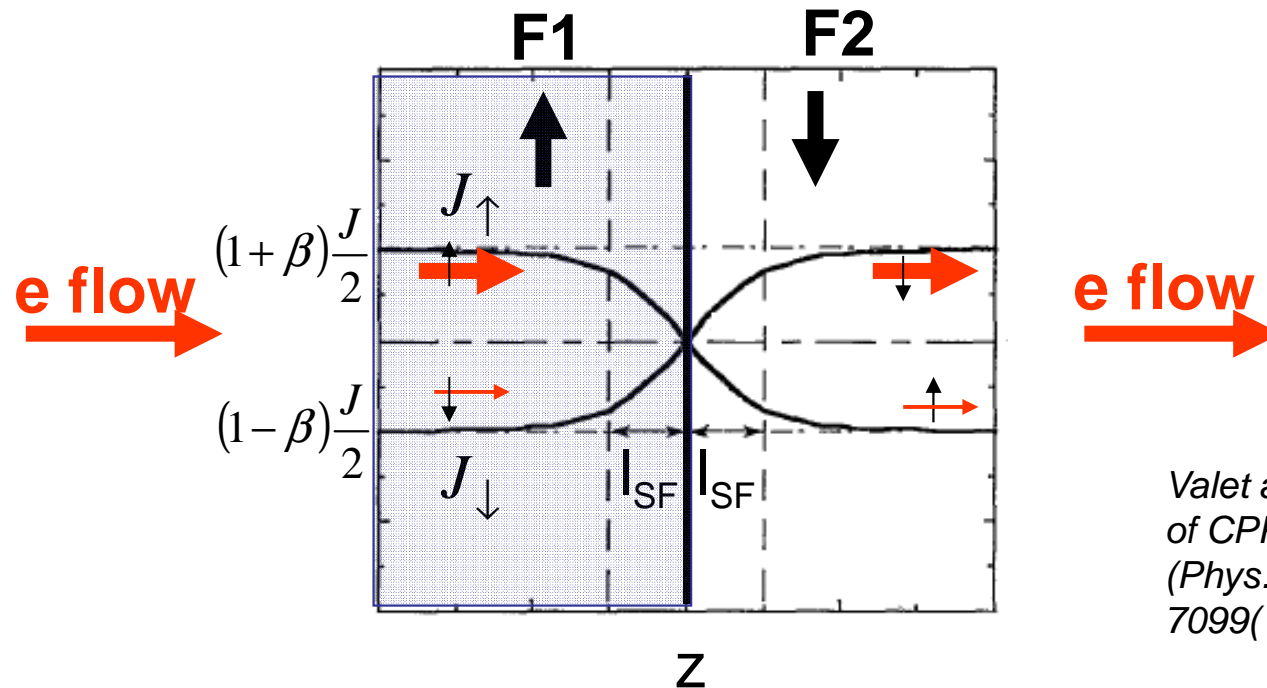
(a) Parallel magnetic configuration :



(b) Antiparallel magnetic configuration :



Spin accumulation – spin relaxation in CPP geometry



*Valet and Fert theory
of CPP-GMR
(Phys.Rev.B48,
7099(1993))*

In F1: Different scattering rates for spin \uparrow and spin \downarrow electrons
 \Rightarrow different spin \uparrow and spin \downarrow currents.
 Larger scattering rates for spin \downarrow : $J_{\uparrow} \gg J_{\downarrow}$ far from the interface.

In F2: Larger scattering rates for spin \uparrow : $J_{\downarrow} \gg J_{\uparrow}$ far from the interface.

Majority of incoming spin \uparrow electrons, majority of outgoing spin \downarrow electrons
 Building up of a spin \uparrow accumulation around the interface balanced in steady state by
 spin-relaxation

Starting point : Valet and Fert theory of CPP-GMR (Phys.Rev.B48, 7099(1993))

μ_σ : spin-dependent chemical potential

In homogeneous material, $\mu = \varepsilon_F - e\phi$

Spin-dependent current driven by $\vec{\nabla}\mu$

$$J_\sigma = \frac{1}{e\rho_\sigma} \frac{\partial \mu_\sigma}{\partial z}$$

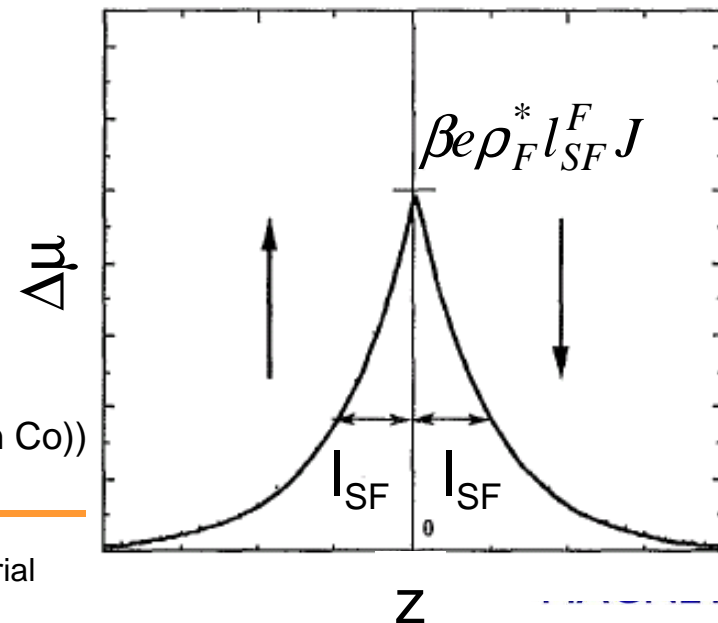
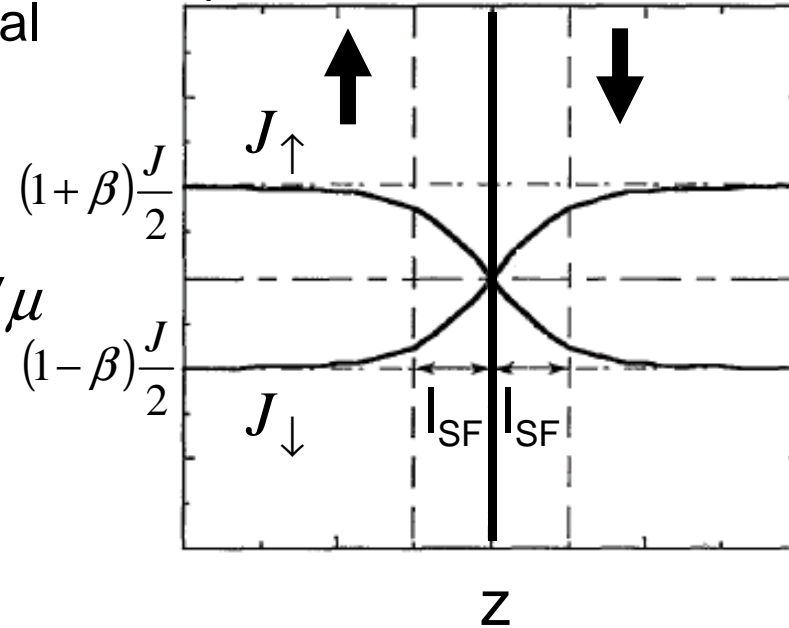
Generalization of Ohm law

Spin relaxation :

$$e\rho_\sigma \frac{\partial J_\sigma}{\partial z} = \frac{\mu_\sigma - \mu_{-\sigma}}{2l_{SF}^2}$$

l_{SF} = spin-diffusion length (~5nm in NiFe, ~20nm in Co))

Spin-relaxation at F \uparrow /F \downarrow interface:



Interfacial boundary conditions

$$\mu_{i+1}^{\uparrow(\downarrow)}(z_{i+1}) - \mu_i^{\uparrow(\downarrow)}(z_{i+1}) = r_{i+1}^{\uparrow(\downarrow)} J_i^{\uparrow(\downarrow)}(z_{i+1}) \quad (\text{Ohm law at interfaces})$$

$$J_{i+1}^{\uparrow(\downarrow)}(z_{i+1}) = J_i^{\uparrow(\downarrow)}(z_{i+1}) \quad (\text{if no interfacial spin-flip is considered})$$

Note: Interfacial spin memory loss can be introduced by :

$$J_{i+1}^{\uparrow(\downarrow)}(z_{i+1}) = \delta J_i^{\uparrow(\downarrow)}(z_{i+1})$$

30% memory loss as at Co/Cu interface yields $\delta=0.7$

Input microscopic transport parameters to describe macroscopic CPP properties :

Within each layer :

- The measured resistivity ρ .
- The scattering asymmetry β .
- The spin diffusion length l_{sf} .

$$\rho_{\uparrow(\downarrow)} = 2\rho^* [1 - (+)\beta]$$

$$\rho_{measured} = \frac{\rho_{\uparrow}\rho_{\downarrow}}{\rho_{\uparrow} + \rho_{\downarrow}} = \rho^* (1 - \beta^2)$$

At each interface :

- The measured interfacial area*resistance product $r_{measured}$
- The interfacial scattering asymmetry γ .

$$r_{\uparrow(\downarrow)} = 2r^* [1 - (+)\gamma]$$

$$r_{measured} = \frac{r_{\uparrow}r_{\downarrow}}{r_{\uparrow} + r_{\downarrow}} = r^* (1 - \gamma^2)$$

Examples of bulk parameters

Material	Measured resistivity 4K/300K	β Bulk scattering asymmetry	l_{SF}
Cu	0.5-0.7 $\mu\Omega$.cm 3-5	0 0	500nm 50-200nm
Au	2 $\mu\Omega$.cm 8	0 0	35nm 25nm
$Ni_{80}Fe_{20}$	10-15 22-25	0.73-0.76 0.70	5.5 4.5
$Ni_{66}Fe_{13}Co_{21}$	9-13 20-23	0.82 0.75	5.5 4.5
Co	4.1-6.45 12-16	0.27 – 0.38 0.22-0.35	60 25
$Co_{90}Fe_{10}$	6-9 13-18	0.6 0.55	55 20
$Co_{50}Fe_{50}$	7-10 15-20	0.6 0.62	50 15
$Pt_{50}Mn_{50}$	160 180	0 0	1 1
Ru	9.5-11 14-20	0 0	14 12

Review on
CPP-GMR:
Bass, JMMM 408 (2016)
244–320



Examples of interfacial parameters

Material	Measured R.A interfacial resistance	γ Interfacial scattering assymetry
Co/Cu	0.21 m Ω . μm^2 0.21-0.6	0.77 0.7
Co ₉₀ Fe ₁₀ /Cu	0.25-0.7 0.25-0.7	0.77 0.7
Co ₅₀ Fe ₅₀ /Cu	0.45-1 0.45-1	0.77 0.7
NiFe/Cu	0.255 0.25	0.7 0.63
NiFe/Co	0.04 0.04	0.7 0.7
Co/Ru	0.48 0.4	-0.2 -0.2
Co/Ag	0.16 0.16	0.85 0.80

Review on
CPP-GMR:
Bass, JMMM 408 (2016) 244–320

Spinelectronics: From Basic Phenomena to Applications

OUTLINE

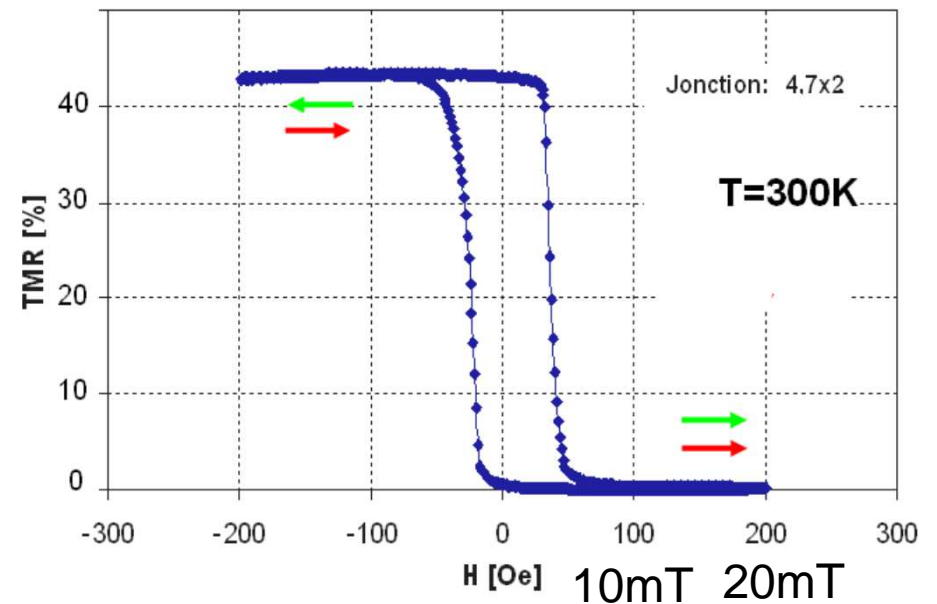
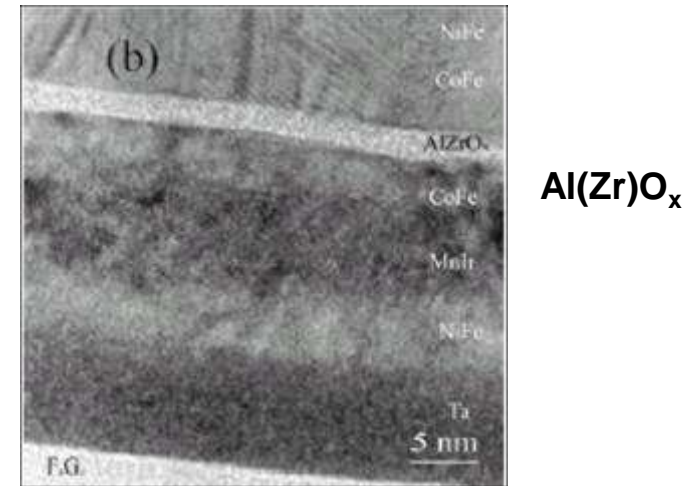
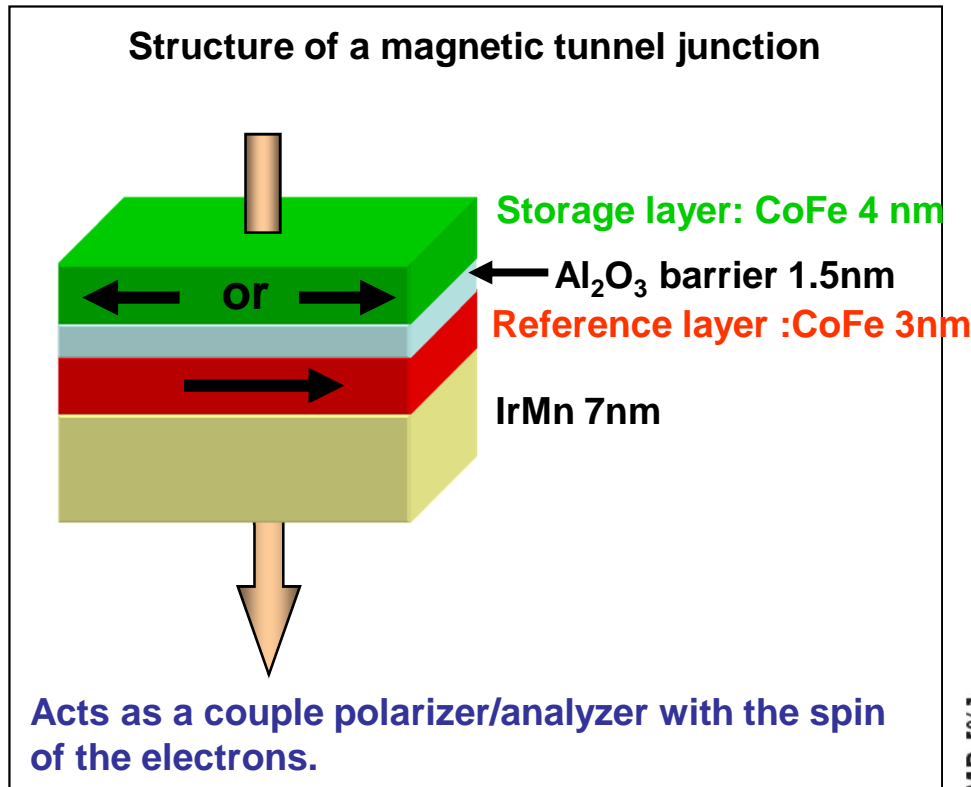
- **Part 1 : Basic phenomena in spintronics:**

- Giant Magnetoresistance
- **Tunnel magnetoresistance (TMR)**
- Spin-Transfer Torque (STT)
- Spin-orbit Torques (SOT)

- Part 2 : Spintronics main applications

- Magnetic Recording (Hard disk drives Read-heads)
- MRAMs
- Magnetic field sensors
- RF applications

Magnetic tunnel junctions – Tunnel magnetoresistance



- First observation of TMR at low T in MTJ:

Julliere (1975) (Fe/Ge/Co)

- TMR at 300K :

Moodera *et al*, PRL (1995);

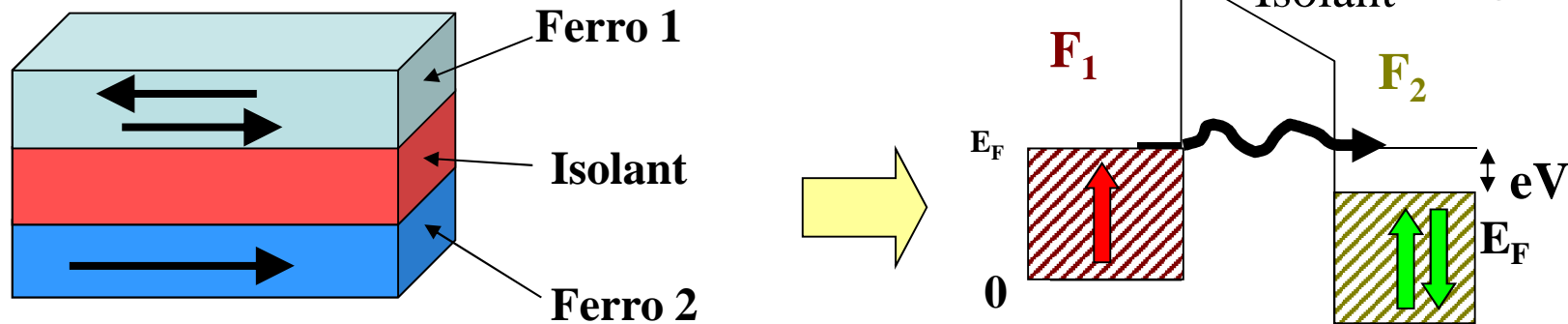
Myazaki *et al*, JMMM(1995).

in AlO_x based junctions

$$\Delta R/R \sim 50\%$$

Julliere model of tunnel magnetoresistance (TMR)

Jullière, Phys. Lett. A54 225 (1975)



Fermi Golden rule: proba of tunneling $P^\sigma \propto \langle i|W|f \rangle^2 D_2(E_F)$

Nb of electrons candidate for tunneling $\propto D_1(E_F)$

\Rightarrow tunneling current in each spin channel $J^\sigma \propto D_1^\sigma(E_F) \times D_2^\sigma(E_F)$

Parallel configuration

$$J^{parallel} \propto D_1^\uparrow D_2^\uparrow + D_1^\downarrow D_2^\downarrow$$

Antiparallel configuration

$$J^{antiparallel} \propto D_1^\uparrow D_2^\downarrow + D_1^\downarrow D_2^\uparrow$$

$$P = \frac{D^\uparrow(E_F) - D^\downarrow(E_F)}{D^\uparrow(E_F) + D^\downarrow(E_F)}$$

$$TMR = \frac{\Delta R}{R_P} = \frac{2 P_1 P_2}{1 - P_1 P_2}$$

$$TMR = \frac{\Delta R}{R_{AP}} = \frac{2 P_1 P_2}{1 + P_1 P_2}$$

P~50% in Fe, Co

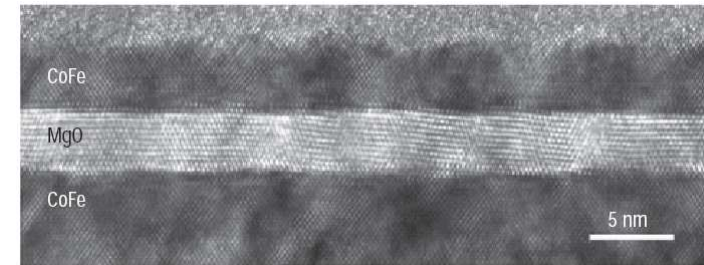
$\Delta R/R \sim 40 - 70\%$ with alumina barriers

Giant TMR of MgO tunnel barriers

S.S.P.Parkin et al, Nature Mat. (2004), nmat1256.

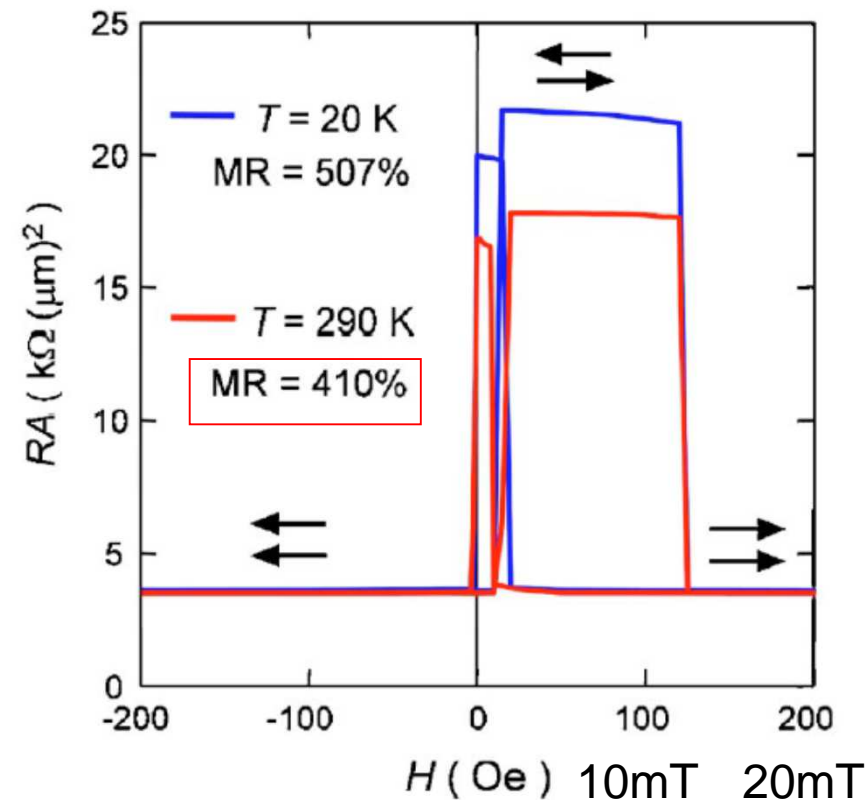
S.Yuasa et al, Nature Mat. (2004), nmat 1257.

Very well textured MgO barriers grown by sputtering or MBE on bcc CoFe or Fe magnetic electrodes, or on amorphous CoFeB electrodes followed by annealing to recrystallize the electrode.



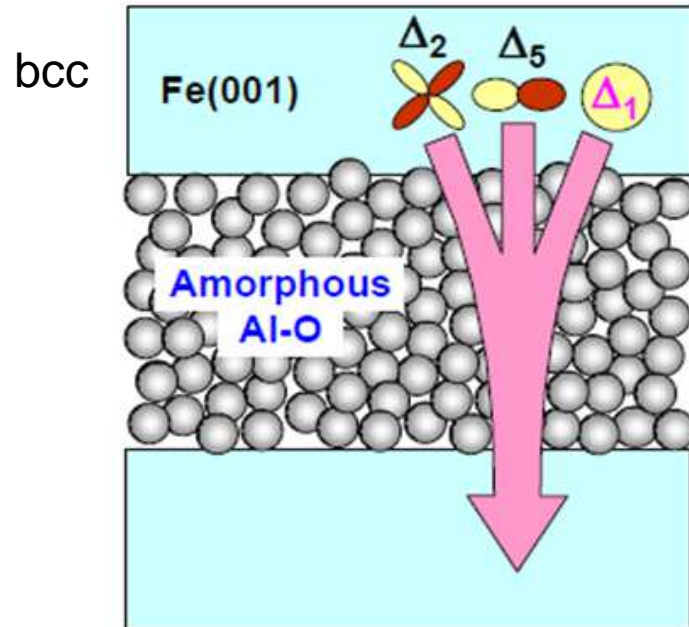
Au cap 50 nm
Ir-Mn 10 nm
Fe(001) 10 nm
Co(001) 0.57 nm
MgO(001) 2.2 nm
Co(001) 0.57 nm
Fe(001) 100 nm
MgO(001) 20 nm
MgO(001) sub.

Yuasa et al, APL89, 042505(2006)

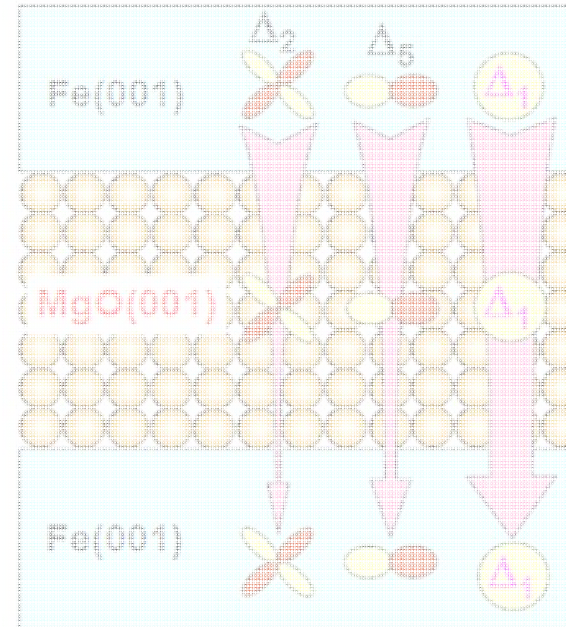


Amorphous barrier Vs Crystalline barrier

Amorphous barrier
ex: amorphous AlO



Crystalline barrier
ex: MgO(001)



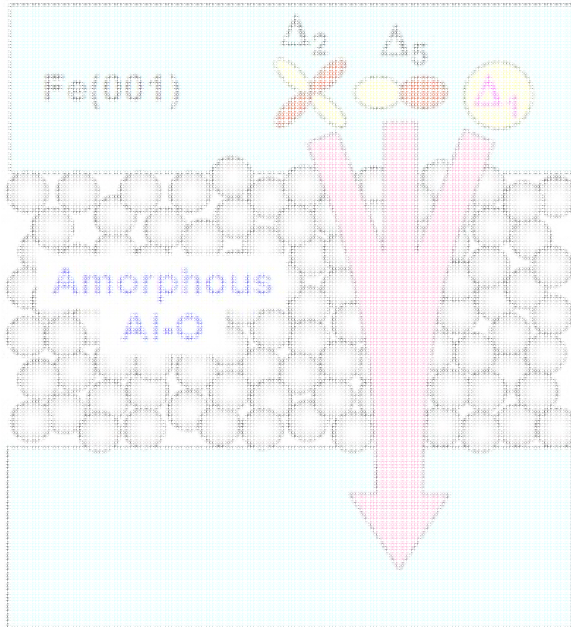
No crystallographic symmetry in the barrier:

- Incoherent tunneling: Bloch states are not conserved during tunneling.
- Every electron symmetry contributes equally to the tunneling process.
- Observed TMR < 100% @RT

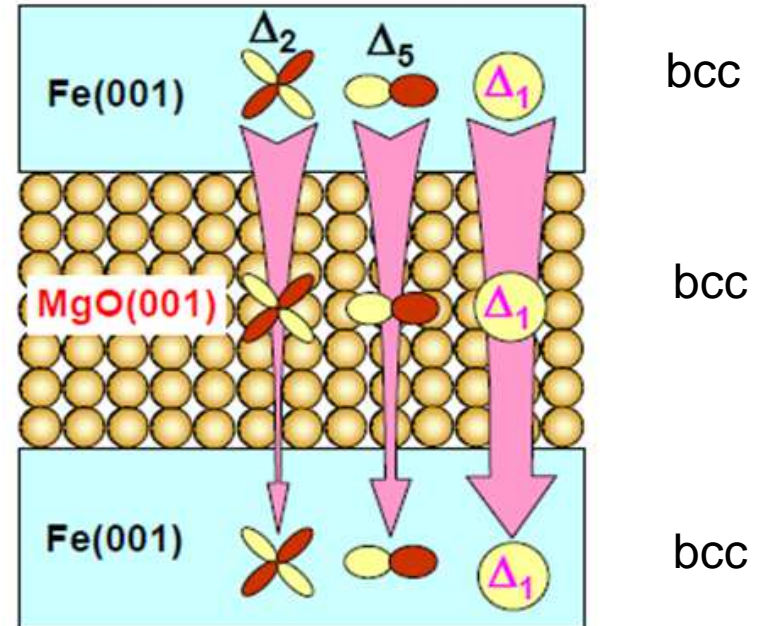
Butler et al., PRB 2001 ; Khvalkovskiy et al., J. Phys. D Appl. Phys 2013

Amorphous barrier Vs Crystalline barrier

Amorphous barrier
ex: amorphous AlO



Crystalline barrier
ex: MgO(001)

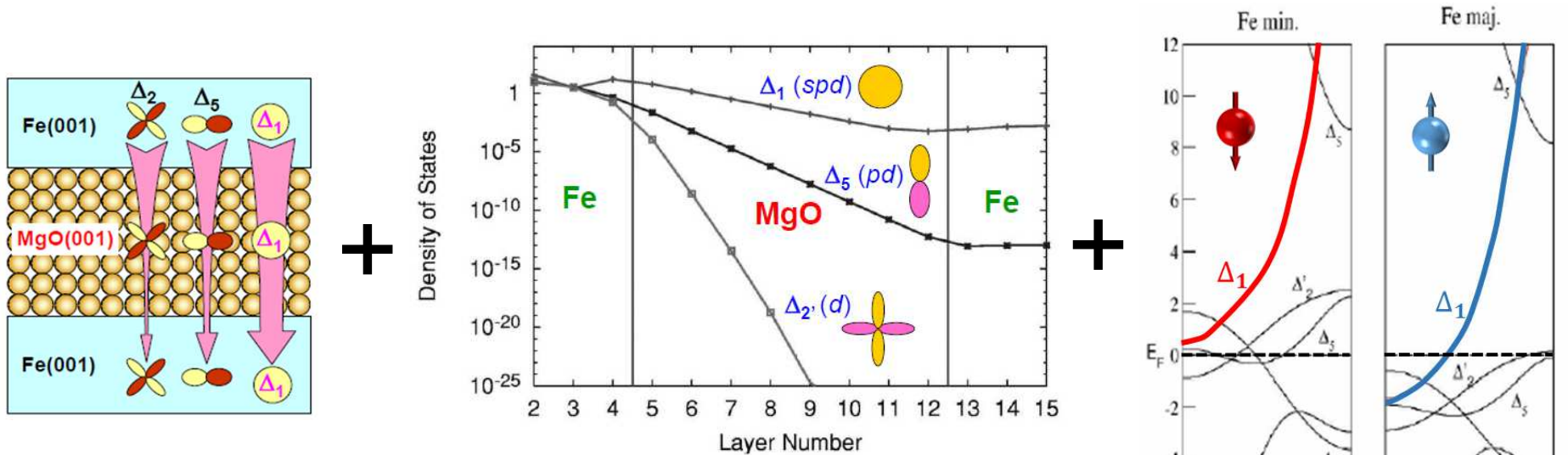


Epitaxially grown crystalline barrier:

- Coherent tunneling: the electrons' wave-functions in the FM are coupled with evanescent wave-functions having the same symmetry in the barrier.
- Tunneling probability of e^- strongly depends on its orbital symmetry
→ possible effective symmetry filtering of the tunneling current.

Butler et al., PRB 2001 ; Khvalkovskiy et al., J. Phys. D Appl. Phys 2013

Crystalline barrier – The example of Fe/MgO/Fe

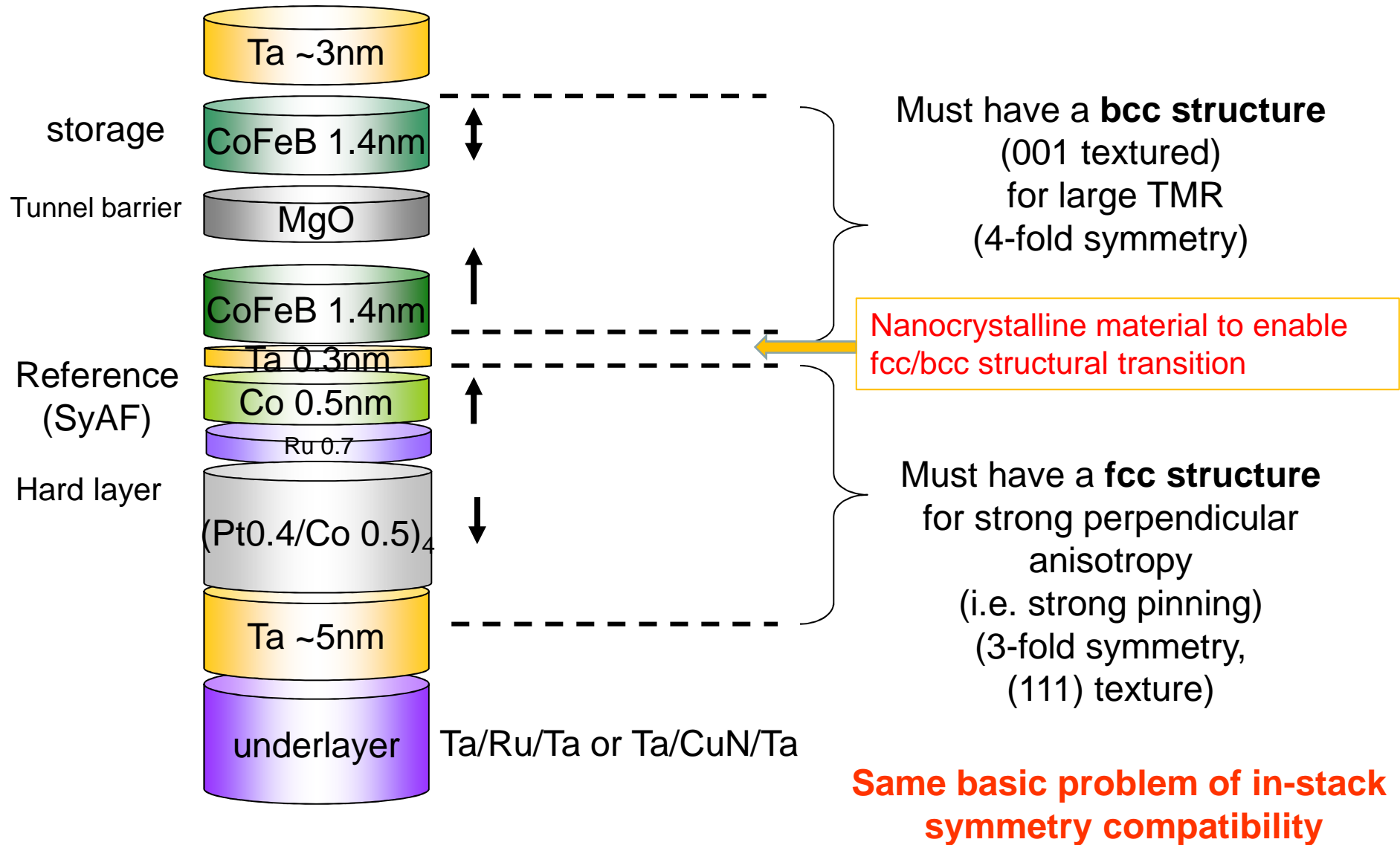


- Exponential tunneling decay is much stronger for Δ_2 and Δ_5 states than for Δ_1 states
- Both majority and minority Δ_2 and Δ_5 symmetry states can be found at the Fermi level \rightarrow low P.
- Only majority electrons fill Δ_1 symmetry states, implying a full polarization $P_{\Delta_1} = 100\%$.

\Rightarrow *Spin filtering* of the wave functions : large values of TMR expected in epitaxial or highly textured structures (TMR>1000% @RT).

Butler et al., PRB 2001 ; Khvalkovskiy et al., J. Phys. D Appl. Phys 2013

Standard out-of-plane MTJ stack

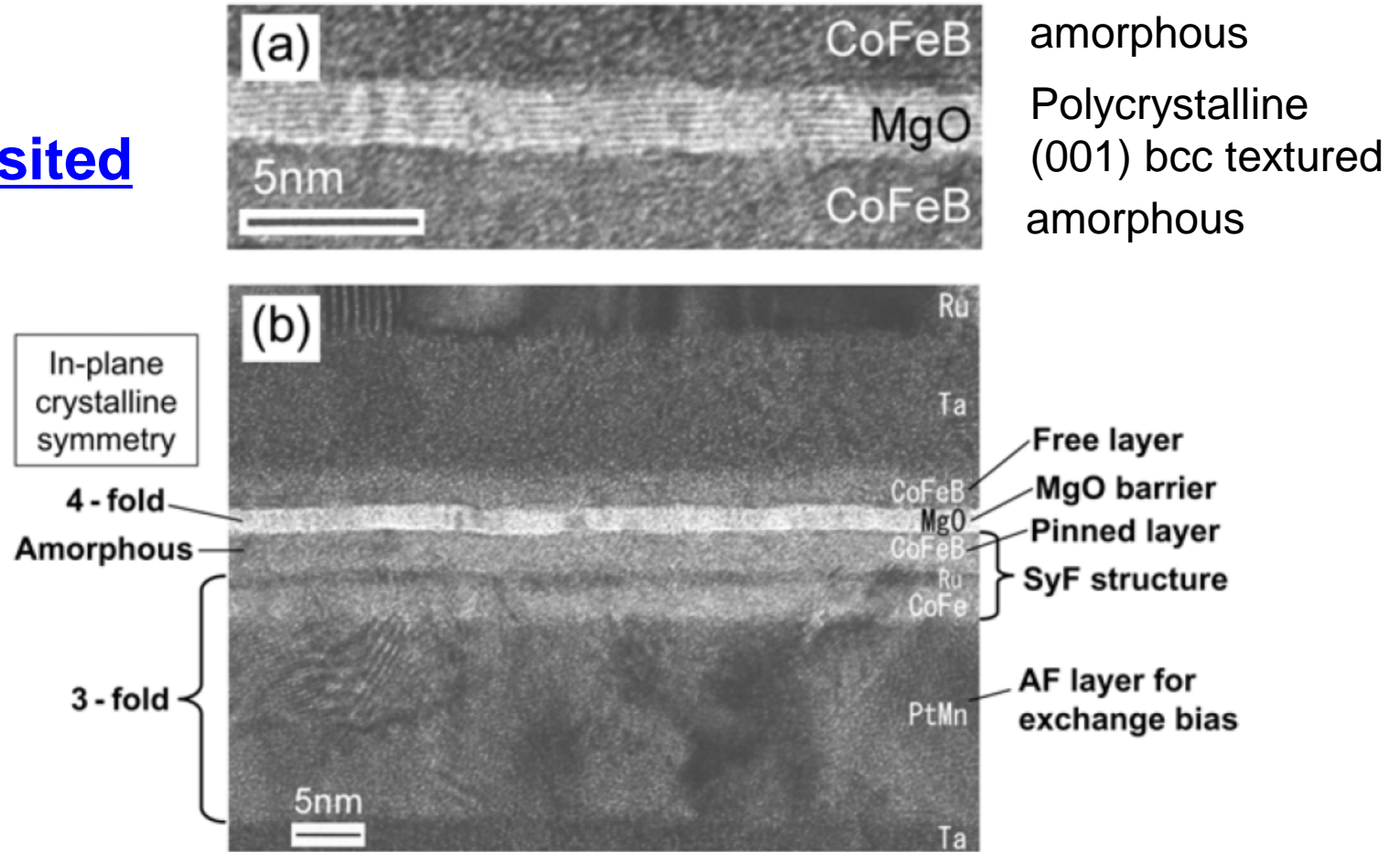


Growth and annealing of the tunnel barrier

Djayaprawira D D et al, *Appl. Phys. Lett.* 86 092502 (2005)

Problem of symmetry compatibility solved by using amorphous CoFeB electrodes during growth

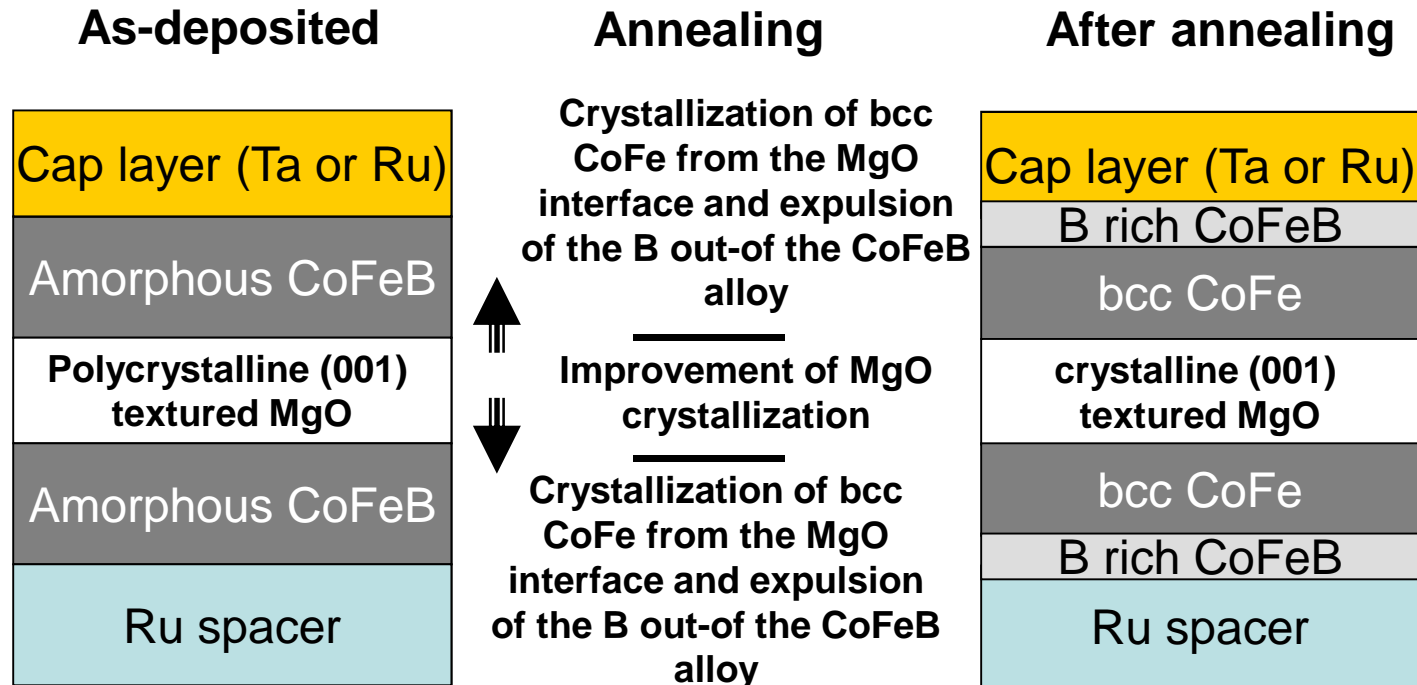
As-deposited



Annealing of the magnetic tunnel junction

Annealing at $T_{\text{anneal}} \sim 300^\circ\text{C} - 400^\circ\text{C}$.

The higher T_{anneal} , the better from the barrier formation standpoint

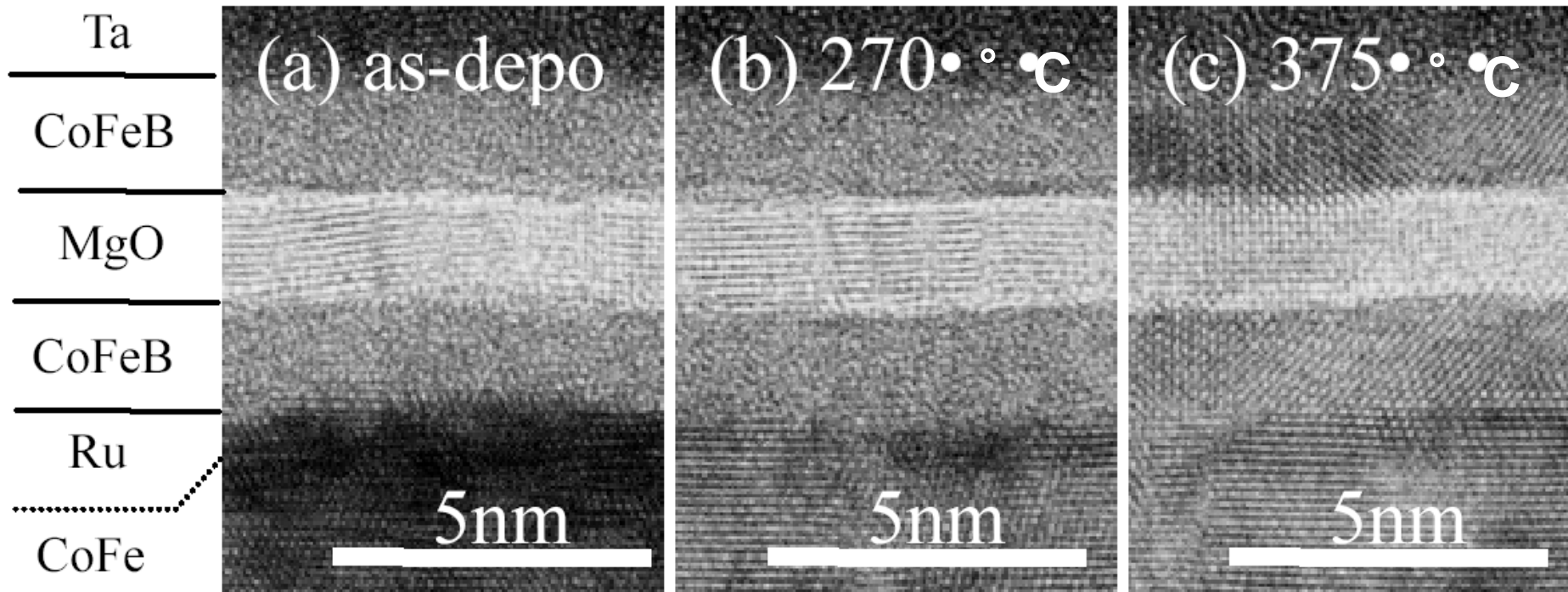


- Important to attract B away from the tunnel barrier during the crystallization process. Choose materials which are **good B getters** on the opposite side of the free (storage) and reference layers (**Ta, Ru, W, Mo, Nb, Zr, Hf,...**).

Magnetic tunnel junctions based on MgO tunnel barriers

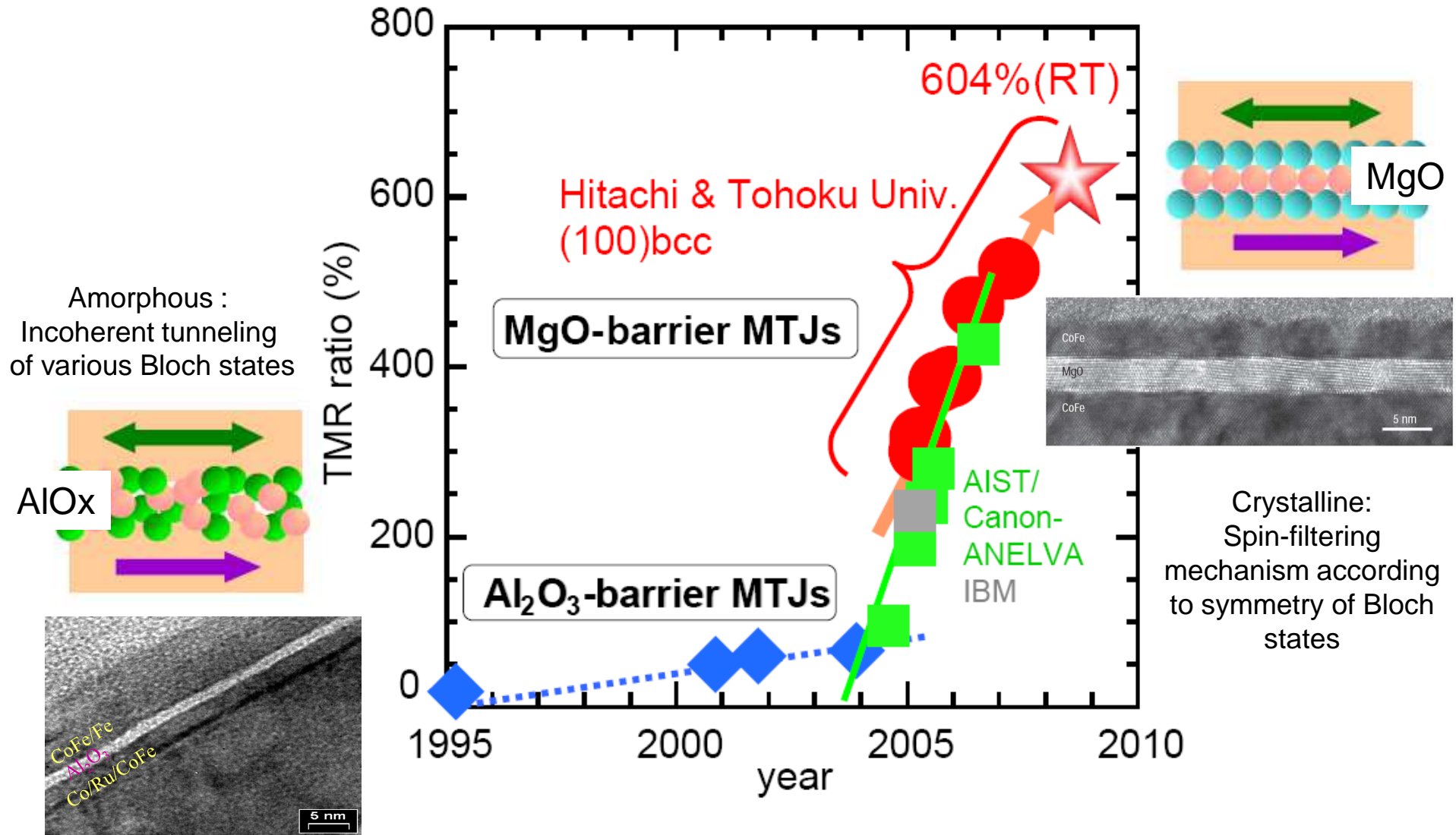
- As-deposited, CoFeB amorphous, MgO polycrystalline
- Upon annealing, recrystallization of CoFeB from the MgO interfaces and improvement in MgO crystallinity with (100) bcc texture

J. Hayakawa et al. Jap. J. Appl. Physics 2005



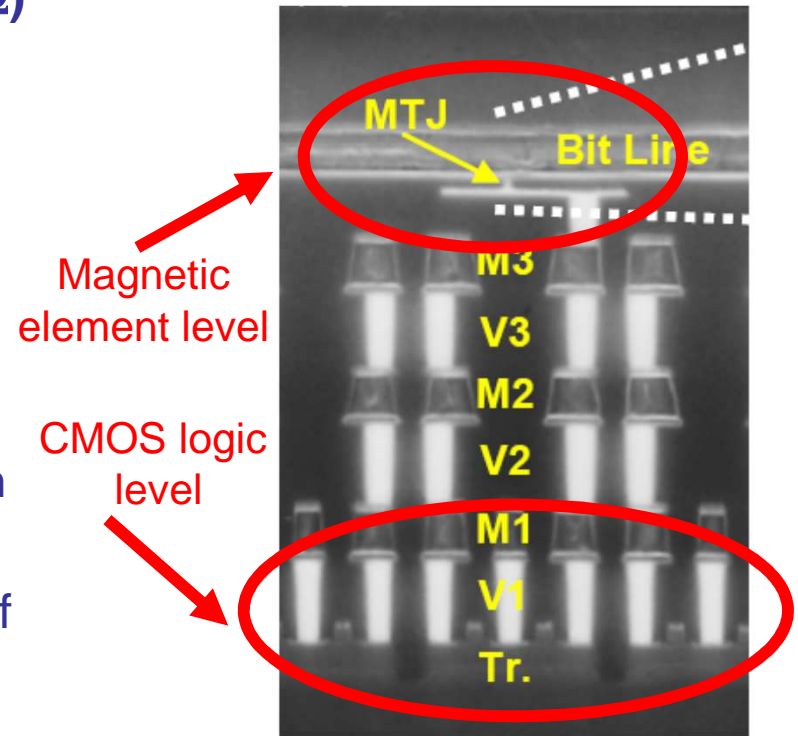
Also, Yuasa et al. Applied Physics Letters, 2005

Giant TMR of MgO tunnel barriers



MTJ : a reliable path for CMOS/magnetic 3D integration

- Resistance compatible with CMOS (cell R ~ k Ω)
- MTJ used as a variable resistance driven by field or current/voltage.
- MTJ can be deposited at any metallic level in the CMOS technology in replacement of a via.
- Above IC technology ('end-of-back-end' process)
- Front-end contamination under control
- Low-T BE process (250°C-350°C) compatible with Cu interconnect process
- Easy / cheap to embed (3 add-masks, no trade-off with logic process)



Rapid progress in technology maturity thanks to the involvement of major IDM and equipment manufacturers.

No CMOS contamination during the integration

Etching of MTJ remains the main difficulty at advanced nodes

More and more fabs now enabled with 200/300mm magnetic BEOL lines

Spinelectronics: From Basic Phenomena to Applications

OUTLINE

- **Part 1 : Basic phenomena in spintronics:**

- Giant Magnetoresistance
- Tunnel magnetoresistance (TMR)
- **Spin-Transfer Torque (STT)**
- Spin-orbit Torques (SOT)

- Part 2 : Spintronics main applications

- Magnetic Recording (Hard disk drives Read-heads)
- MRAMs
- Magnetic field sensors
- RF applications

Spin-Transfer Torque (STT)

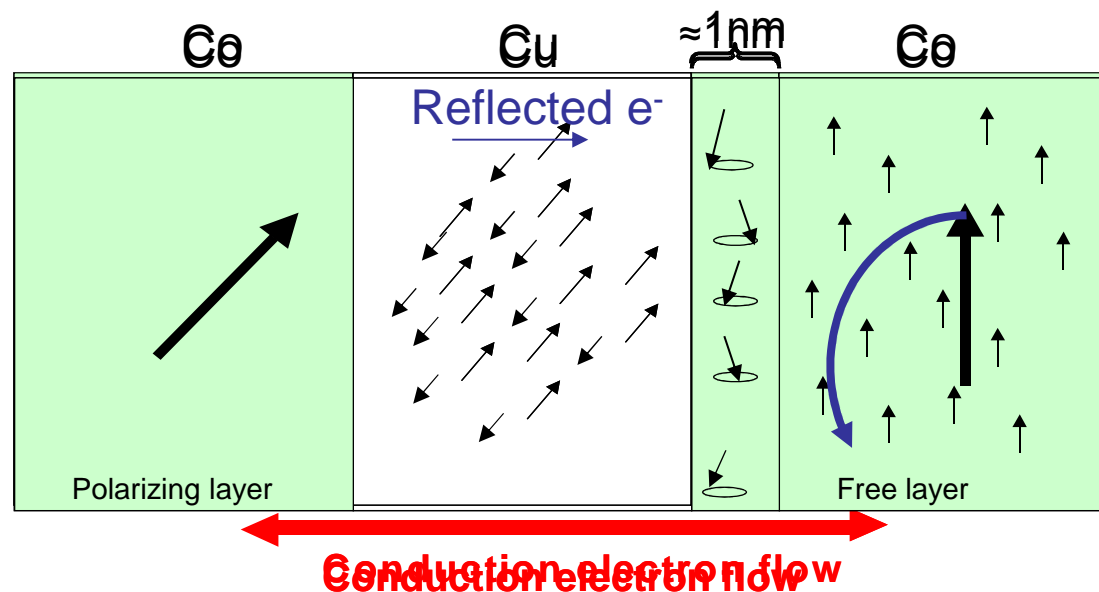
Predicted by Slonczewski (JMMM.159, L1(1996)) and Berger (Phys.Rev.B54, 9359 (1996))

Giant or Tunnel magnetoresistance:

Acting on electrical current via the magnetization orientation

Spin transfer is the reciprocal effect:

Acting on the magnetization via the spin polarized current

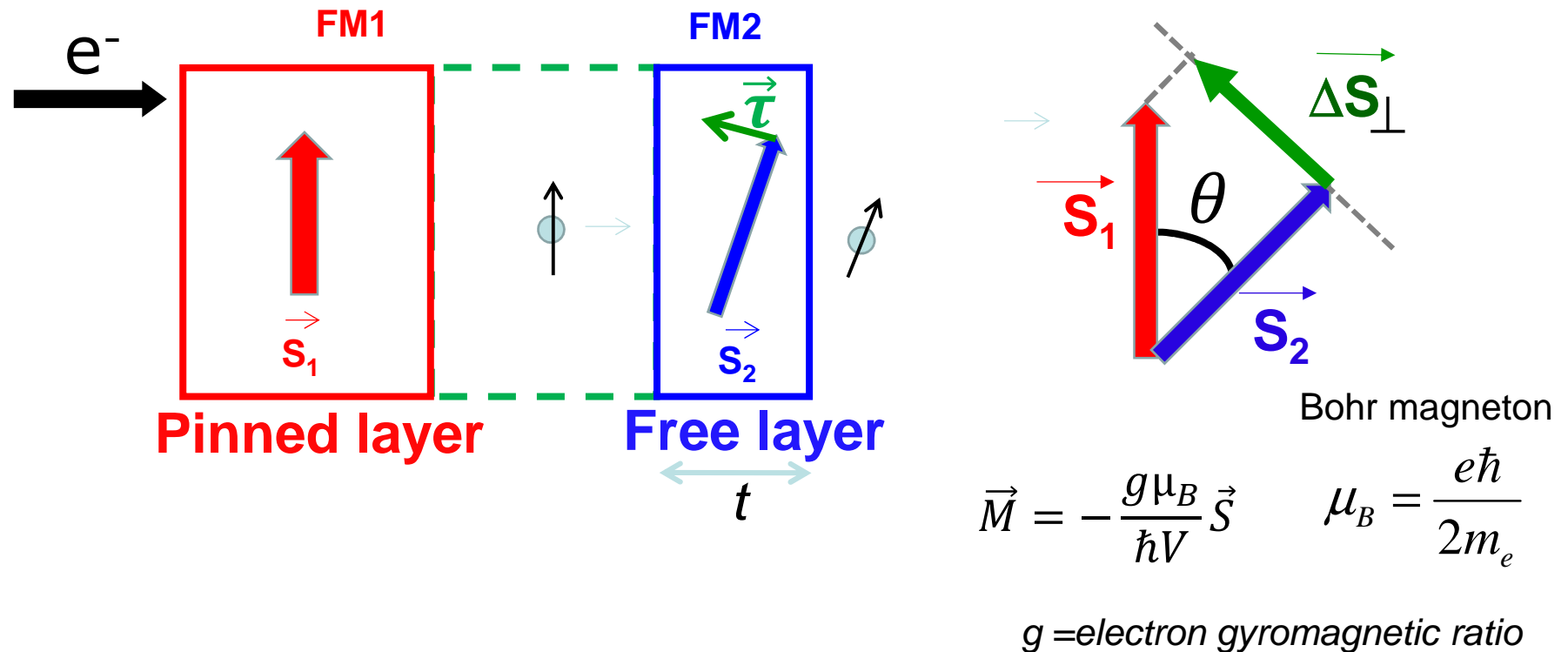


*M.D. Stiles et al,
Phys.Rev.B.66,
014407 (2002)*

Reorientation of spin polarization \Rightarrow **Torque on the free layer magnetization**

A new way to manipulate the magnetization of magnetic nanostructures

Classical expression of the Spin Transfer torque



- ✓ The whole transverse part of spin current is absorbed next to the interface
- ✓ Incident spin direction is aligned along the magnetization of the pinned layer FM₁

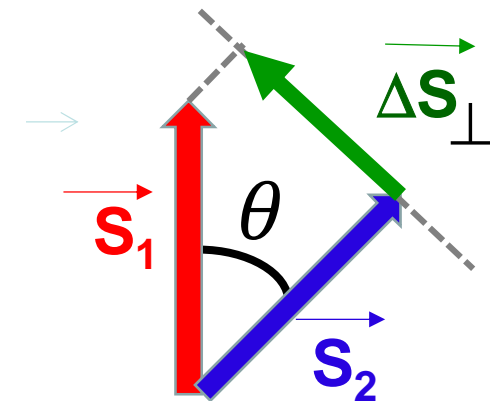
➤ Torque acting on the magnetization of FM₂ ?

Classical expression of the Spin Transfer torque

$$\vec{\tau}_{STT} = \frac{d\vec{M}_2}{dt} \propto \text{absorbed transverse spin current}$$

- ✓ Transverse spin component for one incoming electron :

$$\left. \begin{array}{l} |\Delta S_{\perp}| = S \sin(\theta) \\ \Delta S_{\perp} \perp \vec{S}_2 \end{array} \right\} \Rightarrow \vec{\Delta S}_{\perp} = \frac{\hbar}{2} \vec{m}_2 \times (\vec{m}_2 \times \vec{m}_1)$$



- ✓ Contribution to magnetization: $\vec{\Delta M} = -\frac{g\mu_B}{\hbar V} \vec{\Delta S}$

- ✓ Volume : $V = \mathcal{A} \cdot t = \text{Area} \cdot \text{thickness}$

- ✓ Number of incoming electrons per second :

$$\frac{dN_{e^-}}{dt} = \frac{I}{e} = \frac{J \cdot \mathcal{A}}{e}$$

- ✓ Number of incoming spins per second :

$$\frac{dN_S}{dt} = P_{spin} \frac{J \cdot \mathcal{A}}{e}$$

$$\frac{d\vec{M}_2}{dt} = -P_{spin} \frac{J \mathcal{A}}{e} \frac{g\mu_B}{\hbar \mathcal{A} t} \frac{\hbar}{2} (\vec{m}_2 \times (\vec{m}_2 \times \vec{m}_1))$$

$$\vec{m}_{1(2)} = \frac{\vec{M}_{1(2)}}{\|\vec{M}_{1(2)}\|}$$

$$\vec{\tau}_{STT} = \frac{d\vec{M}_2}{dt} = -P_{spin} \frac{J}{e} \frac{g\mu_B}{2t} (\vec{m}_2 \times (\vec{m}_2 \times \vec{m}_1))$$

Expression derived by
Slonczewski, JMMM 1996

Magnetization dynamics under Spin Transfer Torque (STT)

➤ Landau-Lifshitz-Gilbert-Slonczewski equation (LLGS) :

$$\frac{d\vec{m}_2}{dt} = \boxed{-\gamma_0(\vec{m}_2 \times \vec{H}_{eff})} - \boxed{\alpha \left(\vec{m}_2 \times \frac{d\vec{m}_2}{dt} \right)} + \boxed{P_{spin} \frac{J}{e} \frac{g\mu_B}{2M_{S_2}t} (\vec{m}_2 \times (\vec{m}_2 \times \vec{m}_1))}$$

✓ **Precessional torque (precession around H_{eff})**

$$\vec{H}_{eff} = \vec{H}_{applied} + \vec{H}_{anisotropy} + \vec{H}_{demag}$$

✓ **Damping torque (dissipation)**

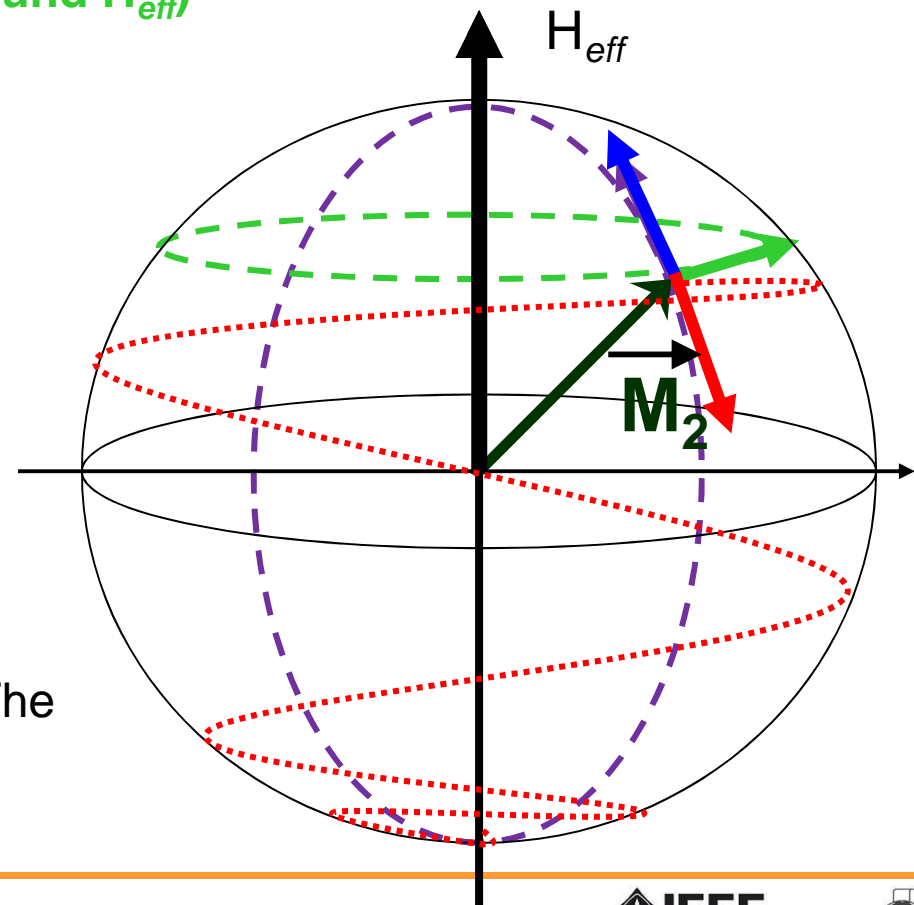
✓ **Spin transfer torque depends on the sign of the current**

- *parallel to damping torque*

- *opposite to damping torque*

→ Above a **threshold current**: the spin transfer torque causes the **effective damping to become negative**.

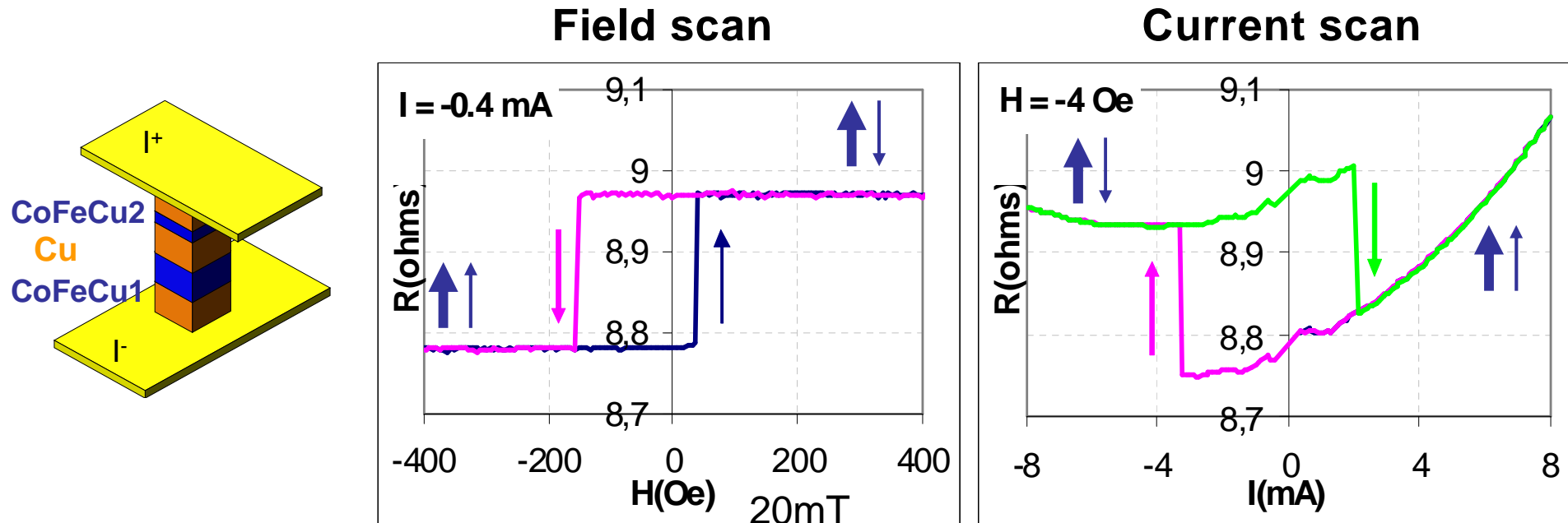
→ Equilibrium state becomes unstable: The magnetization spirals away from the direction of H_{eff} → **Switching**



Magnetization switching induced by a polarized current

STT magnetization switching first observed in metallic pillars (2000)

Katine et al, *Phys.Rev.Lett.*84, 3149 (2000) on Co/Cu/Co sandwiches ($J_c \sim 2-4 \cdot 10^7 \text{A/cm}^2$)



$$j_c^{P-AP} = 1.9 \cdot 10^7 \text{A/cm}^2$$
$$j_c^{AP-P} = 1.2 \cdot 10^7 \text{A/cm}^2$$

By spin transfer, a spin-polarized current can be used to manipulate the magnetization of magnetic nanostructures instead of by magnetic field.

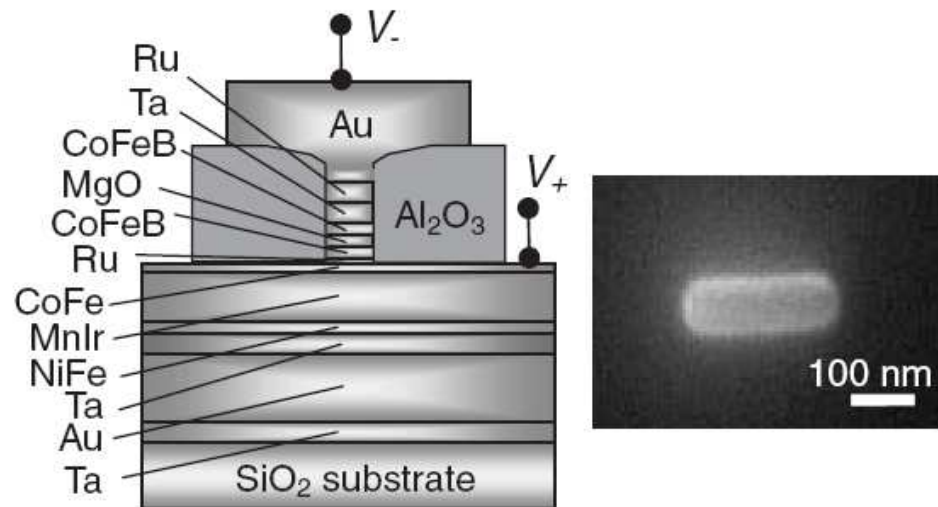
⇒ Can be used as a **new write scheme in MRAM**

Magnetization switching induced by a polarized current

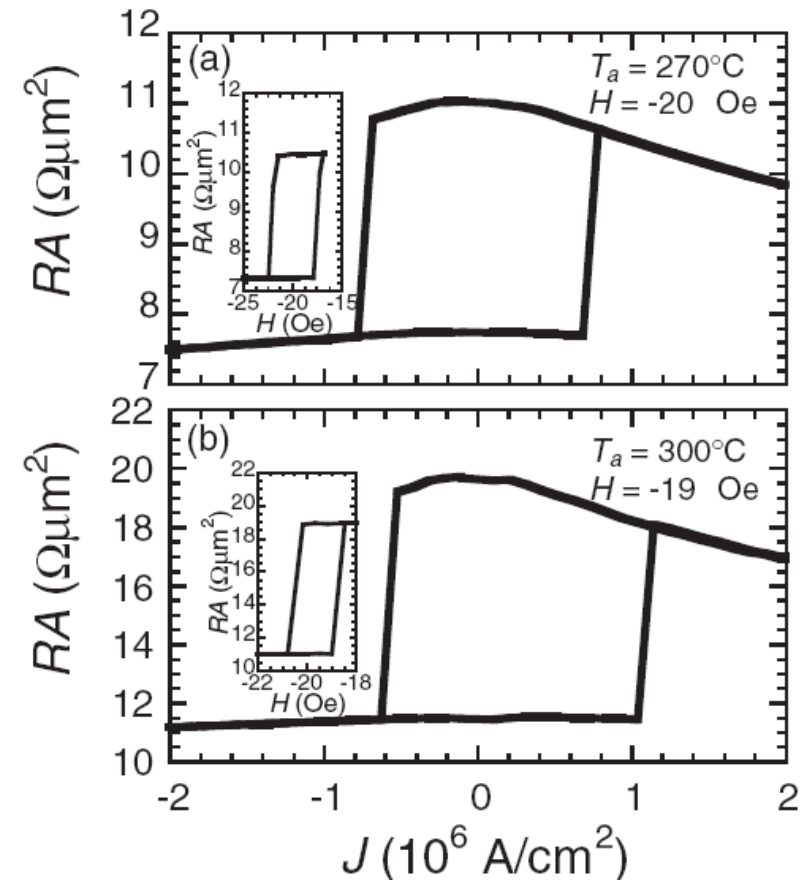
STT magnetization switching in MTJ (2004): *Huai et al, APL (2004); Fuchs et al, APL (2004)*

The bipolar current flowing through the MRAM cell is used to switch the magnetization of the storage layer.

Reading at lower current density then writing so as to not perturb the written information while reading.



*Hayakawa et al,
Japanese Journal of Applied Physics
44, (2005),L 1267*



Spinelectronics: From Basic Phenomena to Applications

OUTLINE

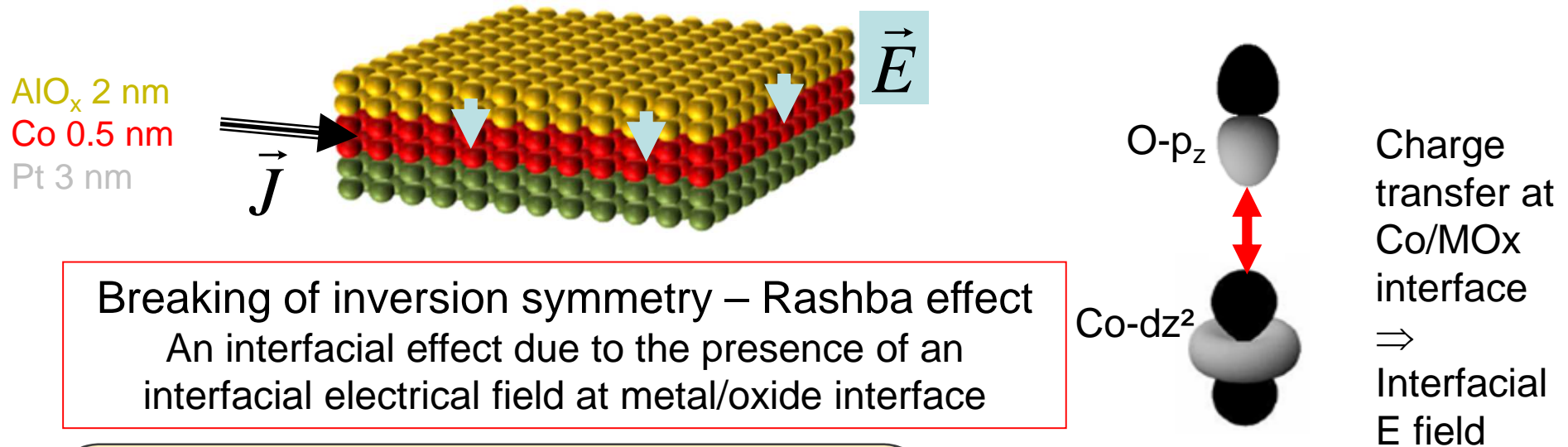
- **Part 1 : Basic phenomena in spintronics:**

- Giant Magnetoresistance
- Tunnel magnetoresistance (TMR)
- Spin-Transfer Torque (STT)
- **Spin-orbit Torques (SOT)**

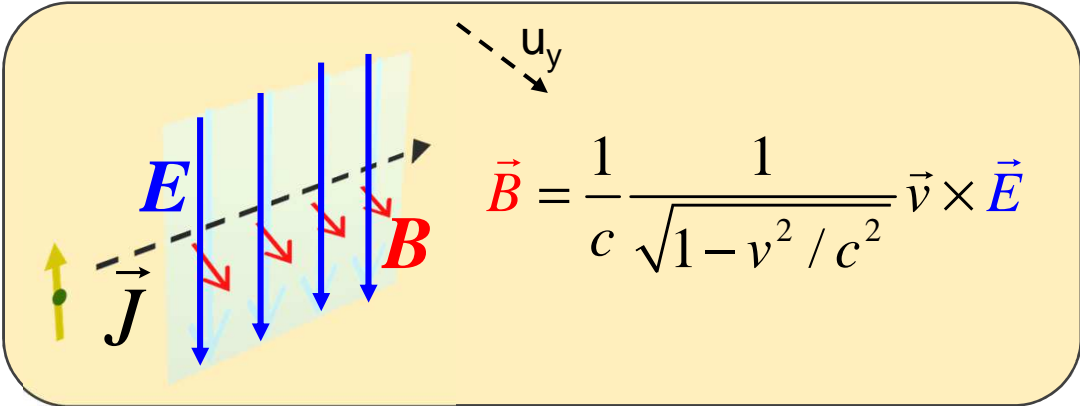
- Part 2 : Spintronics main applications

- Magnetic Recording (Hard disk drives Read-heads)
- MRAMs
- Magnetic field sensors
- Others...

Rashba effect in thin MTJ electrodes with in-plane current



Breaking of inversion symmetry – Rashba effect
An interfacial effect due to the presence of an interfacial electrical field at metal/oxide interface



Manchon et al., PRB 78, 212405 (2008)
Hane et. al .PRB (2013)
H. Yang et. al,PRL (2014)

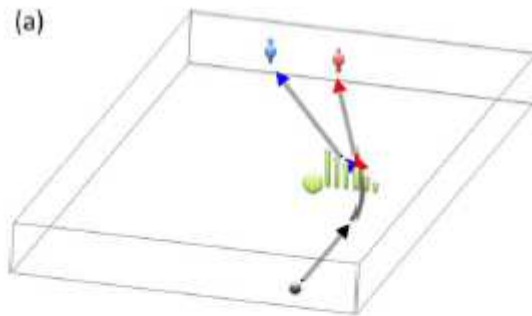
Pulse of in-plane current generates a pulse of in-plane transverse field

→ **Field like torque $\tau \sim \vec{J} \times \vec{m} u_y$**

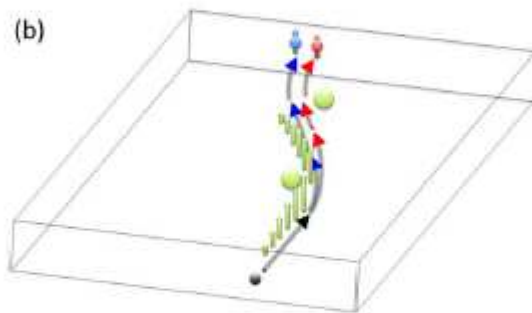
Spin-Hall effect

In presence of spin-orbit interaction in heavy metals (Pt, Au, Bi etc), spin-up and spin-down electrons are differently deviated during scattering.

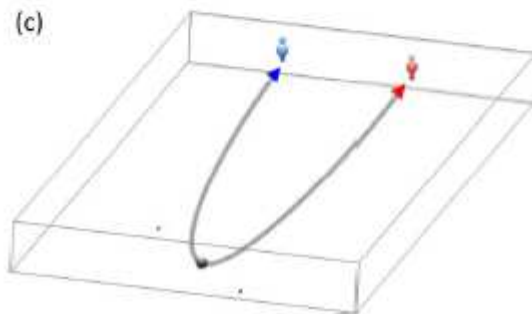
Used in Mott detectors to measure the spin polarization of spin polarized electron beams.



Skew scattering



Side jump

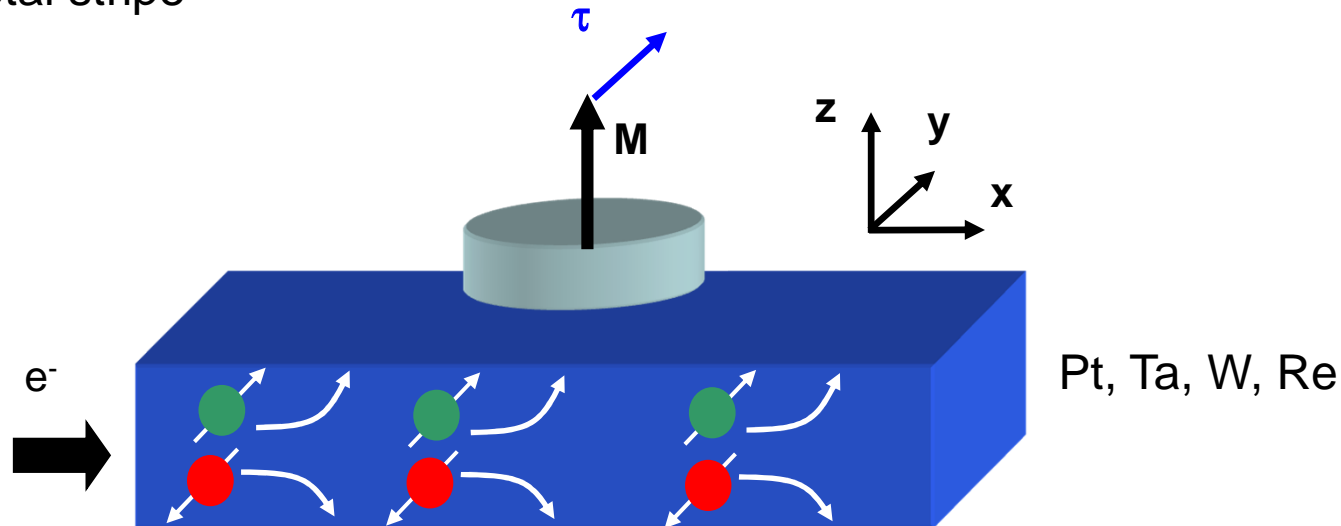


Intrinsic Hall effect due to band structure


A.Hoffmann, IEEE TRANSACTIONS ON MAGNETICS, 49, 5172 (2013)

Switching by spin-Hall effect

Spin Hall effect provides another spin-torque contribution originating from the bulk of the heavy metal stripe



- Vertical spin-current with transverse polarisation u_y .
- Spin-current related to Spin Hall angle θ_{SH} and charge current by: $J_s = \theta_{SH} J$
- **Damping like torque** $\tau \sim \theta_{SH} J m \times (m \times u_y)$

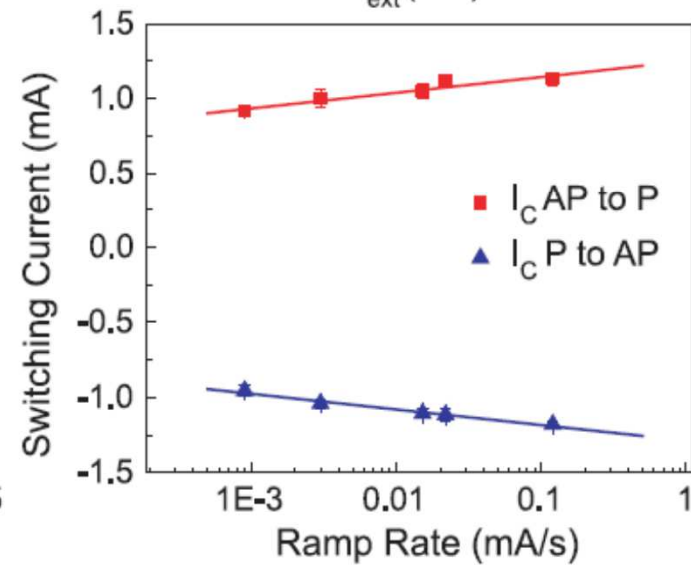
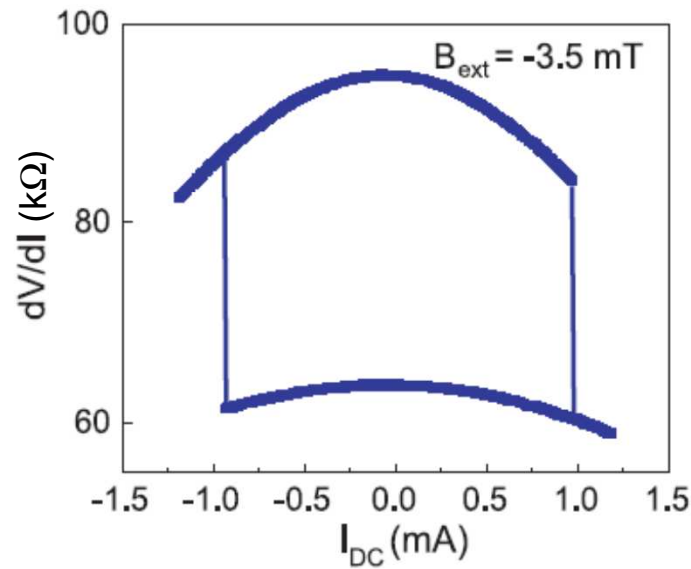
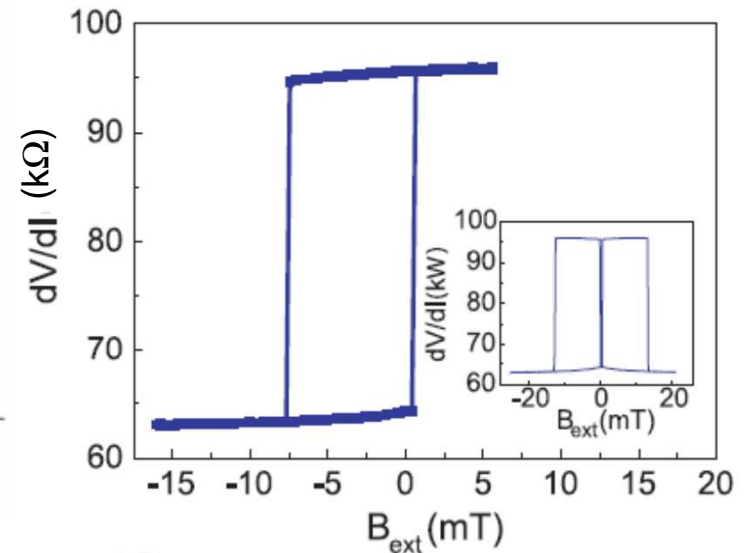
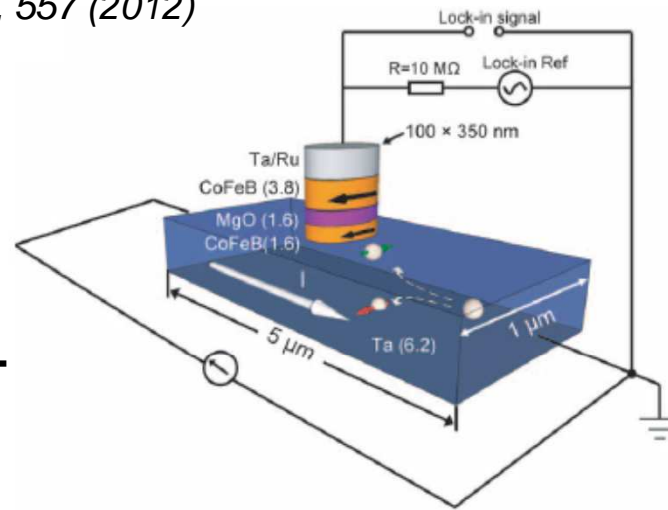
 Liu et al., (Science 2012), Liu et. al (2012); Kim, Hayashi et al. Nature Mater. (2013);

 X. Fan, J. Xiao et. al, NatCom (2014)

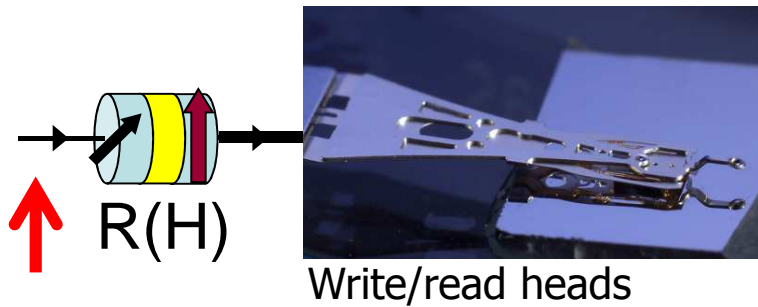
Switching by spin-Hall effect

Liu et al, SCIENCE, 336, 557 (2012)

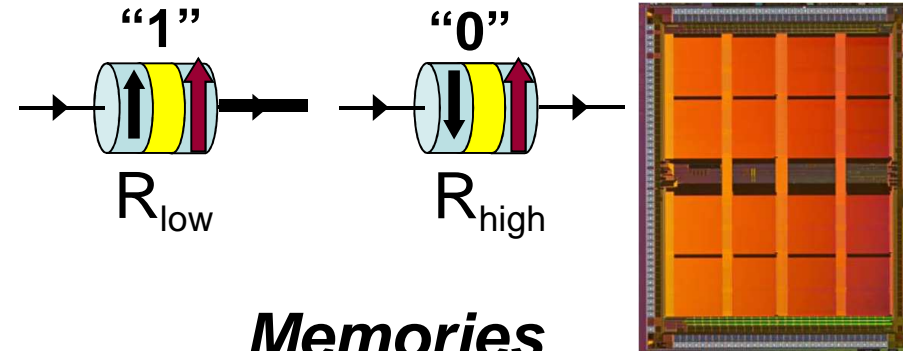
Switching by an in-plane current in a 3-terminal device



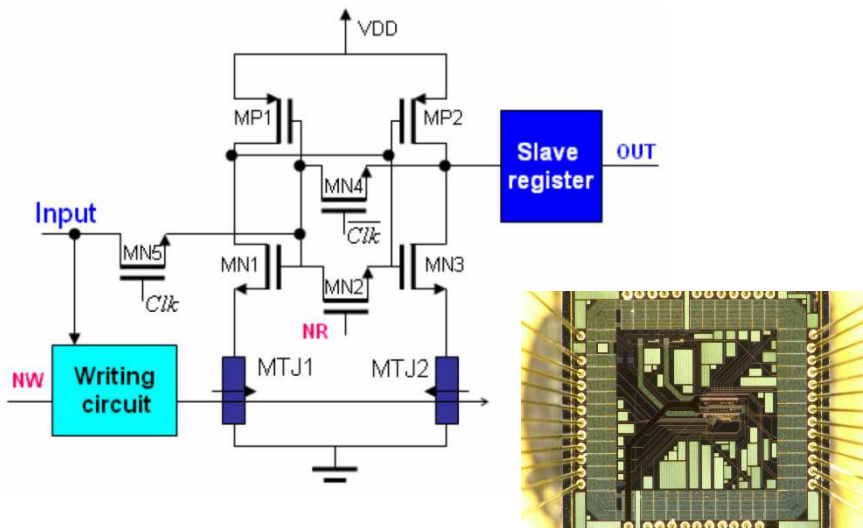
Spintronic components



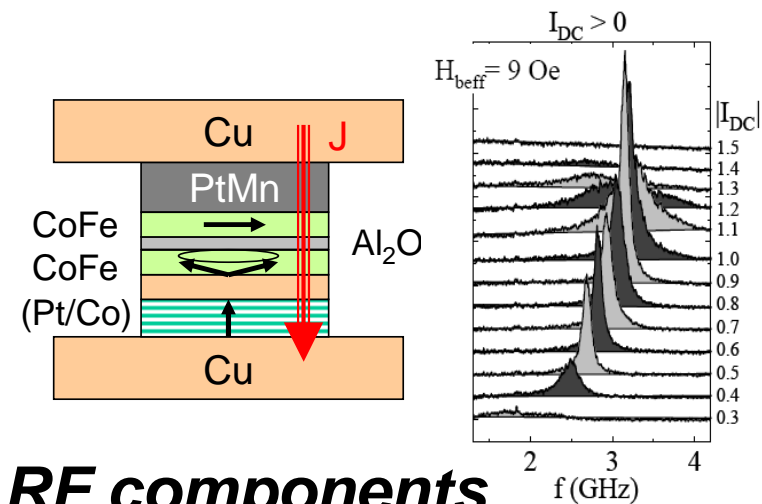
Magnetic field sensors



Memories



Logic circuits



RF components

End part I

Questions ?

Coffee break

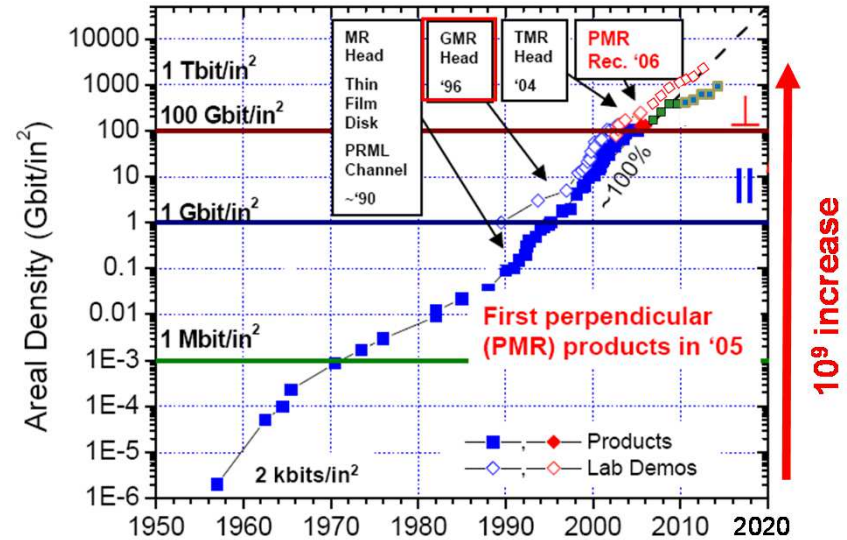
Spinelectronics: From Basic Phenomena to Applications

OUTLINE

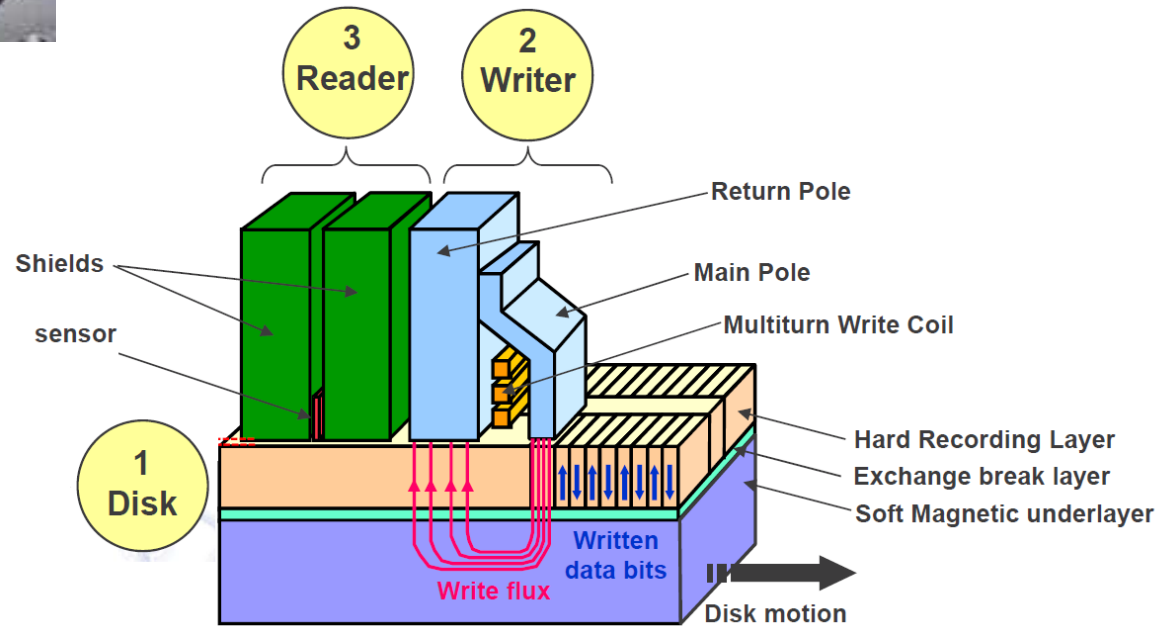
- Part 1 : Basic phenomena in spintronics:
 - Giant Magnetoresistance
 - Tunnel magnetoresistance (TMR)
 - Spin-Transfer Torque (STT)
 - Spin-orbit Torques (SOT)
- **Part 2 : Spintronics main applications**
 - **Magnetic Recording (Hard disk drives Read-heads)**
 - MRAMs
 - Magnetic field sensors
 - RF applications

Magnetic recording technology has stimulated R&D in spintronics for more than 20 years

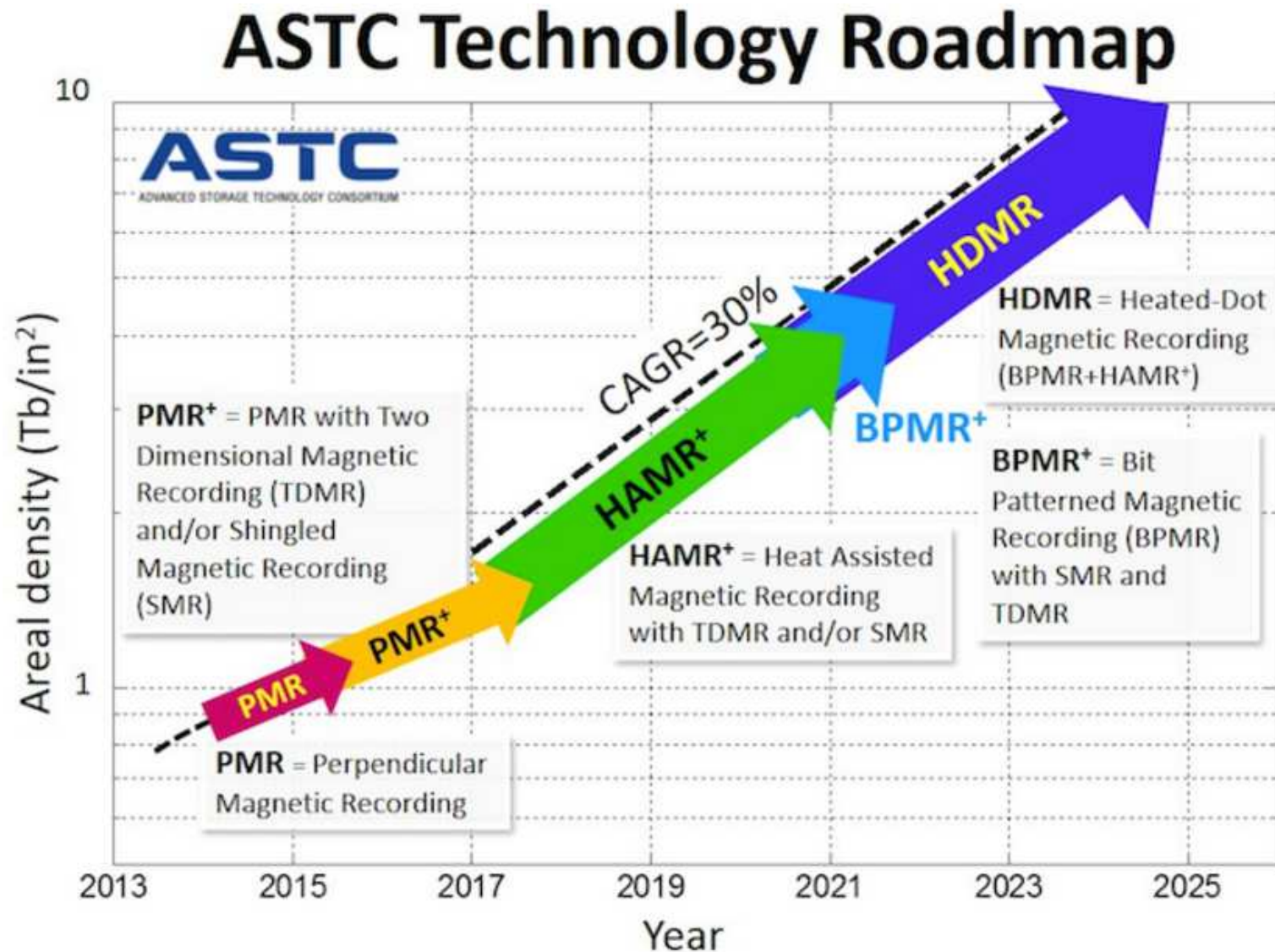
Hard Disk Drive (HDD)



GMR spin-valve heads from 1998 to 2004,
TMR heads since 2004



Progresses in magnetic recording technology more and more difficult to achieve



HDD R&D increasingly difficult but increasing demand for data storage

Coexistence of **Solid State Drives** (based on Flash memories: charge based storage) and **Hard Disk Drives** (magnetic « cold » storage)

Handheld devices
Laptops, cell-phones...



SSD

Servers farms

SSD+HDD

HGST "Active Archive" System
Complete data storage system for cloud data centers

7ft tall **4.7PB** raw capacity per rack

Highest Density
Lowest Power per TB with Fast Data Access

Magnetic storage (capacity, low cost)
588 Helium HDD's (8 TB each)

Charge storage (speed)
+ performance SSDs

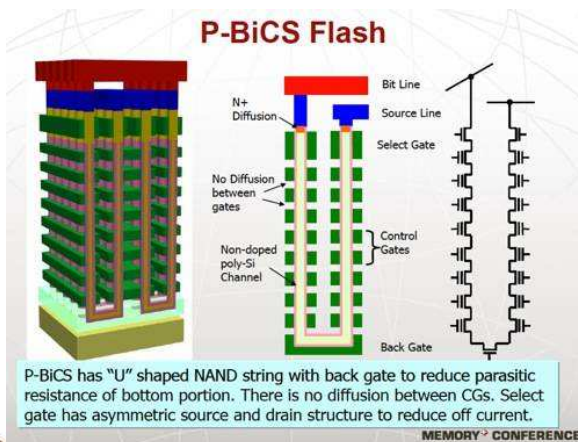
+ Servers and Controllers

+ Specialized Software
AMPLIDATA

+ Drive-Optimized Enclosure.

Need 4 racks to store all the books in the US Library of Congress!

3D-Flash allows significantly increase the density of Flash disks



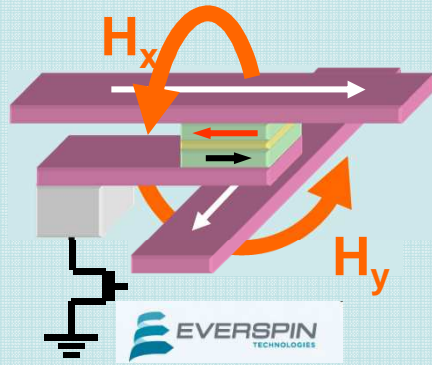
Spinelectronics: From Basic Phenomena to Applications

OUTLINE

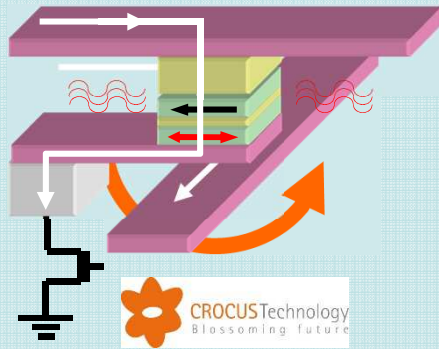
- Part 1 : Basic phenomena in spintronics:
 - Giant Magnetoresistance
 - Tunnel magnetoresistance (TMR)
 - Spin-Transfer Torque (STT)
 - Spin-orbit Torques (SOT)
- **Part 2 : Spintronics main applications**
 - Magnetic Recording (Hard disk drives Read-heads)
 - **MRAMs**
 - Magnetic field sensors
 - RF components

Various MRAM families

Field-driven

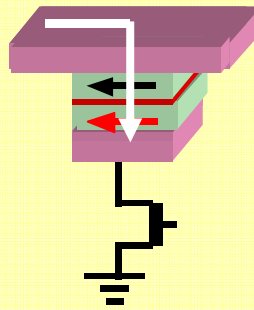


Thermally Assisted (TAS)

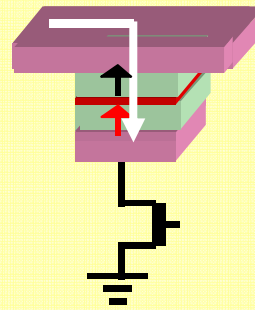


STT (STT MRAM)

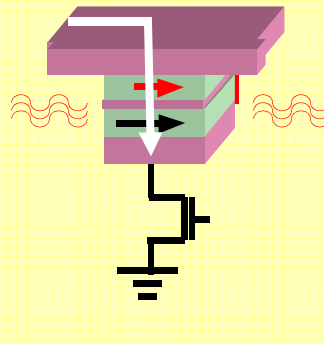
Planar



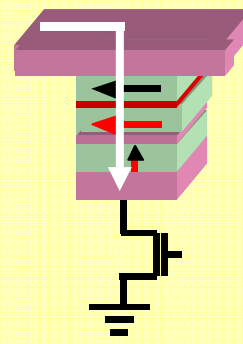
Perpendicular



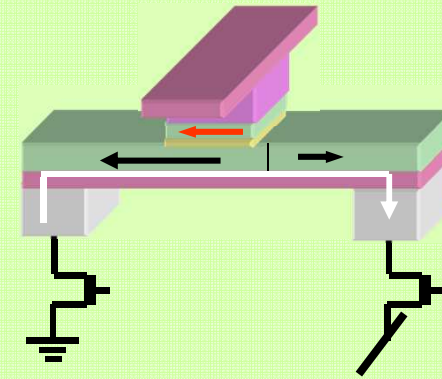
STT-TAS



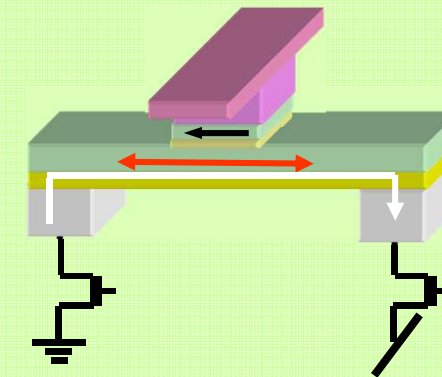
Precessional



DW motion

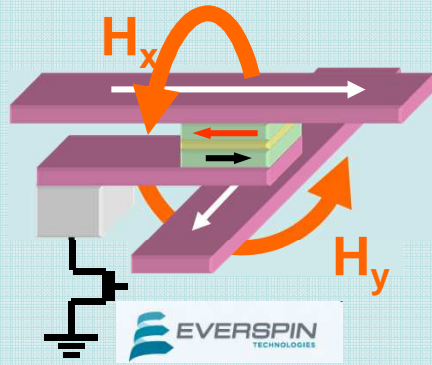


Spin-orbit torque (spin-Hall, Rashba)



Various MRAM families

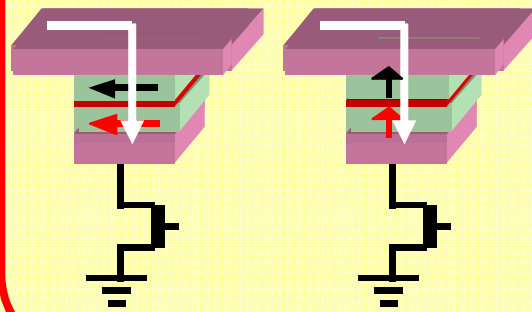
Field-driven



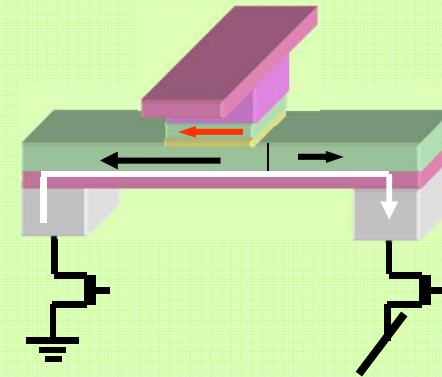
STT (STT MRAM)

Planar

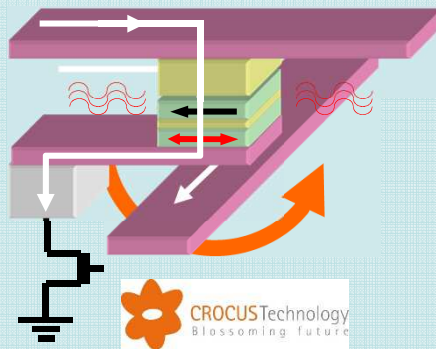
Perpendicular



DW motion

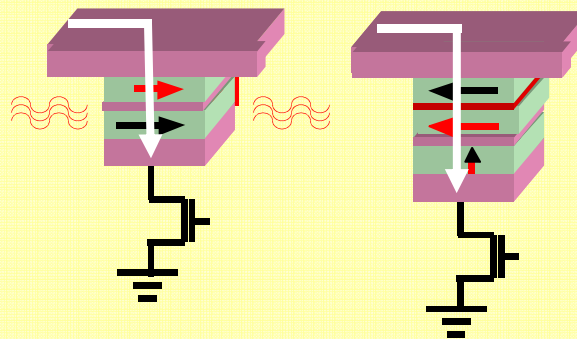


Thermally Assisted (TAS)

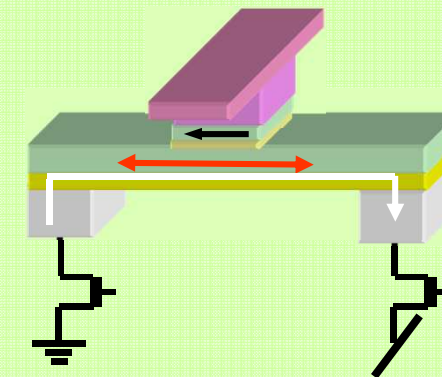


STT-TAS

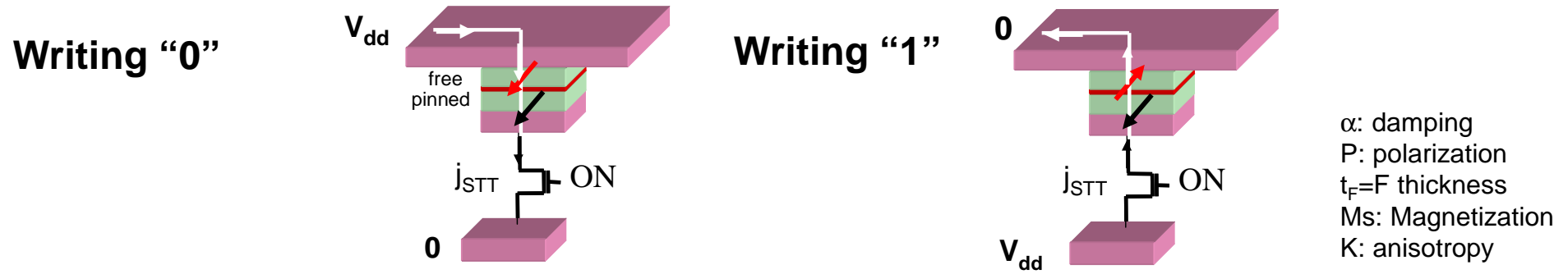
Precessional



Spin-orbit torque (spin-Hall, Rashba)



STT MRAM – scalability of write current



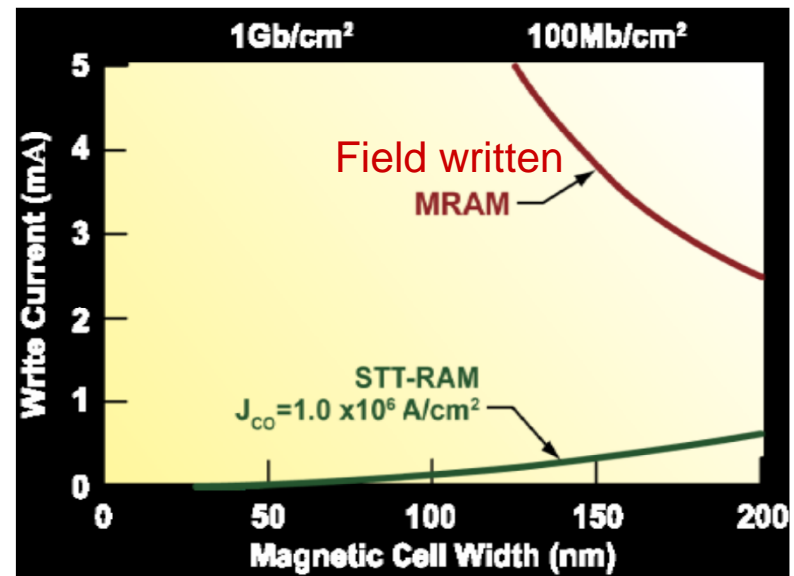
• Writing determined by a current density $j_{WR\ in-plane} = \left(\frac{2e}{\hbar}\right) \frac{\alpha t_F}{P} \left(\frac{\mu_0 M_s^2}{2} + 2K\right)$

• Current through cell proportional to MTJ area

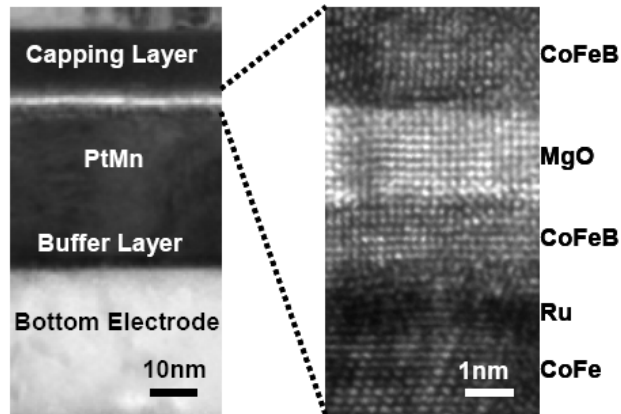
• $j_{write\ SST\ in-plane} \sim 8 \cdot 10^5 \text{ A/cm}^2$ quasistatic
 $\sim 3 \cdot 10^6 \text{ A/cm}^2 @ 10\text{ns}$

Huai et al, *Appl. Phys. Lett.* 87, 222510 (2005);
 Hayakawa, *Jap. Journ. Appl. Phys.* 44 (2005) L1246

Write current $\sim 15\text{-}40\mu\text{A}$ at sub-20nm node



STT-MRAM – Write – influence of current pulse width

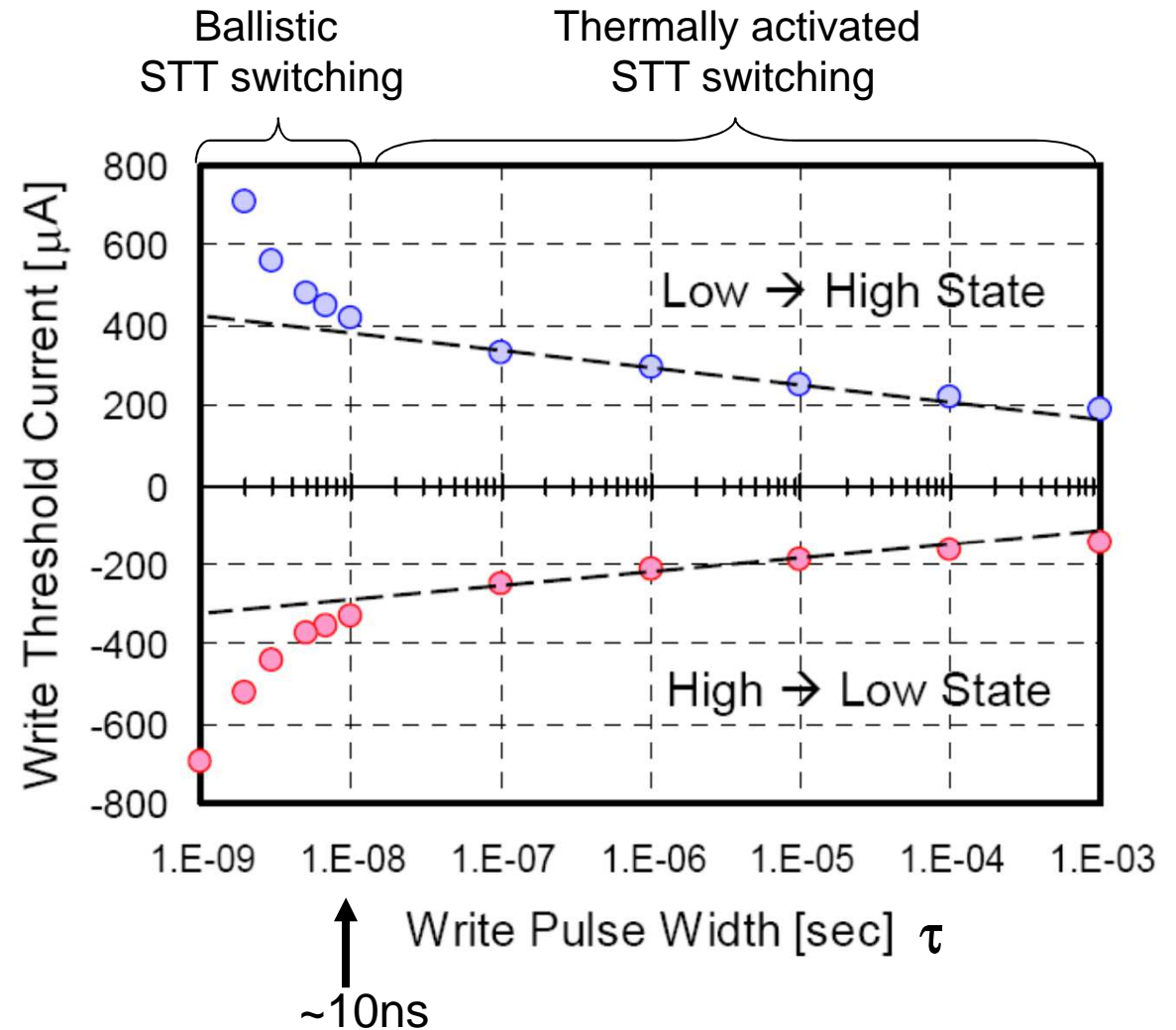


In-plane magnetized MTJ

Elliptical shape

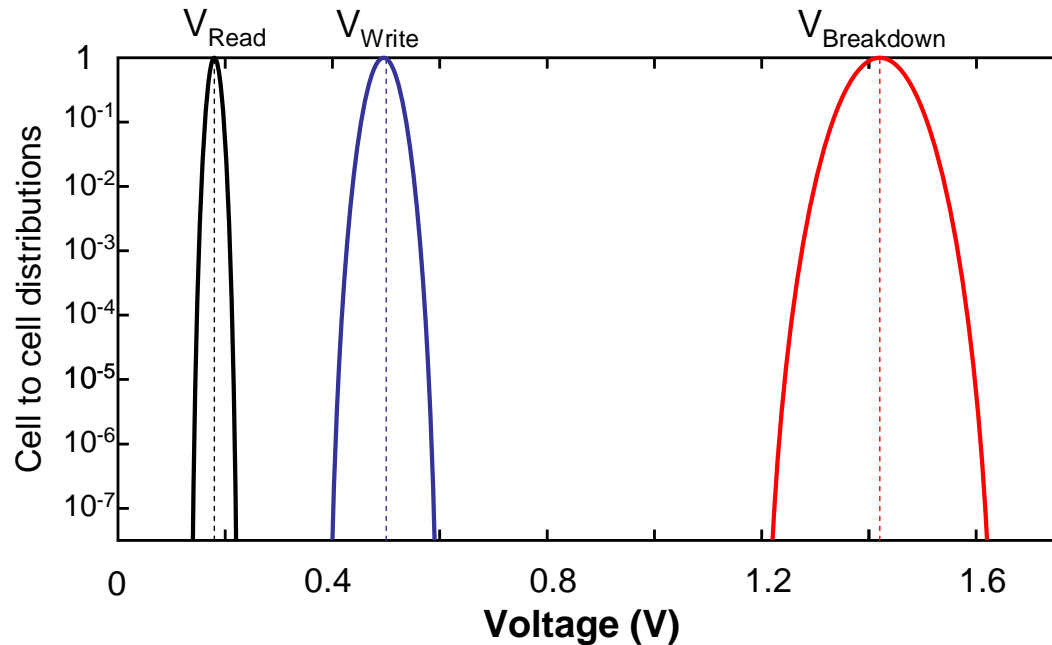
115nm*155nm

Hosomi et al, Sony, 4Kbit demo (2005)



STT-MRAM – Distributions consideration

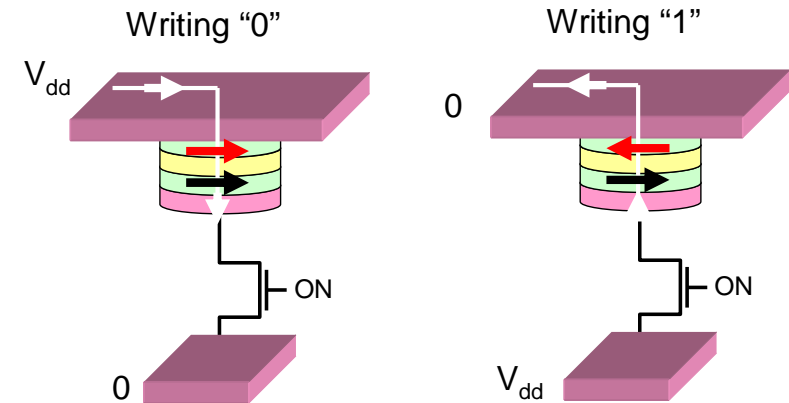
Read **STT Write** **Breakdown**



0.15-0.2V

0.40-0.50V

1.2V-1.6V



$V_{switch} \ll V_{breakdown}$ for good write endurance

$V_{read} \ll V_{switch}$ to avoid disturb during read

V_{read} large enough for reasonable read speed (~10ns).

STT-MRAM – Key parameters

- Δ (**thermal stability factor**) \Rightarrow data retention, read disturb, operating temperature range, downsize scalability

Δ should be between 30 and 90 depending on chip density and retention.

- **TMR (read signal)** \Rightarrow read speed, sense margin, tolerance on RA dispersion

TMR above 200% to achieve fast (sub 10ns) read-out. The larger, the better.

- J_{c0} (**write current density**) \Rightarrow cell size, write speed, write consumption, reliability

J_c below $1 \cdot 10^6 \text{ A/cm}^2$ is desirable to insure select transistor size smaller than MTJ.

- V_{bd} (**MTJ breakdown voltage**) \Rightarrow reliability, endurance

V_{bd} should be above 3 times write voltage (typically $V_{bd} \sim 1.5\text{V}$ at 10ns and $V_{write} \sim 0.5\text{V}$)

to achieve a write endurance above 10^{16} cycles.

2013: 1st STT-MRAM product



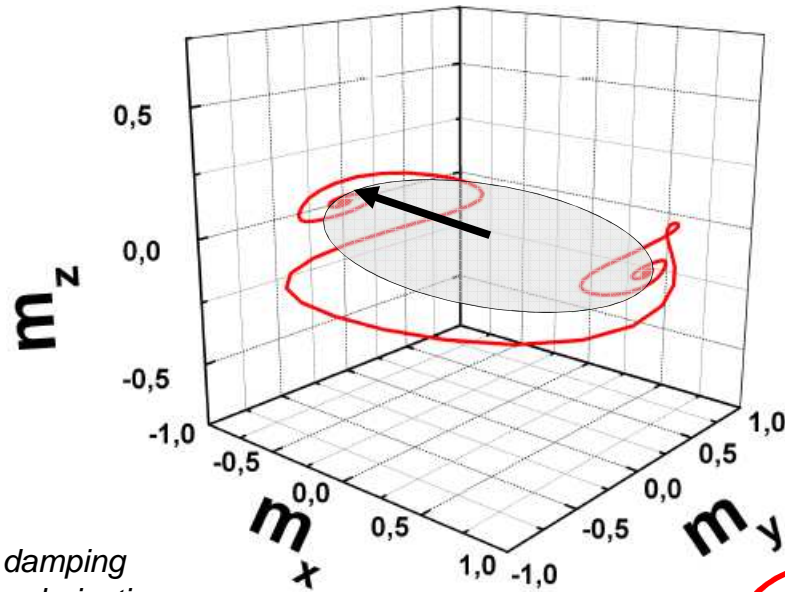
Everspin Introduces The 64Mb DDR3 ST-MRAM



November 2012

In-plane versus out-of-plane STT switching

In-plane magnetized MTJ



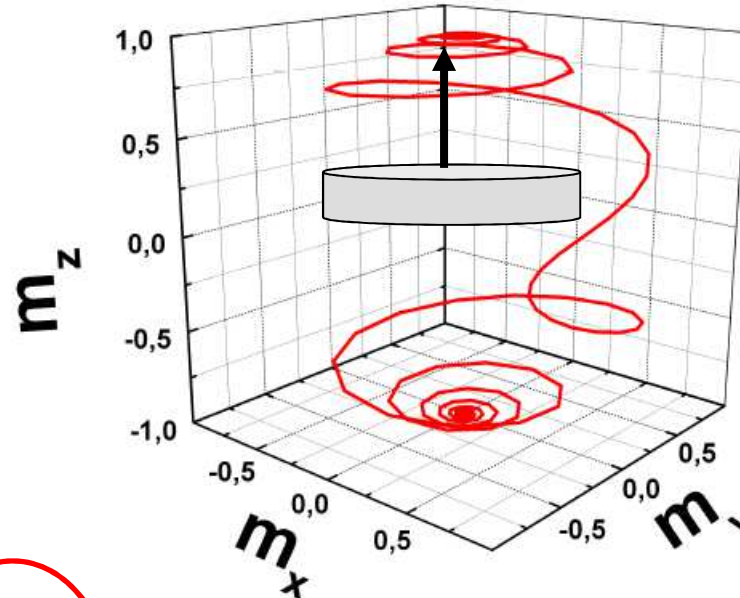
α = damping
 P = polarization
 A = Area
 $g(0) \sim 1$

$$j_c^{in-plane} = \left(\frac{4e}{\hbar} \right) \frac{\alpha k_B T}{g(0) p A} \left(\Delta + \frac{\pi M_s^2 V}{k_B T} \right)$$

Thermal stability determined by in-plane anisotropy (shape anisotropy)

Simpler materials but additional penalty in j_c due to out-of-plane precession

Out-of-plane magnetized MTJ



$$j_c^{perp} = \left(\frac{4e}{\hbar} \right) \frac{\alpha k_B T}{g(0) p A} \Delta$$

More complex materials but lower j_c expected thanks to direct proportionality between J_c and thermal stability Δ

Perpendicular Magnetic Anisotropy (PMA) at magnetic metal/oxide interface

Surprisingly large perpendicular anisotropy at magnetic metal/oxide interface

(Monso et al APL 2002)

S.Monso, et al, APL 80 (2002), 4157-9.

B.Rodmacq et al, Journ. Appl. Phys. 93, (2003), 7513.

A.Manchon et al, Journ. Appl. Phys. 104, 043914 (2008).

B.Rodmacq et al, Phys. Rev. B 79, 024423 (2009)

L.Nistor et al, IEEE Trans Mag., 46 (2010), 1412

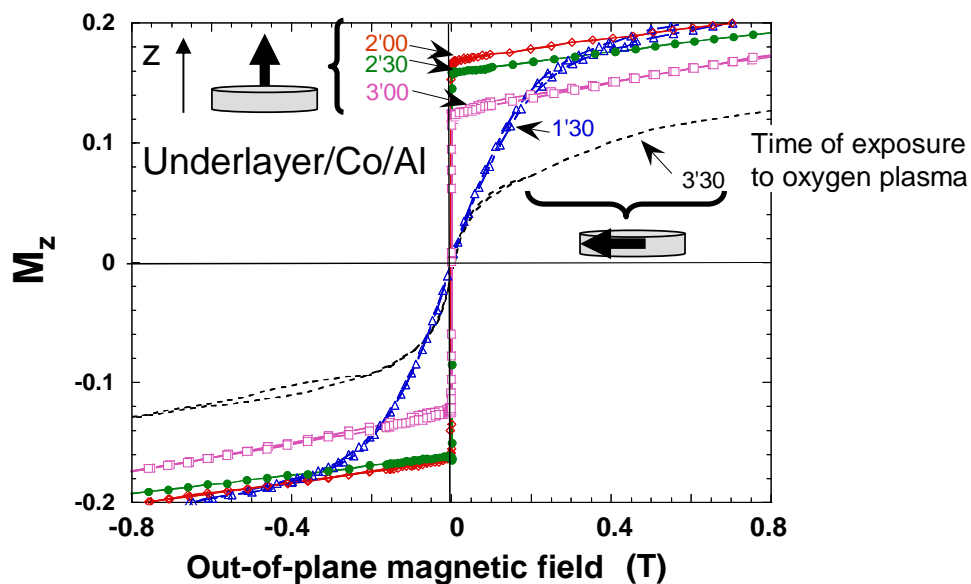
First observation of PMA at Co/AlOx

PMA at Co or CoFe/MgO, CrO, TaO

XPS, XAS, interpretation of PMA at M/Ox

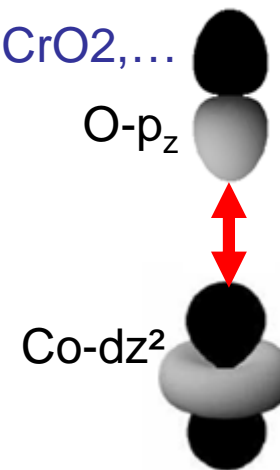
Influence of annealing on PMA at Co/AlOx

Correlation PMA -TMR at CoFe(B)/MgO



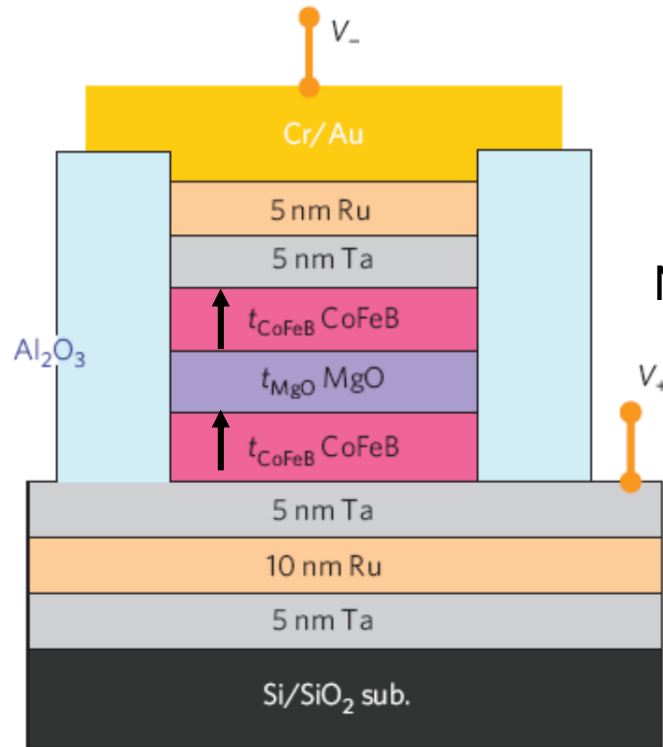
Very general phenomenon of perpendicular anisotropy observed at a wide variety of M/Ox interfaces with $M=Co, CoFe, CoFeB$ and $Ox= AlOx, MgO, TaOx, CrO_2, \dots$

Due to hybridization between Co dz^2 and O sp orbitals

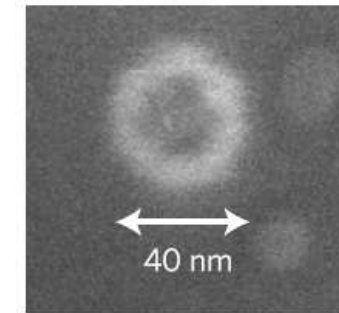


P-MTJ based on interfacial PMA (i-PMA)

Ikeda et al, Nat.Mat.2804 (2010)

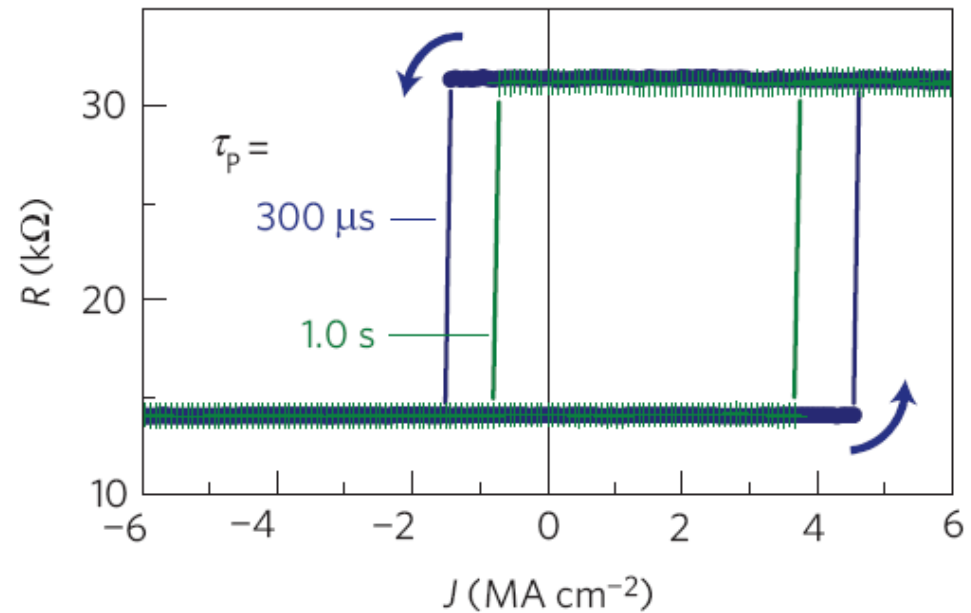


No Pt nor Pd in the stack



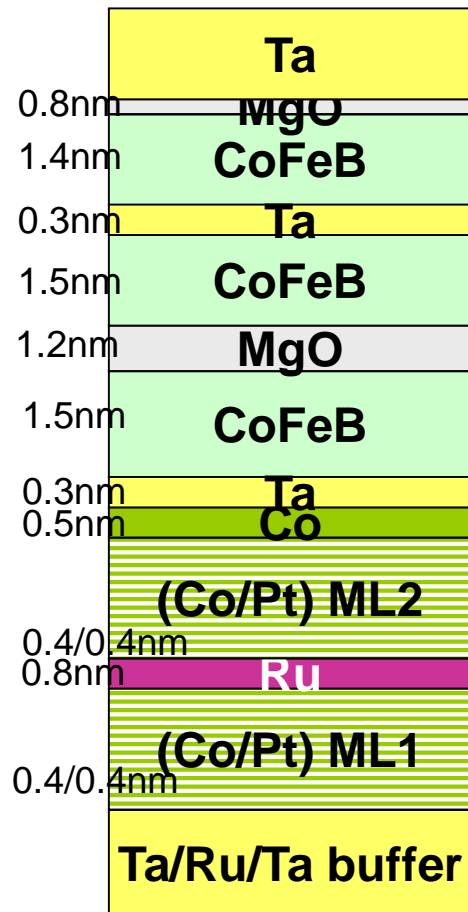
TMR=124%
RA=18Ω.μm²

Δ=43
(70 required for 1Gbit)

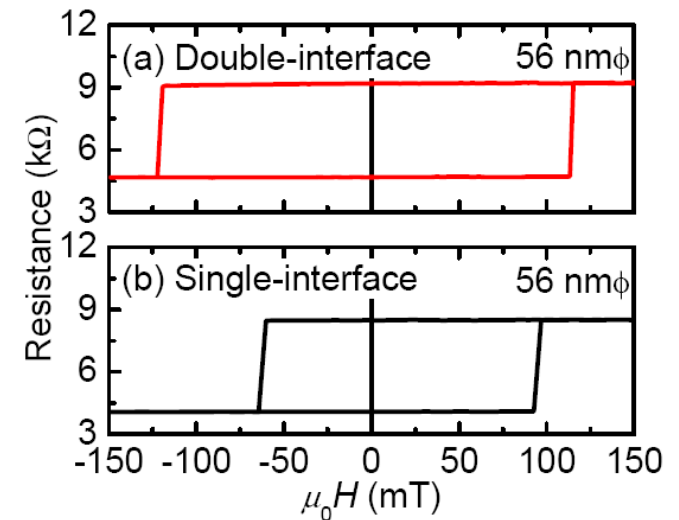
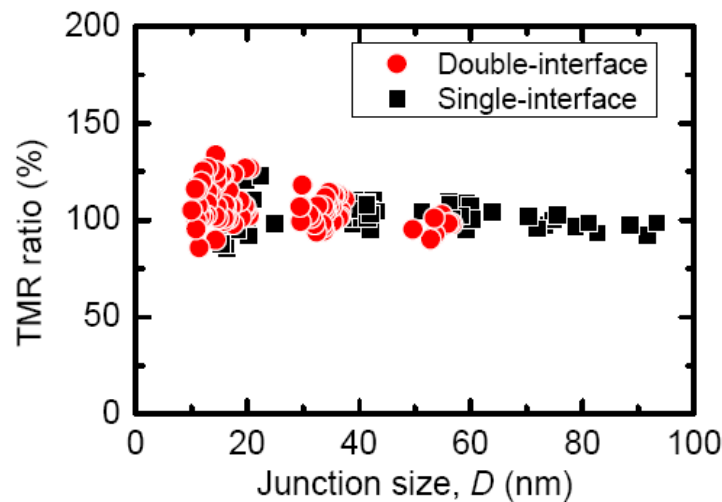


Sub-20nm STT-MRAM

Bottom pinned with double MgO barrier:



Benefit from the PMA at these two interfaces.
Increases the thermal stability of the free layer.

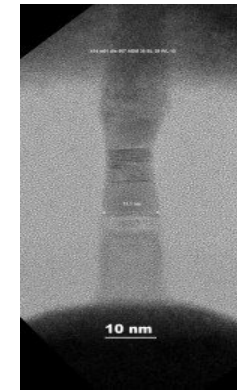
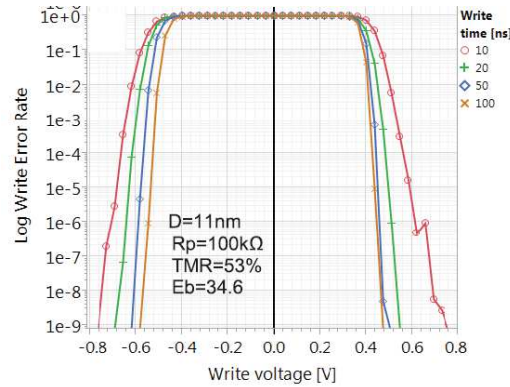


TMR ~100-130%

H. Ohno's group (Tohoku Univ 2013), IEDM 2014

STT-MRAM assets

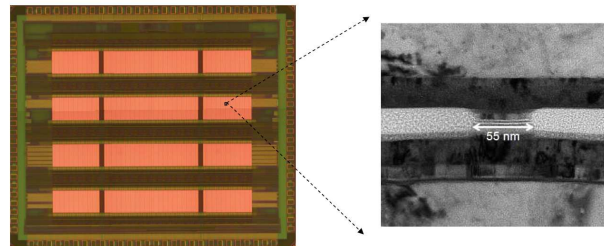
- Non-volatility



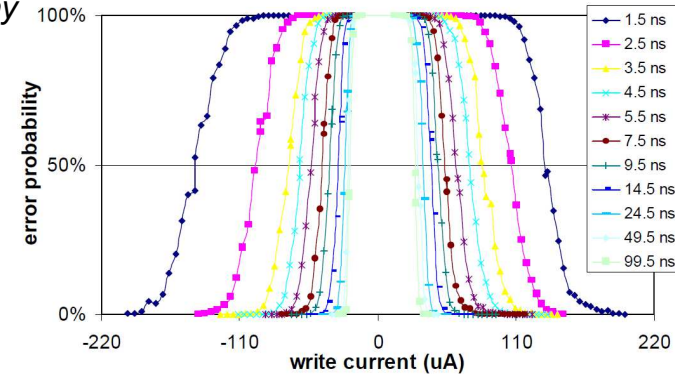
11nm STT-MRAM cell (IBM)
Janusz et al, IEEE Mag.Lett.7, 3102604(2016)

- Downsize scalability

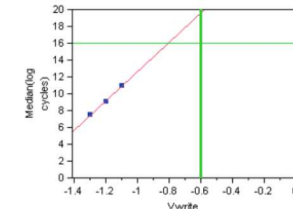
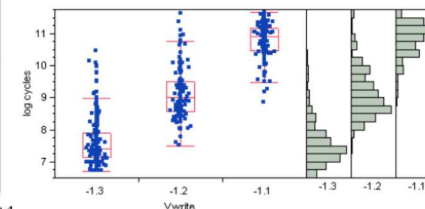
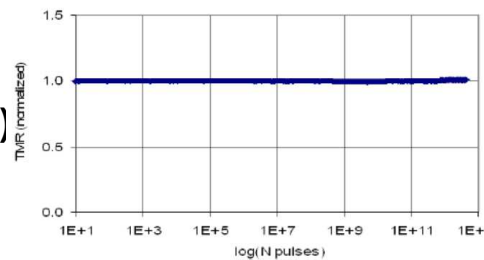
8 Mbit fully functional demo from TDK/Headway
 Techno now transferred to TSMC



- Write speed



- Write endurance (at least for pulse duration >20ns)



10²⁰ cycles à 0.6V

➔ 1) e-FLASH, 2) non-volatile SRAM 3) Non-volatile DRAM

An increasing number of industrial actors active in the MRAM arena



Samsung Electronics Starts Commercial Shipment of eMRAM Product Based on 28nm FD-SOI Process

Korea on March 6, 2019

Samsung's eMRAM will further strengthen the company's technology leadership in embedded memory

Samsung Electronics the world leader in semiconductor technology, today announced that it has commenced mass production of its first commercial embedded magnetic random access memory (eMRAM) product based on the company's 28-nanometer(nm) fully-depleted silicon-on-insulator (FD-SOI) process technology, called 28FDS.

As eFlash has faced scalability challenges due to a charge storage-based operation, eMRAM has been the most promising successor since its resistance-based operation allows strong scalability while also possessing outstanding technical characteristics of memory semiconductors such as nonvolatility, random access, and strong endurance. With today's announcement, Samsung has proved its capability to overcome technical hurdles and demonstrated the possibility for further scalability of embedded memory technology to 28nm process node and beyond.

Samsung's 28FDS-based eMRAM solution offers unprecedented power and speed advantages with lower cost. Since eMRAM does not require an erase cycle before writing data, its writing speed is approximately a thousand times faster than eFlash. Also, eMRAM uses lower voltages than eFlash, and does not consume electric power when in power-off mode, resulting in great power efficiency.

Conclusion on p-STT-MRAM

- Perpendicular MTJs offer better downsize scalability than in-plane magnetized MTJs due to larger anisotropy and lower write current for a given thermal stability factor.
- In p-MTJs, taking advantage of the interfacial anisotropy at CoFe/MgO interface allows to circumvent the issue of combining large PMA with low Gilbert damping.
- Etching of the MTJ stack remains the main technological difficulty at sub-28nm node yielding too large variability. However, great progress are made and demonstrators of embedded STT-MRAM at 28nm node have been successfully realized.
- Main foreseen applications:
 - Replacement of embedded FLASH
 - Replacement of SRAM
 - Remplacement of DRAM (longer time goal....)

Spinelectronics: From Basic Phenomena to Applications

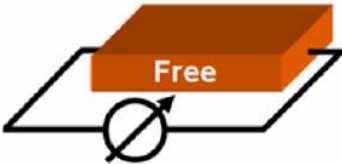
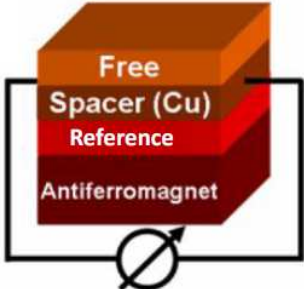
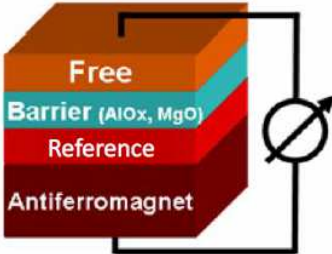
OUTLINE

- Part 1 : Basic phenomena in spintronics:
 - Giant Magnetoresistance
 - Tunnel magnetoresistance (TMR)
 - Spin-Transfer Torque (STT)
 - Spin-orbit Torques (SOT)
- **Part 2 : Spintronics main applications**
 - Magnetic Recording (Hard disk drives Read-heads)
 - MRAMs
 - **Magnetic field sensors**
 - RF components

Different kinds of magnetoresistive sensors

Freitas, P.; Ferreira, R., Cardoso, S. ; PROCEEDINGS OF THE IEEE, 104, 1894-1918 (2016)

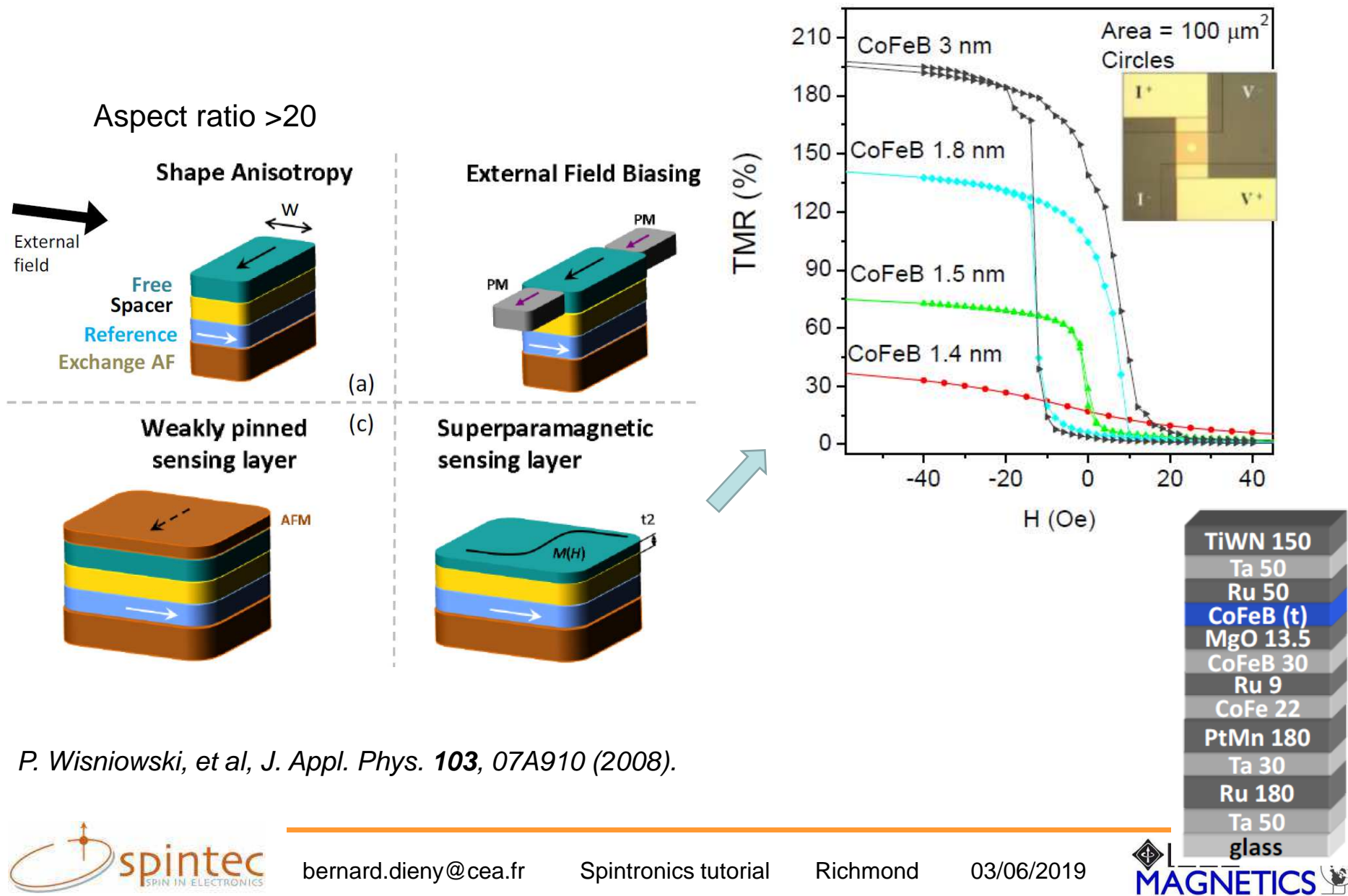
TYPICAL KEY PROPERTIES OF MAGNETORESISTIVE SENSORS

	AMR	GMR - Spinvalves	TMR - Magnetic Tunnel Junctions
Physical principle	Anisotropic MR	Giant MR	Spin dependent tunneling
Thin film structure	Simple Buffer/free/cap	Multilayers, several material compositions Buffer/free/spacer/reference/pinning/cap	Complex multilayers, several material compositions Buffer/free/barrier/reference/pinning/cap
Magnetoresistance (MR) [%] [#]	2-6	6-20	50% (Al ₂ O ₃ amorphous barrier) 300% (MgO crystalline barrier)
Sensor linear range [mT] ^{&}	0.1-1	1-5	2-10
Thermal treatment [°C] [§]	Not required	Typically 220-280°C	Typically 280-340°C
Reference layer	No, needs external	Yes (interface exchange biased trough an antiferromagnetic film)	Yes (interface exchange biased trough an antiferromagnetic film)
Electrical robustness against electrostatic discharge	Excellent	Excellent	Good
General geometry and readout scheme			

Sensors matrix (from NIST, 2003)

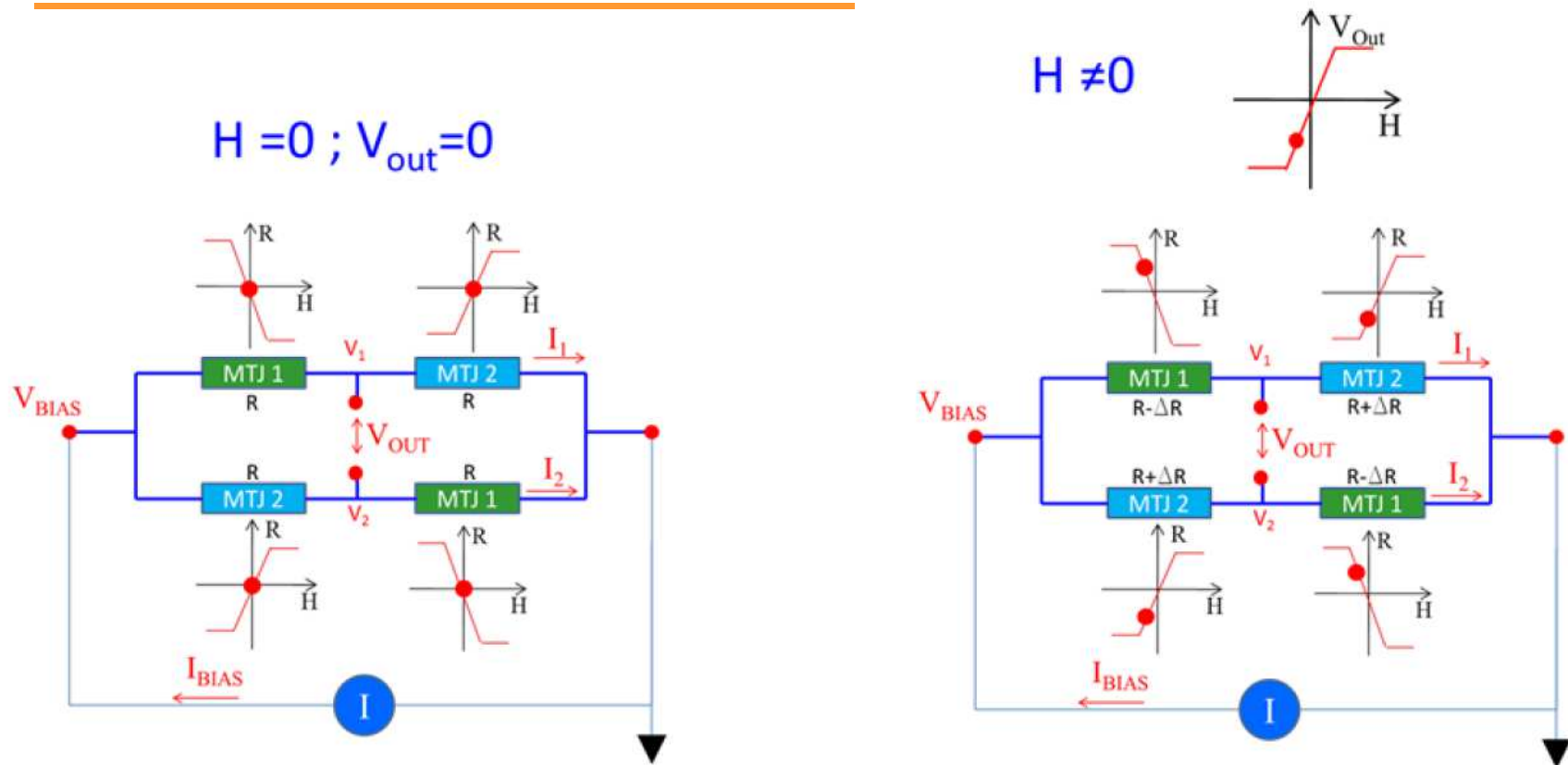
Sensor type	Sensitivity/ Field range	Frequency Range	Operation Temperature	Minimum sensor size/ Scalability	Vectorial/ scalar	Cost	Advantages	Disadvantages	Status
Search coil	30 fT	>1 Hz	RT	1 mm	vector	Moderate	Low cost for the sensitivity	Limited to > 1Hz, sensitive to angular vibrations, Loose sensitivity as decrease size	Mature
Hall probe/EMR	100 nT/ 1nT	< 1kHz	RT	< 1 μ m	Vector	Moderate	Large range, linear	Temperature dependent	Mature
Fluxgate	1 pT/Hz) ^{0.5} @ 1Hz	< 1kHz	RT	Loose S/N scaling down	Vector	Moderate	High sensitivity	Cost, size, energy consumption	Bulk films versions possible
SQUID	1 fT	<1kHz	<77K	< 1 μ m (system large)	Vector	Expensive	Sensitivity	Need for low temperature	mature
GMR	20 nT	0- 5 GHz	RT	< 1 μ m	Vector	Cheap	Low cost in large quantities. Small sensors. Wide frequency range		
TMR	1 nT	0-1 GHz	RT	< 1 μ m	Vector	Cheap	Large MR, low cost in large quantities	High 1/f noise, hysteretic	
GMI	100 pT	<500 kHz	RT	1 mm	Vector	Moderate		Cost, size, high power	
Magneto-optic	100 pT	0-5GHz	RT	. 1 mm	Vector	Moderate	No electrical connection		
Resonance		DC	RT		Scalar	Expensive			
Optical pumping	10-1000 fT	< 100 Hz	RT	10 mm	Scalar or vector	Expensive	Insensitive to angular vibrations	Cost, power consumption, loss of sensitivity at higher frequencies	
Magnetostrictive /	1 nT		RT	10 μ m	Vector	Moderate	Low power Large output	Sensitive to vibrations	

Various approaches for linearization of magnetoresistive sensors



P. Wisniowski, et al, J. Appl. Phys. **103**, 07A910 (2008).

Magnetoresistive sensors often used in Wheastone bridge configuration



Difficulty is to set the two pairs of sensors in opposite pinning directions:

- Use different deposits (different field during deposition or AF with different TB or SAF differently compensated...)
- Or use local heating lines
- Or use local field generating lines

P.P.Freita et al, SPIN, Vol.1, 71 (2011)
J.Cao et al, J.Appl.Phys. 107, 9 (2010)

Example of bridge magnetoresistive sensor

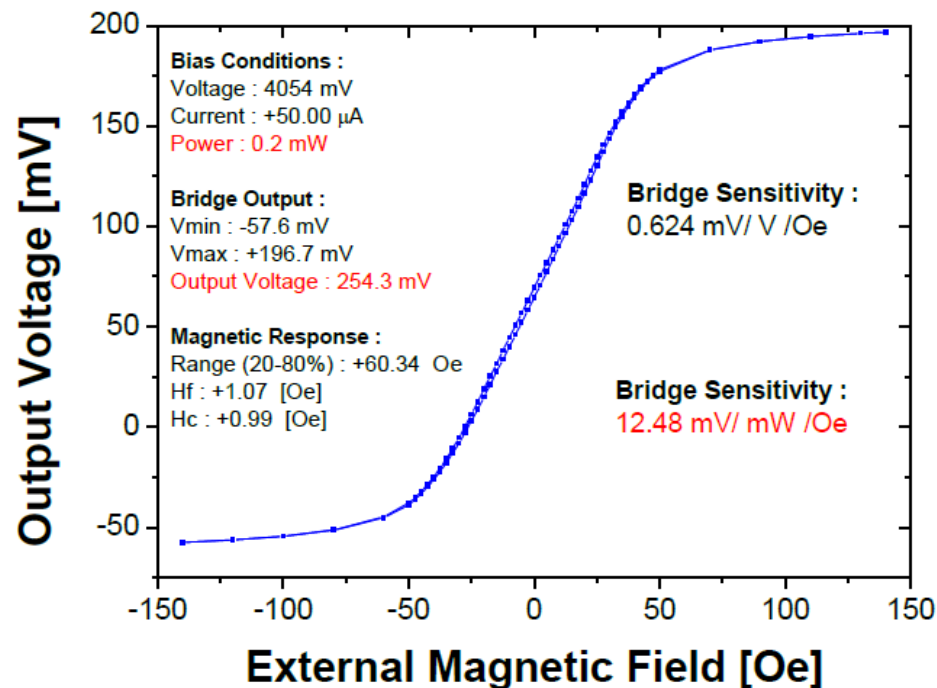
Example: spin-valve based bridge sensor

Glass/Ta 2nm / NiFe 3nm / CoFe 2 / Cu 1.9 / CoFe 2 / Ru 8 / CoFe 1.5 / MnIr 6 / Ta 3nm

GMR=8%

30 GMR elements in series in each branch with individual dimension 3*170nm

Very elongated shape to insure single domain behavior



J.Cao and P.P.Freitas, Wheatstone bridge sensor composed of linear MgO magnetic tunnel junctions, *Journal of Applied Physics*, 107, 9, (2010)

With TMR : bridge sensitivity 32mV/V/Oe or 26.7 mV/mW/Oe

Spintronics sensors for ultra-low field detection

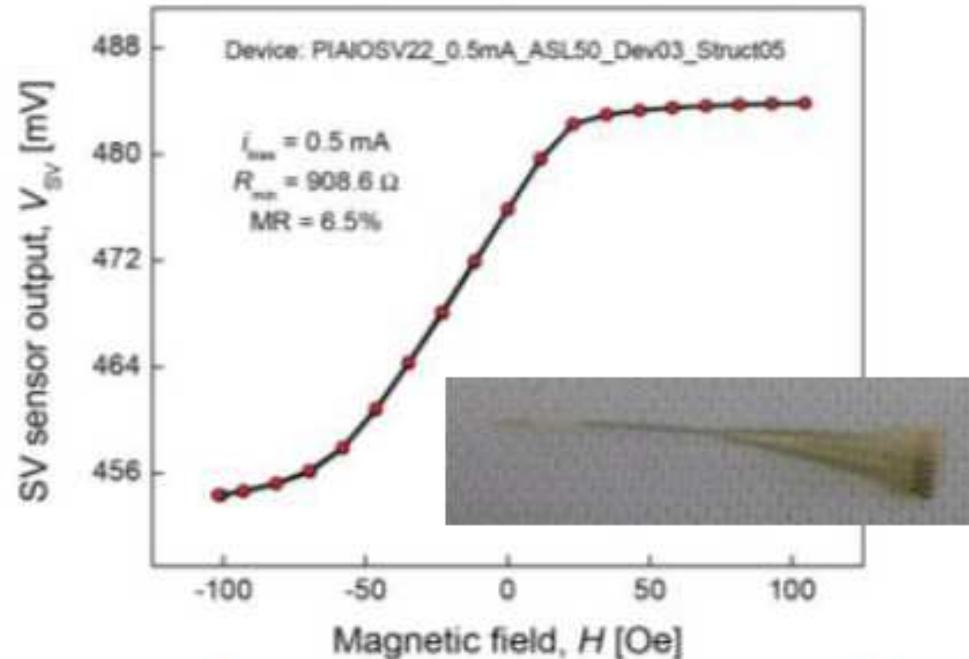
S.Cardoso et al, *Microsyst .technol* (2014) 20, 793.

Table 1 Summary of characteristics and achievements of competing technologies (based on magnetoresistance) for ultra-low field detection

Active sensor	Details	Magnetic flux guides	Operation temperature	Detectivity at 1 Hz (T/Hz ^{0.5})	Device footprint	Reference
AMR-bridge	Honeywell comercial AMR HMC1001	N	RT	100 pT	N/A	Stutzke et al. (2005)
GMR-bridge	NVE commercial GMR devices	Y	RT	4 nT	N/A	Stutzke et al. (2005)
GMR-single	Spin valves with ferromagnetic FGs	Y	RT	7–20 nT	>470 × 400 μm ^{2b}	Leitao et al. (2012); Guedes et al. (2007)
GMR-single	Spin valves with MEMs–FGs	Y	RT	40–600 nT ^a	900 × 2,400 μm ^{2b}	Guedes et al. (2008, 2012)
<i>GMR-single</i>	<i>Spin-valve with YBaCuO loop</i>	<i>Y</i>	<i>77 K</i>	<i>~200 fT</i>	<i>3 × 3 cm^{2c}</i>	<i>Pannetier et al. (2004)</i>
<i>GMR-bridge</i>	<i>GMR wheatstone bridge with Nb loop</i>	<i>Y</i>	<i>4 K</i>	<i>3 pT</i>	<i>3 × 3 cm^{2c}</i>	<i>Pannetier-Lecoeur et al. (2011)</i>
TMR-single	MTJ	N	RT	350 nT	N/A	Mazumdar et al. (2007)
TMR-bridge	NVE SDT	N	RT	~4 nT	N/A	Stutzke et al. (2005)
TMR-series	MTJ series	N	RT	16.2 nT	500 × 500 μm ²	Guerrero et al. (2009)
TMR-single	Al ₂ O ₃ MTJ with ferromagnetic FGs	Y	RT	534 pT	2,210 × 1,775 μm ^{2b}	Jander et al. (2003)
TMR-single	MgO MTJ sensor with ferromagnetic FGs	Y	RT	300 pT	500 × 500 μm ^{2b}	Chaves et al. (2007, 2011)

Integration of sensors on flexible substrates possible

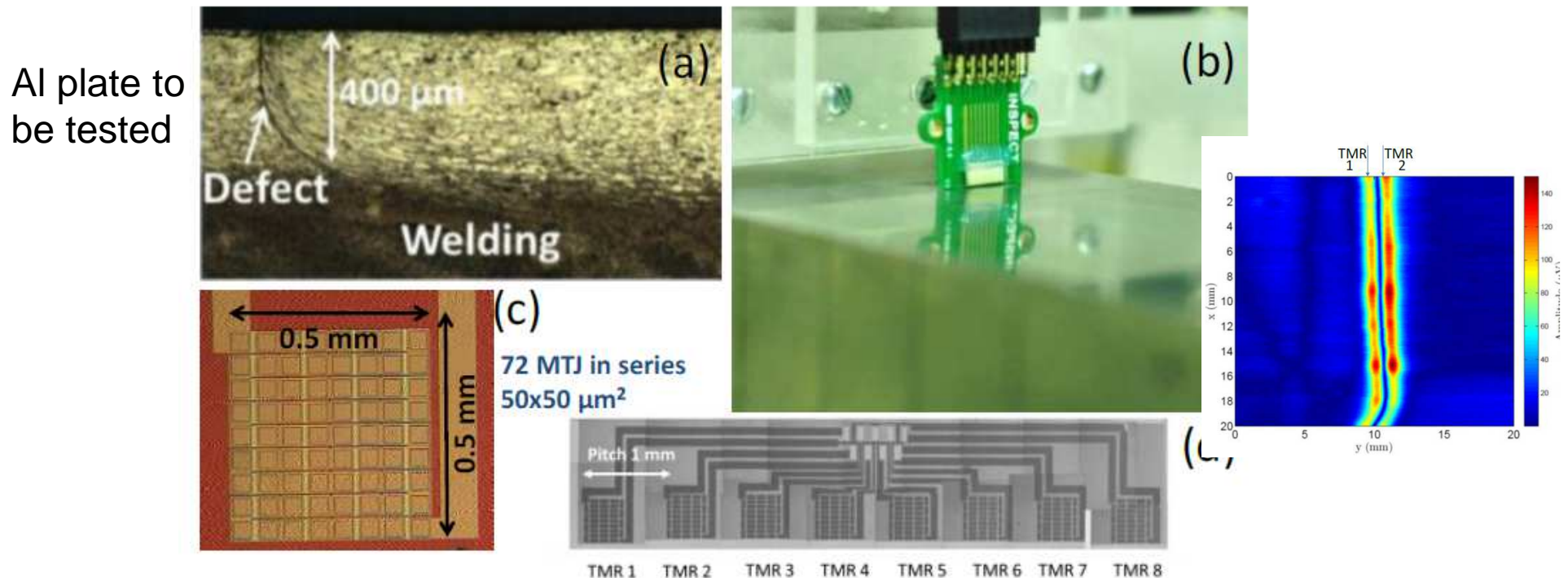
Interesting for instance for implantable devices, bendable electrodes (neurosciences).
Example: GMR spin-valves on polyimide



- M. Melzer, G. Lin, O. G. Schmidt, *Adv. Mater.* 2012, DOI: 10.1002/adma.201201898
- C. Barraud et al, *Appl. Phys. Lett.* 96, 072502 (2010)
- M. Melzer, D. Makarov, A. Calvimontes, et al, *Nano Lett.* (2011), 11, 2522–2526
- J. Gaspar et al, presented at INTERMAG conference, Beijing (2015)

Applications: 1) metal surface inspection

Principle: To excite the metal surface with a RF field at $\sim 1\text{MHz}$ and detect the stray field due to eddy current from the metal surface. Eddy currents are very sensitive to local resistivity which changes significantly if a defect is present.



E. E. Kriezis et al, *Proceedings of the IEEE*, 80(10), 1559-1589, 1992

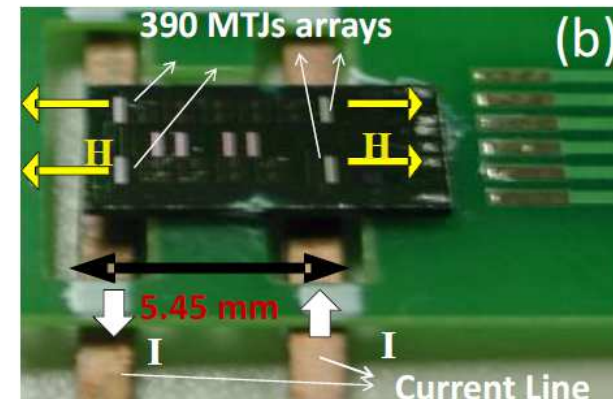
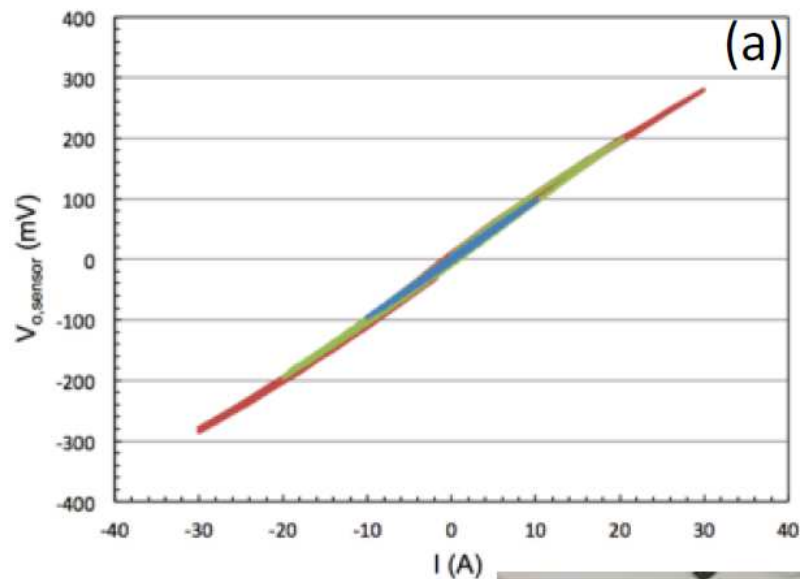
T. Dogaru et al, *IEEE Trans.Magn.*, 37, 3831 (2001).

Y. Dalichaouch, et al, *Proc. SPIE*, 3994, 2 (2000).

L. Rosado et al, *Sensors and Actuators A:Physical*, 212, 58 (2014).

F. Cardoso et al, *J.Appl.Phys.* 115, 17E516 (2014).

Applications: 2) MR sensors for Power measurements



Contactless
measurement of the
stray field created by a
current flowing in a wire

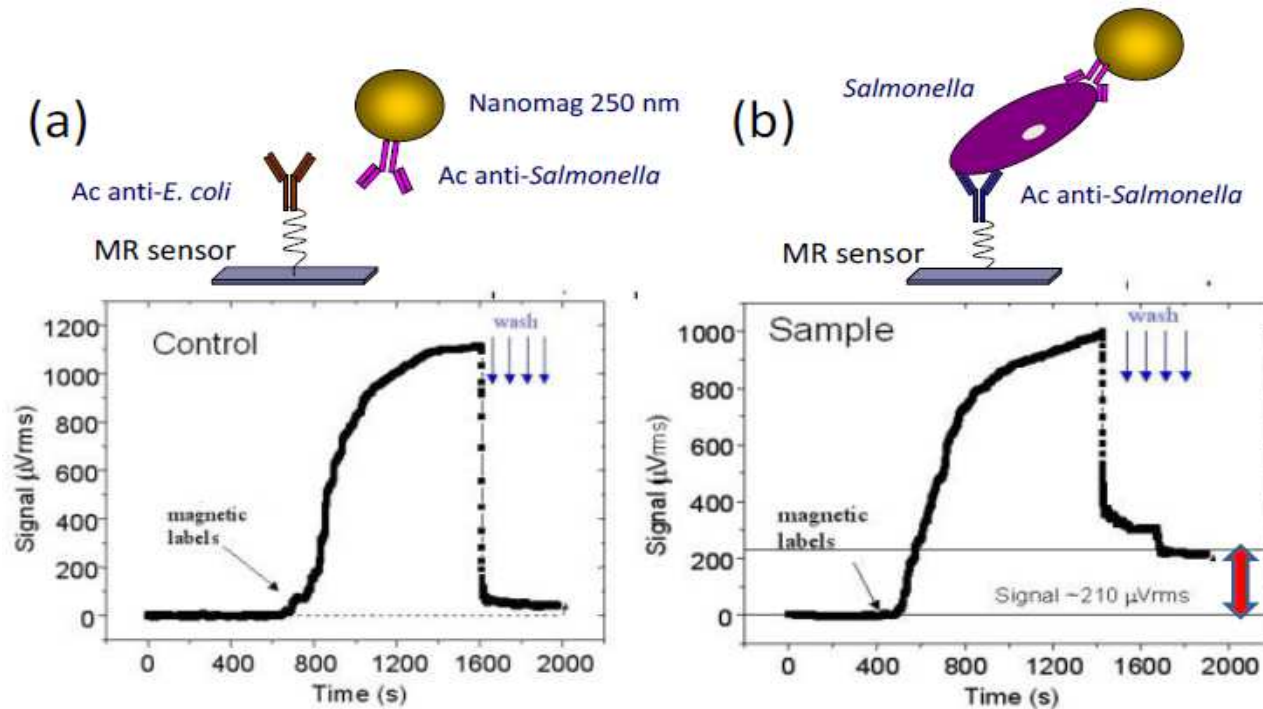


D. Ramírez Muñoz et al "Active power analog front-end based on a Wheatstone-type magnetoresistive sensor", Sensors & Actuators A 169 (2011), 83-88

J. Sánchez et al, "Magnetic tunnel junction current sensor for industrial applications", IEEE Trans. Magn. 48 (11), pp. 2823-2824 (2012)

Applications: 3) Medical/biological diagnosis Biosensing through magnetic nanoparticles labelling

Use MR sensors to detect magnetic particles flowing in a microfluidic channel



Startups:

<http://www.magarray.com>

(Stanford, Pr S.Wang)

<http://www.zeptolife.com>

(Minnesota)

<http://www.magnomics.pt>

(INESC, Portugal)

P.P. Freitas et al, Spintronic platforms for biomedical applications, Lab-on-Chip, 2012, 12 (3), 546 – 557

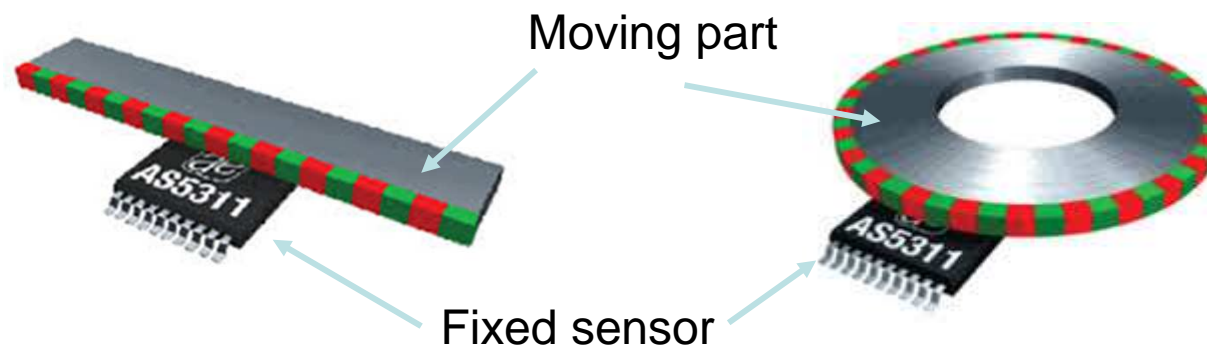
G.Li et al, Model and experiment of detecting multiple magnetic nanoparticles as biomolecular labels by spin valve sensors. *IEEE Transactions on Magnetics*, 40, 3000-3002 (2004)

V. C Martins et al, Femtomolar Limit of Detection with a Magnetoresistive Biochip, *Biosensors and Bioelectronics* 24, 2690 (2009),

Ferreira, H.A. et al. Rapid DNA hybridization based on ac field focusing of magnetically labeled target DNA, *Appl. Phys. Lett.* 87, 013901 (2005)

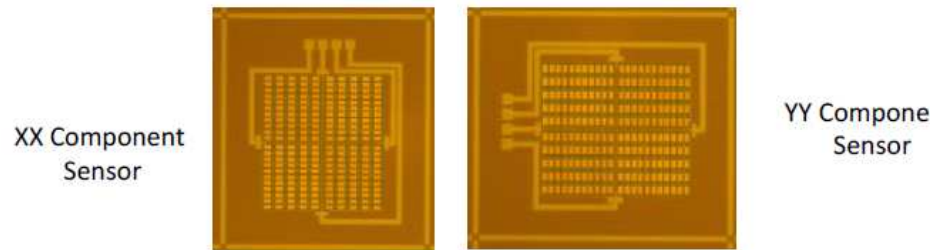
Germano, J. et al., *Sensors* 9(6), 4119-4137 (2009).

Applications: 4) Position/rotation encoders



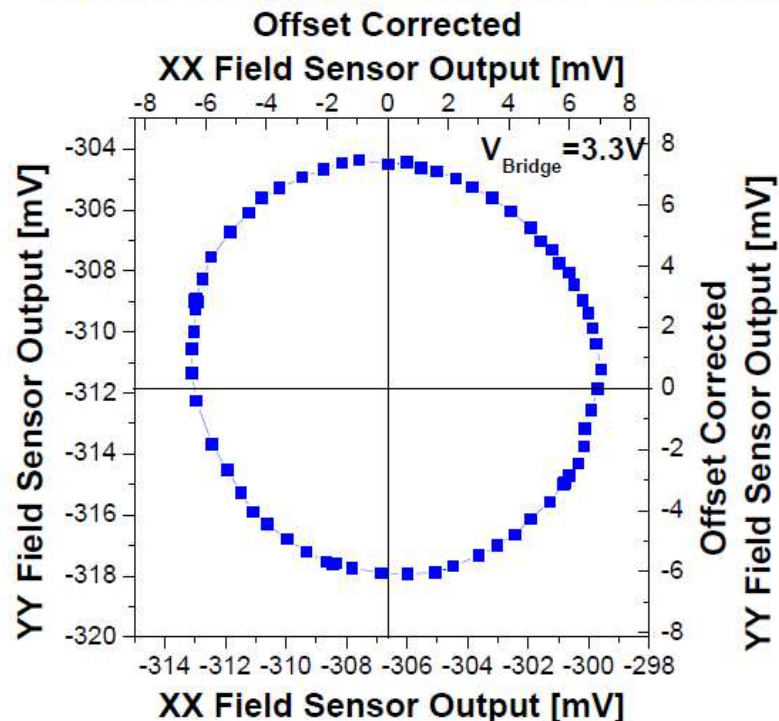
- MR sensors used as linear or rotation encoders
- More than 100 of them in a car. Often based on Hall sensors but GMR increasingly used.
- One difficulty with GMR or TMR is the **temperature sensitivity**. Must be somehow compensated (example: anisotropy field $H_k(T)$ decreasing at same rate as GMR(T) amplitude versus T so that $dR/R/dH$ remains constant vs T)
- Must be very low cost.

Applications: 5) MR sensors used as compass



Sensitive to earth field

Sensor output during a 360° rotation



13.3 mV/V/Oe sensitivity \rightarrow 0.31 Oe field

R. Ferreira, E.Paz, P.P.Freitas, 2-Axis Magnetometers Based on Full Wheatstone Bridges Incorporating Magnetic Tunnel Junctions Connected in Series, IEEE Transactions on Magnetics, 48, 4107 (2012)

Can complement GPS signal when the latter is not available (tunnels, underground parking lot, GPS breakdown...)

3D sensing also developed:
Difficulty is to measure B_z with integrated components (these sensors must be low cost)

Industrial actors in MR sensors



Allegro
MicroSystems, LLC
High-Performance Semiconductors

(USA)

PRODUCTS

- Current Sensor ICs
- Magnetic Digital Position Sensor ICs
- Magnetic Speed Sensor ICs
- Sanken Products
- Magnetic Linear and Angular Position Sensor ICs
- Motor Driver and Interface ICs
- Regulators and Lighting

AsahiKASEI

(Japan)

Honeywell

(USA)

Infineon

(Germany)

Melexis
Microelectronic Integrated Systems

(Belgium)

MEMSIC *Powerful Sensing Solutions*

(USA)

MICRONAS

(Switzerland)

NXP

(Netherlands)

amun

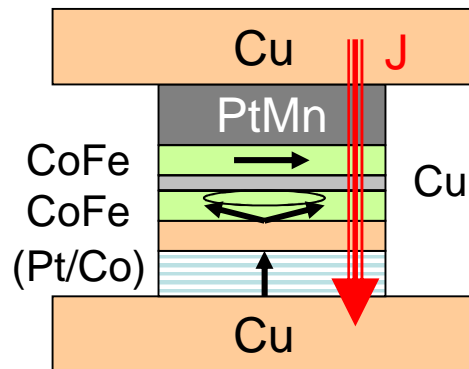
(Austria)

Spinelectronics: From Basic Phenomena to Applications

OUTLINE

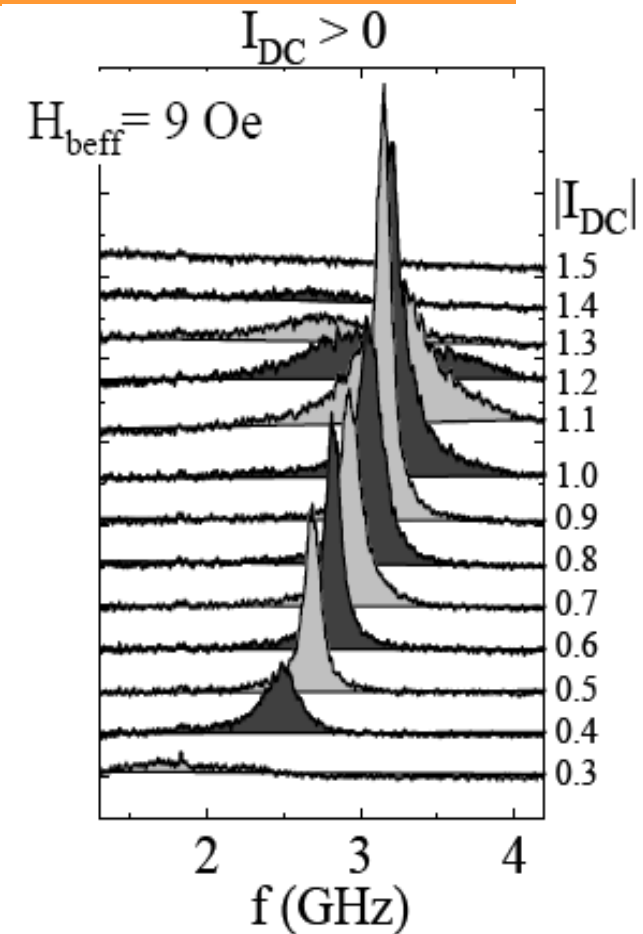
- Part 1 : Basic phenomena in spintronics:
 - Giant Magnetoresistance
 - Tunnel magnetoresistance (TMR)
 - Spin-Transfer Torque (STT)
 - Spin-orbit Torques (SOT)
- **Part 2 : Spintronics main applications**
 - Magnetic Recording (Hard disk drives Read-heads)
 - MRAMs
 - Magnetic field sensors
 - **RF components**

RF oscillators based on spin-transfer torque



*D.Houssamedine et al,
Nat.Mat 2007*

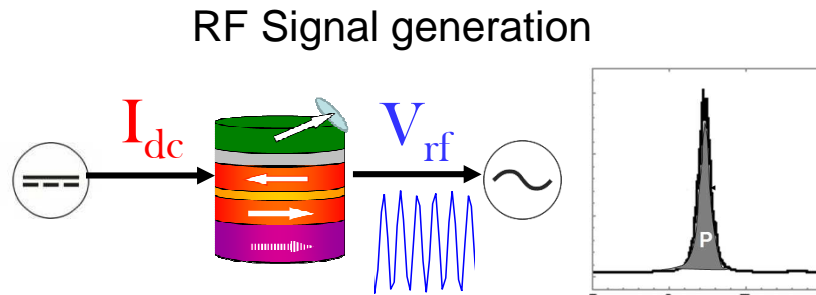
- Injection of electrons with out-of-plane spins in a layer of in-plane magnetization;
- Steady precession of the magnetization of the soft layer adjacent to the tunnel barrier.



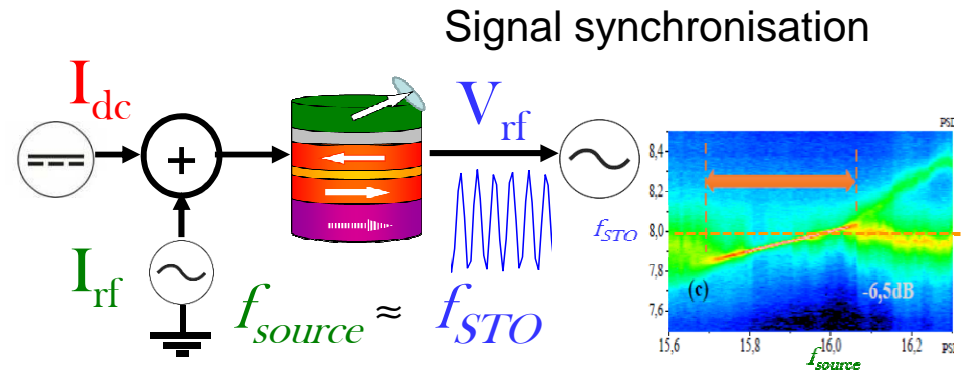
Precession (2GHz-40GHz) + Tunnel MR \Rightarrow RF voltage
Large-band frequency tunable RF oscillators

Spintronics RF Functions

Function 1: DC-to-RF converter

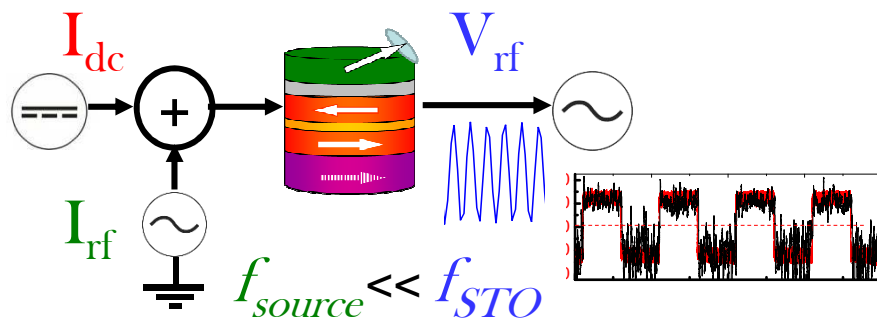


Function 2: Injection locking



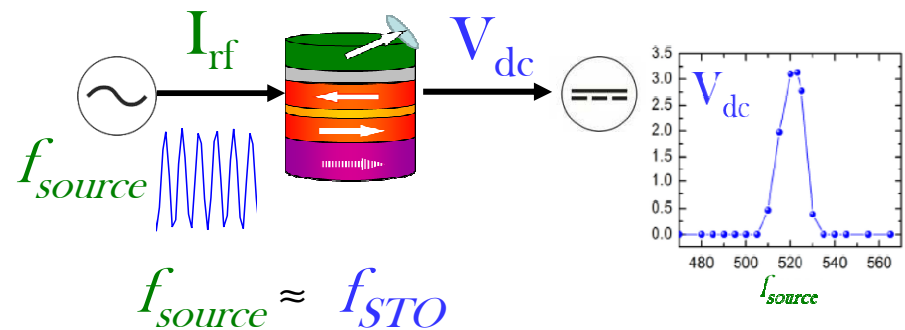
Function 3: Modulation and Mixing

Communication



Function 4: RF-to-DC conversion

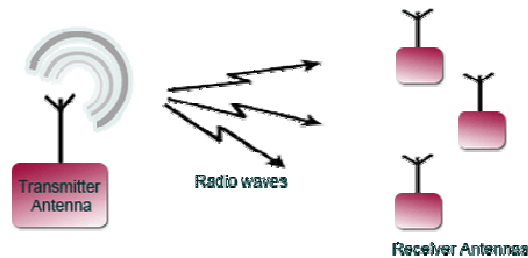
Frequency selective microwave detection



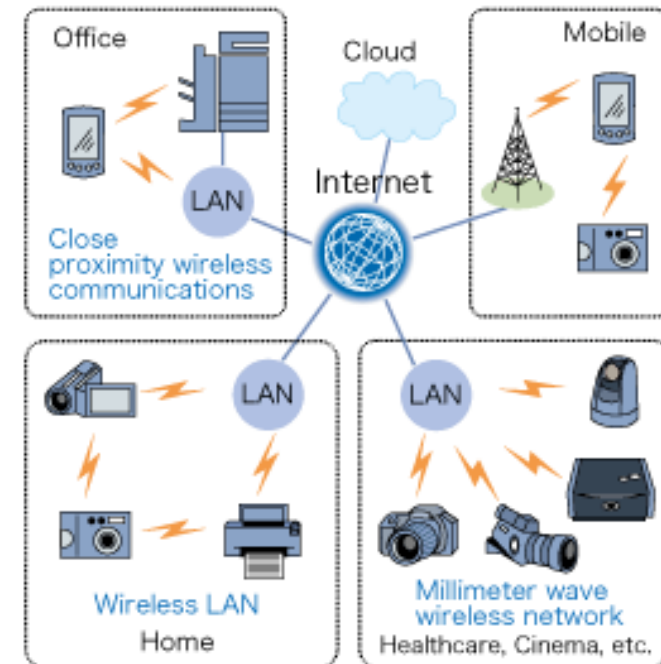
Assets of spintronics RF components

- **Low power**, active device
- **Nanoscale dimension** – small chip size, compact alternative to LC tanks
- **Large range of base frequencies** (configuration)
- **Frequency tuning** via I and H – reconfigurable communication
- **Multifunctional** (signal generation, injection locking, modulation, detection)
- **CMOS compatible** and radiation hard

Wireless communications



Wireless sensors network



However, not yet ready for practical applications....

Remaining problems towards practical spintronics RF oscillators

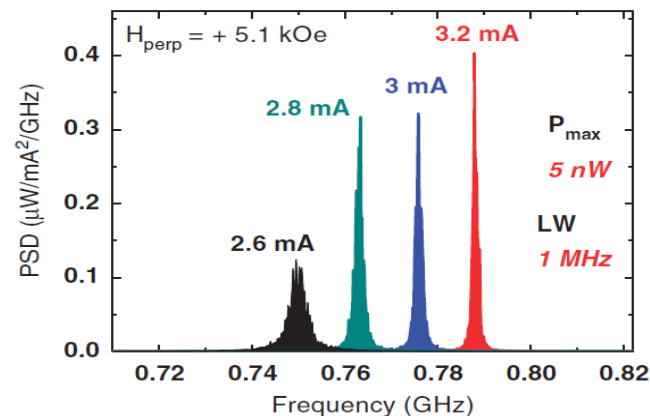
1) RF power still too low :

Large microwave generation from current-driven magnetic vortex oscillators in magnetic tunnel junctions, A.Dussaux et al, Nature Com.2010, DOI: [10.1038/ncomms1006](https://doi.org/10.1038/ncomms1006)

PtMn 15 nm / CoFe 2.5 nm / Ru 0.85 nm / CoFeB 3 nm / MgO 1.075 nm / NiFe 15 nm / Ru 10 nm.

170nm pillar diameter

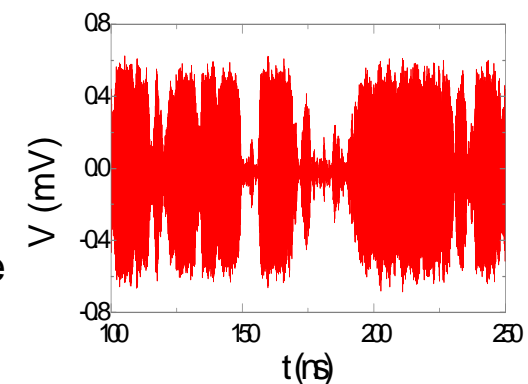
Free layer in vortex configuration



Vortex oscillators provide the largest output power among all STO but weak tunability and **power still too low** for practical applications (by several orders of magnitude).

2) Instability of the precessional motion:

Large tunability is intrinsically associated with large non-linearity in magnetization dynamics (frequency depends on magnetization trajectory amplitude). But then thermal fluctuations, by perturbing the magnetization trajectories, more strongly hamper the coherence of the magnetization dynamics yielding **large noise**.



Most probable first application : RF rectifiers: spin-torque diodes

ARTICLES

PUBLISHED ONLINE: 20 OCTOBER 2013 | DOI: 10.1038/NMAT3778

nature
materials

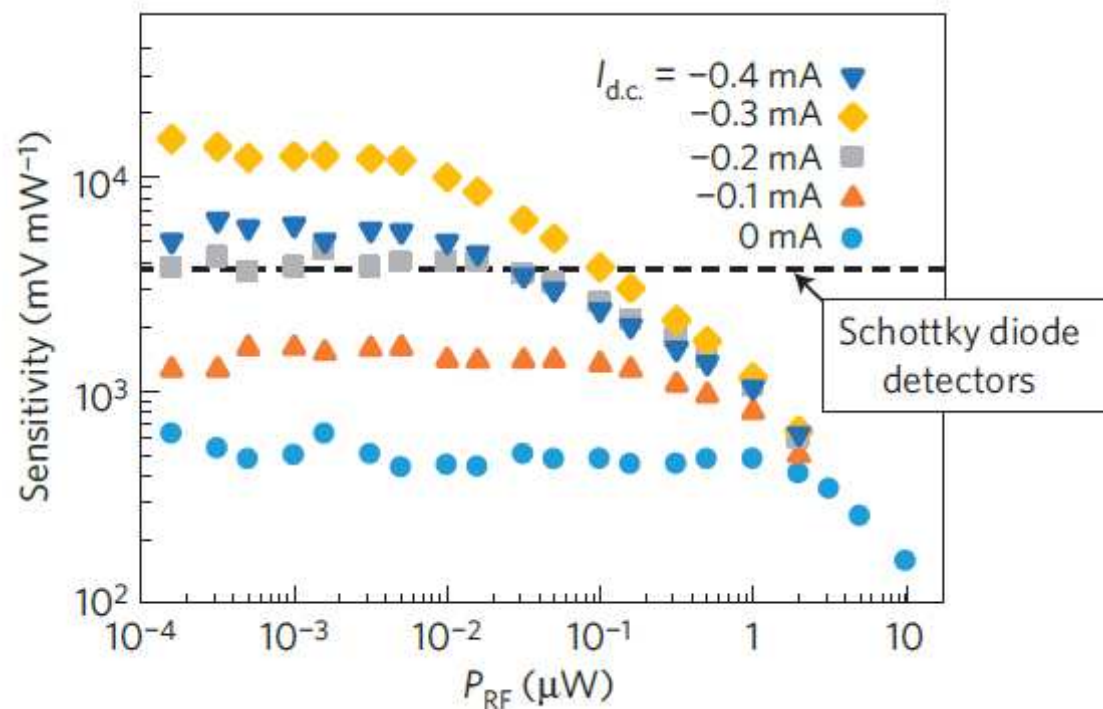
Highly sensitive nanoscale spin-torque diode

S. Miwa^{1†}, S. Ishibashi^{1,2†}, H. Tomita¹, T. Nozaki^{1,2}, E. Tamura¹, K. Ando¹, N. Mizuochi¹, T. Saruya^{2‡}, H. Kubota², K. Yakushiji², T. Taniguchi², H. Imamura², A. Fukushima², S. Yuasa² and Y. Suzuki^{1,2★}

Highly sensitive microwave devices that are operational at room temperature are important for high-speed multiplex telecommunications. Quantum devices such as superconducting bolometers possess high performance but work only at low temperature. On the other hand, semiconductor devices, although enabling high-speed operation at room temperature, have poor signal-to-noise ratios. In this regard, the demonstration of a diode based on spin-torque-induced ferromagnetic resonance between nanomagnets represented a promising development, even though the rectification output was too small for applications (1.4 mV mW^{-1}). Here we show that by applying d.c. bias currents to nanomagnets while precisely controlling their magnetization-potential profiles, a much greater radiofrequency detection sensitivity of $12,000 \text{ mV mW}^{-1}$ is achievable at room temperature, exceeding that of semiconductor diode detectors ($3,800 \text{ mV mW}^{-1}$). Theoretical analysis reveals essential roles for nonlinear ferromagnetic resonance, which enhances the signal-to-noise ratio even at room temperature as the size of the magnets decreases.

RF diodes are important components in RF communications for frequency detection.

RF rectifiers: spin-torque diodes

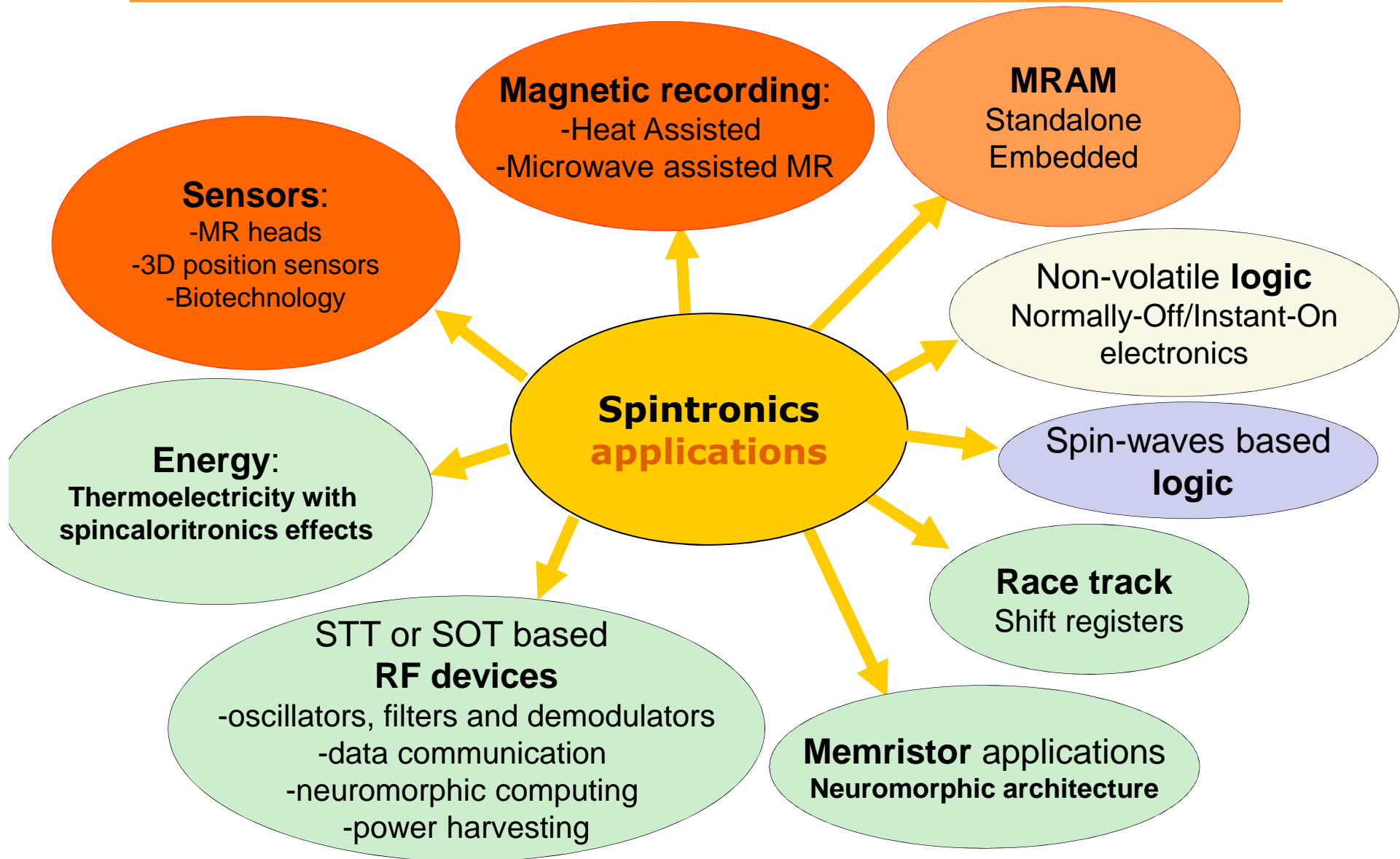


S.Miwa et al, Nat.mat (2013) NMAT 3778

In the sub-threshold regime (just before magnetization switching), high sensitivity of magnetization trajectory on RF power.

In Japan, spin-torque diodes considered as a promising RF application of STT.

Spintronics/nanomagnetism broadening spectrum of interest





Thank you !

Work partly supported by the project



HYMAGINE (ERC2010-2015)

MAGICAL (ERC2015-2020)